

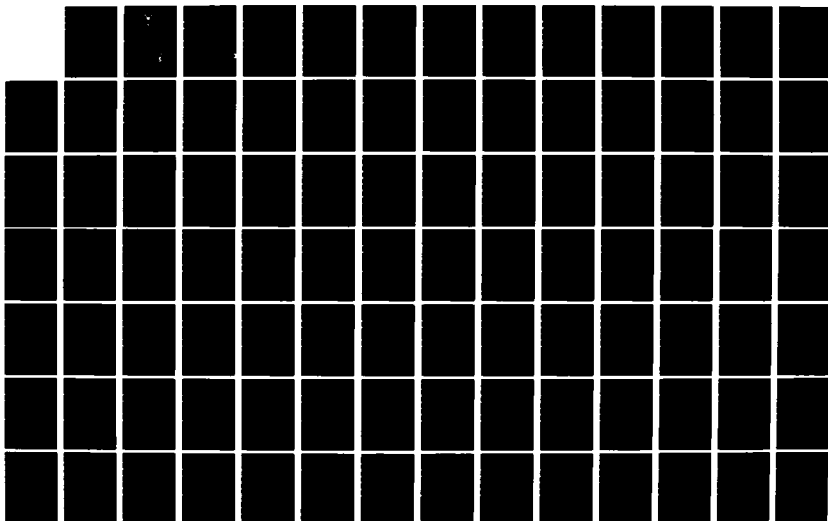
AD-A124 734

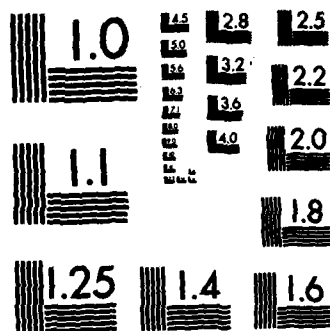
AN EVALUATION OF THE EFFECTIVENESS OF DEPLOYING
ELECTRO-OPTICAL TELESCOPE. (U) AIR FORCE INST OF TECH
WRIGHT-PATTERSON AFB OH SCHOOL OF ENGI. R T SALMON
DEC 82 AFIT/GSO/OS/82D-4 F/G 17/8

1/2

UNCLASSIFIED

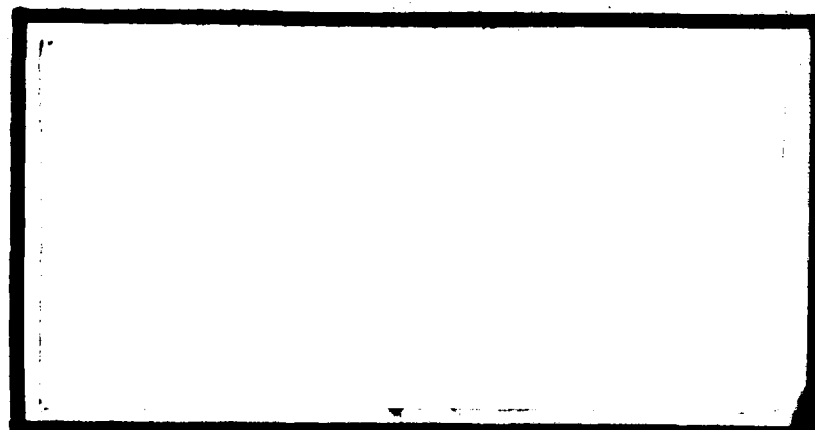
NL





MICROCOPY RESOLUTION TEST CHART
NATIONAL BUREAU OF STANDARDS-1963-A

AD A124734



This document has been approved
for public release and sale; its
distribution is unlimited.

DEPARTMENT OF THE AIR FORCE
AIR UNIVERSITY (ATC)

AIR FORCE INSTITUTE OF TECHNOLOGY

Wright-Patterson Air Force Base, Ohio

DTIC
ELECTE
FEB 22 1983
S A

DTIC FILE COPY

83 02 022 158

OS
AFIT/GSO/82D-4

Accession For	
NTIS GRA&I	<input checked="checked" type="checkbox"/>
DTIC TAB	<input type="checkbox"/>
Unannounced	<input type="checkbox"/>
Justification	
By	
Distribution/	
Availability Codes	
Dist	Avail and/or Special
A	



AN EVALUATION OF THE EFFECTIVENESS OF
DEPLOYING ELECTRO-OPTICAL TELESCOPES
FOR SATELLITE TRACKING ON HIGH
ALTITUDE POWERED PLATFORMS

THESIS

Richard T. Salmon
Capt. USAF
AFIT/GSO/82D-4
OS

DTIC
ELECTE
FEB 22 1983
A

Approved for public release; distribution unlimited

OS
AFIT/GSO/~~OS~~82D - 4

AN EVALUATION OF THE EFFECTIVENESS OF
DEPLOYING ELECTRO-OPTICAL SATELLITE
TRACKING TELESCOPES ON HIGH ALTITUDE
ALTITUDE POWERED PLATFORMS

THESIS

Presented to the Faculty of the School of Engineering
of the Air Force Institute of Technology
Air University
in Partial Fulfillment of the
Requirement for the Degree of
Master of Science

by

Richard T. Salmon

Capt. USAF

Graduate Space Operations

December 1982

Approved for public release; distribution unlimited.

Preface

This research was performed to determine the potential of developing electro-optical satellite tracking telescopes on board high altitude powered platforms. A computerized simulation model was developed to conduct a comparative analysis of a hypothetical system of air based telescopes with the Ground-Based Electro-Optical Deep Space Surveillance (GEODSS) System. Some effort was also devoted to assessing the feasibility of an air based satellite tracking telescope.

Thanks go to Professor Edward Dunne for his guidance in the analysis procedures, Professor James Lange for his assistance in electro-optics, and Capt. Charles Ruberson for his help in obtaining cloud cover data.

Richard T. Salmon

Contents

	Page
Preface	ii
List of Figures	v
List of Tables	vi
Abstract	vii
I. Introduction	1
Background	1
Objective of the Study	5
Modeling Approach	6
Scope, Limitations, and Assumptions	7
Sequence of the Presentation	8
II. Model Overview	9
Definition of Terms	9
User Inputs	10
Basic Physical Principle	15
Orbital Mechanics	15
Sensor Operation	15
Submodel Descriptions	23
SPHERE and CART	23
TARGET and SUNPOS	23
SIGHT	25
VISELE	25
SLWIR	25
SIDEN	25
CLOUD	30
TRACK	30
Main Program EOBASE	30
Input Section	35
Optimization Section	35
Confidence Section	35
Summary	35
III. Model Development	38
Sphere of Operations (Subroutine SPHERE)	38
Placement of Points	38
Ground- and Air-Basing Modes	38
Space-Basing Mode	41
TARGET and SUNPOS	41
SIGHT	43
VISELE AND SLWIR	44

	Page
SIDEN	45
CLOUD	46
OPTIMIZE	48
TRACK	48
Sensor Placement	49
Target and Sensor Movement at Each Δt	50
EOBASE Validation	51
Conceptualization	51
Verification	51
Credibility	54
Confidence	55
IV. Sensor System Basing Mode Analysis	57
Methodology	59
Results and Discussion	63
V. Conclusion	73
Summary	73
Conclusions	75
Recommendations for Further Study	75
Bibliography	78
Appendix A: Use of the Model	81
Appendix B: EOBASE Listing	86
Vita	124

List of Figures

<u>Figure</u>		<u>Page</u>
1	Geocentric Equitorial Reference	16
2	Sunlight Reflection Geometry	18
3	Submodel Sphere Logic Diagram	24
4	Submodel Target Logic Diagram	26
5	Submodel SIGHT Logic Diagram	27
6	Submodel VISBLE Logic Diagram	28
7	Submodel SLWIR Logic Diagram	29
8	Submodel SIDEN Logic Diagram	31
9	Submodel CLOUD Logic Diagram	32
10	Submodel TRACK Logic Diagram	33
11	EOBASE Functional Flow	34
12	Typical Wind Velocity Profile	40

List of Tables

<u>Table</u>		<u>Page</u>
I	User Inputs: General, Sensor, and Mission Data	11
II	Target Type Descriptions	12
III	User Inputs: Ground Site Locations and Air- and Space-Based Sensor Location Parameters	13
IV	User Inputs: Sky Cover Probabilities	14
V	Summary of Submodel Functions	36
VI	Number of Points on Each Latitude	39
VII	Basic Scenario	52
VIII	Experiment Descriptions	53
IX	Experiment Results	53
X	Δ Experiment Results	55
XI	Location of GEODSS Sites	61
XII	Location of Weather Stations	61
XIII	Basic Initialization and Sensor Inputs for GEODSS System Simulation	64
XIV	Results of GEODSS System Encounter with the Four Target Type Target System	66
XV	Average Nighttime Probability of Less Than or Equal To $3/8$ Sky Cover	67
XVI	Inputs Used to Choose Air-Based System	69
XVII	Five Sensor Air-Based System	71
XVIII	Example Scenario	82
XIX	Input Data Format	83
XX	Input Data Form for Preselected Ground-Based Sensors	84
XXI	Input Data Format for Preselected Air- and Space-Based Sensors	84

Abstract

↓ The purpose of this research was to evaluate the possible benefits of an air based system of electro-optical satellite tracking telescopes. A computerized simulation model was developed to conduct a comparative analysis of a hypothetical system of air based telescopes with the Ground-Based Electro-Optical Deep Space Surveillance (GEODSS) System. The simulation includes a first order optimization process for selecting a satellite surveillance system and a many-on-many engagement model to test the effectiveness of the surveillance system selected. In addition, the user can input a preselected surveillance system and test its effectiveness.

The user specifies the characteristics of the surveillance system and the basing locations, if they are preselected. Cloud cover data can be entered with preselected ground sites. Target satellites included four sets of representative satellite systems. The user selects the targets, defines the mission time, and determines the percentage of each target system which must be tracked.

Preliminary results indicate^d that an air based surveillance system with three dispersed telescope platforms could outperform a system of five candidate GEODSS sites. ↑

**AN EVALUATION OF THE EFFECTIVENESS OF DEPLOYING
ELECTRO-OPTICAL TELESCOPES FOR SATELLITE TRACKING
ON HIGH ALTITUDE POWERED PLATFORMS**

I Introduction

Background

Optical sensors provide an important input to the Space Detection and Tracking System (SPADATS), a network of sensors maintained by the Air Force to monitor all man-made objects in space (Ref 1:Ch 2). Unlike radar, optical sensors can with relative ease track a satellite in deep space. The Baker-Nunn camera, classified as a modified Schmidt telescope, is currently SPADATS' primary deep space sensor. This telescope can track an object the size of a basketball at 35,000 nautical miles (Ref 1:Ch 2, 20).

Unfortunately, the presence of the atmosphere limits the utility of these sensors. The atmosphere limits telescopes in five ways (Ref 1:Ch 5, 31-32). The first limitation is due to weather. Clouds, fog, and rain severely degrade atmospheric transmission. The second limitation is that the atmosphere is not transparent to all regions of the electromagnetic spectrum. The atmosphere is actually opaque in some regions of the spectrum. The third problem is that the atmosphere scatters light. Thus an astronomical telescope cannot detect faint objects in daylight, and at night even city lights limit the depth that can be probed by a telescope. The fourth problem is caused by variations in the density of the atmosphere. It is these variations which cause the stars to twinkle. Finally, the fifth limitation is that under some

conditions the atmosphere can emit light. The auroras illustrate this ability. As a result of these limitations, it is desirable to locate optical telescopes at remote sites at high altitudes. This creates severe complications in choosing sites for SPADATS' optical sensors.

Airborne electro-optical telescopes have been proposed as a means of circumventing some of the atmospheric limitations. In 1967, Nortronics (Palos Verdes Peninsula, California) conducted a design study for an airborne electro-optical surveillance system (Ref 2). Since then, the feasibility of using airborne optical sensors for satellite tracking has been demonstrated. In 1970, a long-wavelength infrared search/track radiometer, mounted on a U-2 aircraft, successfully acquired and tracked Pegasus satellites up to a range of 720 nautical miles (Ref 3:81-94).

Most experience with airborne optical sensors has been gained by astronomers using infrared telescopes. Because the atmosphere absorbs infrared radiation, celestial observations from the earth's surface are limited to views from high altitudes through narrow "atmospheric windows" at 1 to 2.5, 3 to 5, 8 to 12, 20, and less clearly at 350 microns (Ref 4). At sea level, most atmospheric absorption of the infrared is due to water vapor and carbon dioxide; however, the water content of the atmosphere decreases rapidly with altitude, and above 40,000 feet, the water content of the air is negligible (Ref 5:118). The two types of vehicles which astronomers have used most successfully as airborne observatories are balloons and airplanes. The balloon has the advantage of high operating altitudes. For example, a 40-inch far-infrared telescope has been carried to 95,000 feet several times by balloon (Ref 6), and the NASA Ames Research Center has sent a

balloon-borne 28-inch telescope to 100,000 feet (Ref 4). The Ames Center also operates a Learjet carrying a 12-inch telescope and a C-141 carrying a 36-inch telescope (Ref 7). Although these aircraft can operate only up to 45,000 feet, they can carry equipment operators in a shirt sleeve environment, the flight path is controlled, and the payload is not at risk. In addition, the C-141 can carry a large payload.

But neither the balloon nor the airplane are practical for satellite surveillance (Ref 8:Sec B.2). Balloons have little station-keeping ability. This imposes a serious constraint since sensor data must be sent to the ground where it can be processed. Airplanes, on the other hand, would be too expensive. Due to expected aircraft availability, at least three planes would be required at each station to assure 16 hours/day operation.

A third kind of high altitude sensor platform is still under development. Both the Air Force (Ref 9) and the Navy (Ref 10) have sponsored programs for the development of an unmanned high altitude airship (or aerostat).

This concept combines some of the advantages of the airplane and the free balloon since the vehicle should be able to maintain a stationary position above the ground at 70,000 feet. The Air Force sponsored program has demonstrated that such an airship can be built. In May of 1970, High Platform II, a solar powered airship, was flown. This vehicle had a design speed of 10.3 meters/seconds at 20 kilometers above sea level. In spite of two attempts, the Navy has not yet sponsored a successful flight, but their effort is perhaps more ambitious. The Navy's High Altitude Superpressured Powered Aerostat

(HASPA) program has built an airship which is designed to maintain a payload of 4,000 pounds at 70,000 feet for 1 year.

The development of a practical high altitude airship has been slowed by two serious problems (Ref 11). The most serious of these problems is developing a suitable hull fabric. The high operating altitudes impose a severe strength to weight ratio requirement. Materials exist which can meet this requirement; but finding a material which also resists abrasion, tolerates temperature extremes, and tolerates ultraviolet light is a problem. The second problem is that the high altitude airship requires a lightweight power system for payload operation and propulsion. Several types of power systems are being studied as alternatives. Perhaps the most probable candidate for long duration flights is a regenerative power source utilizing solar arrays (Ref 11). However, NASA is evaluating the feasibility of powering an aerostat or even an unmanned lightweight airplane with a microwave power system (Ref 12). This should also be suitable for long duration flights. For short duration flights, up to 30 days or more, technology is currently available to assemble a gasoline fueled, turbocharged, reciprocating engine capable of providing sufficient power (Ref 13).

The latest effort to build a practical high altitude airship is a concept called Hi-Spot for high altitude surveillance platform for over-the-horizon targeting (Ref 14). Hi-Spot could hover at 60,000 to 80,000 feet for as long as 155 days. It would be 504 feet long and 154 feet in diameter, would carry a 550-pound payload, and would be propelled by a 27 meter diameter propeller powered by a hydrogen fueled, air breathing engine(s). The Hi-Spot concept is being studied for the

Navy by Lockheed Missile & Space Company for applications including air/sea surveillance, communications relay, remote sensors readout, and signal intelligence (SIGINT) collection missions. The Lockheed design is being considered for a Fiscal 1984 start of a technical risk reduction program and scale model demonstration.

Objective of the Study

In the past (Ref 8:Sec B.2), the high altitude airship has been summarily dismissed as a viable platform option for satellite surveillance because of the relatively high development risk associated with finding a suitable hull fabric and because of the limited station-keeping ability of the proposed designs. However, interest in developing a high altitude airship has continued, and Hi-Spot may soon demonstrate the feasibility of such a vehicle. Furthermore, NASA is now investigating the feasibility of a High Altitude Powered Platform (HAPP) which would be either an unmanned airship or airplane utilizing a microwave power system. The results of their cost/feasibility study appear promising (Ref 15). In addition, NASA has funded user surveys in various areas of application (Ref 16). These surveys suggest that the HAPP system would have the attributes of a low attitude geostationary satellite. It would be particularly useful as a communications relay, and it would also be attractive in some remote sensing applications where very frequent coverage is required.

Since the implementation of a high altitude airship concept in some form appears likely, the practical value of an aerostat for satellite surveillance should be reassessed. The first step in that process should be to determine what practical value the aerostat would

have in operational terms. The problem of interest here is to estimate the effectiveness of a system of airship-based optical sensors in performing the deep space surveillance mission and to compare this to a system of ground-based sensors. Thus the objective of this study is to assess the gain in mission performance due to three major operational advantages conferred by the airship:

1. The optical sensor would be relatively insensitive to weather limitations.
2. The optical sensor could be stationed almost anywhere.
3. The infrared portion of the spectrum would be more readily available to the sensor.

Modeling Approach

The comparison between the different modes of sensor basing, airship versus ground basing, can be made by using a computer program derived from HELBASE, a computer simulation model for the investigation of high energy laser applications in the antisatellite role (Refs 17 and 18). The purpose of HELBASE is (given specific mission requirements) to determine the optimal configuration and number of laser weapons required to "shoot" a given number of satellites with a given probability of success. The program can make these selections regardless of whether the laser weapons are ground-, air-, or spacebased. To determine if a particular system design (number and location of weapons) will meet the mission requirements, the program simulates several battles. If the system is unsatisfactory, the program selects the next "best" weapon/location combination to add to the system. This ensures that the weapons system selected can meet the mission requirements.

Obviously HELBASE needed to be adapted for this thesis. HELBASE has been revised to do the following:

1. Allow the input of selected ground sites with predefined coordinates (latitude, longitude, and altitude) and associated sky cover probabilities.
2. Account for the effect of weather on a ground-based sensor's performance by utilizing sky cover probabilities in Markov chain model.
3. Determine if a target satellite can be tracked based upon the sun/earth shadow, target, and sensor configuration as well as the type of sensor involved.

The output from the model is the average time required to track all of the simulated target satellites. For this study, target satellite orbits were selected which emphasized the ability to detect and track injections from parking orbits into highly elliptical, 12-hour orbits and to detect maneuvers.

Scope, Limitations, and Assumptions

Scope. This effort is limited to comparing the performance of the aerostat-based versus ground-based optical sensors in the role of deep space surveillance and tracking. No comparison of investment and operating costs has been made. The ground-based system against which the aerostat-based system was compared was the Ground-Based Electro-Optical Deep Space Surveillance (GEODSS) system which is now in the process of being deployed.

Limitations and Assumptions. Since there has been only moderate interest, an aerostat-based electro-optical telescope has yet to be built that could meet the requirements for deep space satellite

surveillance. It is somewhat uncertain how such a system would perform. For the purposes of this study, however, it has been assumed that an aerostat based electro-optical telescope can track objects in geosynchronous orbit and that the expected problems with pointing accuracy, position fixing, and weight limits can be overcome at a reasonable cost.

Sites for the aerostat-based system were selected from 13 evenly spaced latitudes from 60 degrees north through 60 degrees south. No other limits were placed upon deployment. This is somewhat unrealistic, however, it is possible that configuration of the aerostat-based systems could be approximated in the real world. The aerostat based optical sensors were assumed to be operating at 70,000 feet and without weather interference. Sites for the ground-based system were placed in the same configuration as those sites selected for the GEODSS system. The sky cover (weather interference) for each of the ground sites was estimated using a model which assumed that the sky cover conditions persisted for at least a 3-hour interval.

The orbital mechanics used in the model assume a simple two body problem with the satellites acting as point masses. The Earth is regarded as a simple sphere of radius 6378.145 kilometers.

Sequence of Presentation

Chapter II provides an overview of the computer simulation model. In addition, some of the basic physical principles used in the model are described. Chapter III contains an explanation of the concepts employed in each of the model's subprograms. Chapter IV gives the results of the basing mode analysis. Chapter V, the conclusion, includes a summary of this thesis, some conclusions derived from this work, and recommendations for further study.

II Model Overview

This chapter presents a general overview of the program EOBASE. The user inputs, the submodels, and some of the basic physical principles which are used in the program are described. The program EOBASE was derived from HELBASE (Refs 17 and 18), and it is analogous to HELBASE in as much as one of its purposes is to select "the most efficient" sensor system. However, EOBASE can also be used to evaluate a system of sensors with user selected sites.

Definition of Terms

1. Basing Mode: This refers to the possible sensor locations. The three alternative locations are the surface of the earth, in an aircraft or aerostat, and in a circular orbit around the earth.
2. Sensor: One electro-optical sensor which either detects visible or infrared radiation from a specific sensor type.
3. Sensor Type: A specific combination of specific electro-optical sensor characteristics.
4. Sensor System: A collection of sensors selected from the available sensor types.
5. Target: A single specific satellite which a sensor may track.

6. Target Type: A group of targets which are related by a common set of mission and orbital parameters.
7. Target System: The collection of all selected targets.
8. Mission: The operational capabilities around which the sensor system is to be defined.
9. Most Efficient: Like HELBASE, EOBASE selects a system which is a first cut approximation of the optimal system. The term "most efficient" is viewed in this sense.

User Inputs

The EOBASE program allows the user two distinct options. The program can be used to select the most efficient sensor system, or it can be used to evaluate a user selected system. Each of these options requires somewhat different input formats. Appendix A illustrates these input formats and provides a description of the various inputs.

However the user chooses to use the program, the following categories of user inputs are required: general, sensor types, target types, and mission data. Table I provides a summary of these inputs.

Up to five sensor types may be input. As illustrated in Table I, both the basing mode and the sensor characteristics are needed to specify a sensor type. One of three basing modes can be chosen for each sensor type, the ground mode, the air mode, or the space basing mode. If the user elects to have the EOBASE program select the sensor system; selection of the ground mode, Mode 1, limits deployment to the latitudes on the surface of the earth; selection of the air mode, Mode 2, limits deployment 21.3 kilometers above latitudes on the surface of the earth; and selection of the space basing mode, Mode 3,

TABLE I

User Inputs: General, Sensor Data, and Mission Data

<u>Input Category</u>	<u>Variable</u>	<u>Dimension</u>
General	SEED	---*
	JCOUNT	---
	NOWT	---
	ICOUNT	---
	DT	Minutes
	P	---
	INPUT	---
	INPUTS	---
	SUNTYP	---
Sensor Data	Basing mode	---
	Sensor	---
	Cutoff/angular resolution	Visual magnitudes/ steradians
	Altitude	Kilometers
	Minimum tracking time per cycle	Seconds
	Dwell time	Seconds
Target Type Selection	Del	---
Mission Data	Target type	---
	Target type tracking percentage	---
	Mission time	Minutes
	Target type tracking priority	---

*Dimensionless parameter.

Note: Several sets of sensor and/or mission data are possible.

limits deployment to circular orbits around the earth at an altitude specified by the user.

The EOBASE program provides the user with the selection of any combination of four target types. These target types are permanently stored in EOBASE, and they are intended to be reasonable representations of real world target possibilities. See Table II for a description of the four types.

TABLE II
Target Type Descriptions

Target Type	I	II	III	IV
Semimajor axis (kilometers)	22,260.0	22,260.0	42,164.0	42,165.0
Orbital eccentricity (dimensionless)	.7	.7	0	0

Orbital inclination (radians)	1.1340	.7854	1.5708	0
Argument of perigee (radians)	4.0143	4.5379	0	0

Longitude of the ascending node (radians)	Random*	Random	Random	0
Mean anomaly	Random*	Random	Random	Random
Number of targets	3	4	3	4

*Each set of targets is evenly spaced over 360 degrees.

A set of mission data inputs must be provided by the user with each target type selection. These inputs define the minimum mission requirements for tracking each type of target, and they are particularly relevant when EOBASE is used to select the most efficient sensor system. The target type tracking percentage is the percentage of a particular type of target which must be tracked to ensure mission accomplishment. The mission time is the maximum time a selected sensor system is allowed to accomplish the mission. This input must be the

same for all target types. A target type tracking priority is assigned to each target type (one is the highest). The tracking priority is used to determine which target is tracked first if two targets can be tracked at the same time. A secondary criterion is the target's range from the sensor. The target with the shortest range, within a particular priority group, is tracked first.

A fifth input category, ground site locations, is used when the user wishes to input previously selected sites for sensors in the ground mode. As shown in Table III, the user enters the latitude, longitude, altitude, and sensor type of each ground-based sensor. Associated with each of these site locations is a sixth input

TABLE III

User Inputs: Ground Site Locations and Air and Space
Based Sensor Location Parameters

<u>Input Category</u>	<u>Variable</u>	<u>Dimension</u>
Ground site locations	Latitude	Radians
	Longitude	Radians
	Altitude	Kilometers
	Sensor type	---
Sky cover probabilities (see Table IV)	Conditional	---
	Unconditional	---
Air and space-based sensor location parameters	Orbital radius or coordinate theta	Kilometers or radians
	Eccentricity	---
	Inclination or coordinate theta	Radians or radians
	Longitude of ascending node	Random
	Argument of perigee	0

*Dimensionless parameter

TABLE IV

User Inputs: Sky Cover Probabilities

<u>Initial Time</u>	<u>Starting Condition</u>	<u>Array # 0 hours</u>	<u>Array # +3 hours</u>	<u>Array # +6 hours</u>	<u>Array # +9 hours</u>	<u>Array # +12 hours</u>
1700 L	0-3/8 4-8/8	1	2 3	4 5	6 7	8 9

2000 L	0-3/8 4-8/8	10	11 12	13 14	15 16	

2300 L	0-3/8 4-8/8	17	18 19	20 21		

0200 L	0-3/8 4-8/8	22	23 24			

0500 L	0-3/8 4-8/8	25				

category, sky cover probabilities. These are the probabilities for the occurrence of less than or equal to 3/8 total cloud cover. These probabilities are used to determine whether or not the sensor has a cloud free line of sight. As shown in Table IV, the sky cover probabilities for each site are inserted into an array which requires 25 inputs for each site. The probabilities are used to simulate cloud cover conditions from 1700 hours to 0700 hours local time. The input values under the 0 hours column are the unconditional probabilities of less than or equal to 3/8 sky cover at the initial time. The remaining

inputs are the conditional probabilities of less than or equal to 3/8 sky cover given the initial sky cover condition and starting time.

Finally, the seventh input category is the air-and space-based sensor location parameters. These inputs are used if the user wishes to evaluate a user selected sensor system which includes air-or space-based sensors. As shown in Table III, there are six inputs in this category. These include the sensor type and the orbital parameters for a space-based sensor or the latitude (coordinate theta) for an air-based sensor.

Basic Physical Principles

The fundamental aspects of orbital mechanics and sensor operation as used in EOBASE are described below.

Orbital Mechanics. The EOBASE program employs the same techniques and principles of orbital mechanics as utilized in the HELBASE simulation (Refs 17 and 18). As stated in Chapter I as an assumption, the techniques used here assume a simple two body problem with the satellite acting as a point mass, and the earth is regarded as a simple sphere of radius 6378.145 kilometers.

The coordinate reference system employed in the model is the geocentric-equatorial system. This system has its origin at the earth's center, and it is essentially fixed with respect to the stars. Figure 1 depicts this reference system.

Sensor Operation. Both of the two classes of electro-optical sensors which can be evaluated with EOBASE have to have two conditions satisfied before they can be used for satellite tracking. First, the sensors have to be located either in space or on the night side of the

- Ω LONGITUDE OF ASCENDING NODE
- v TRUE ANOMALY AT EPOCH
- u ARGUMENT OF PERIGEE
- i INCLINATION

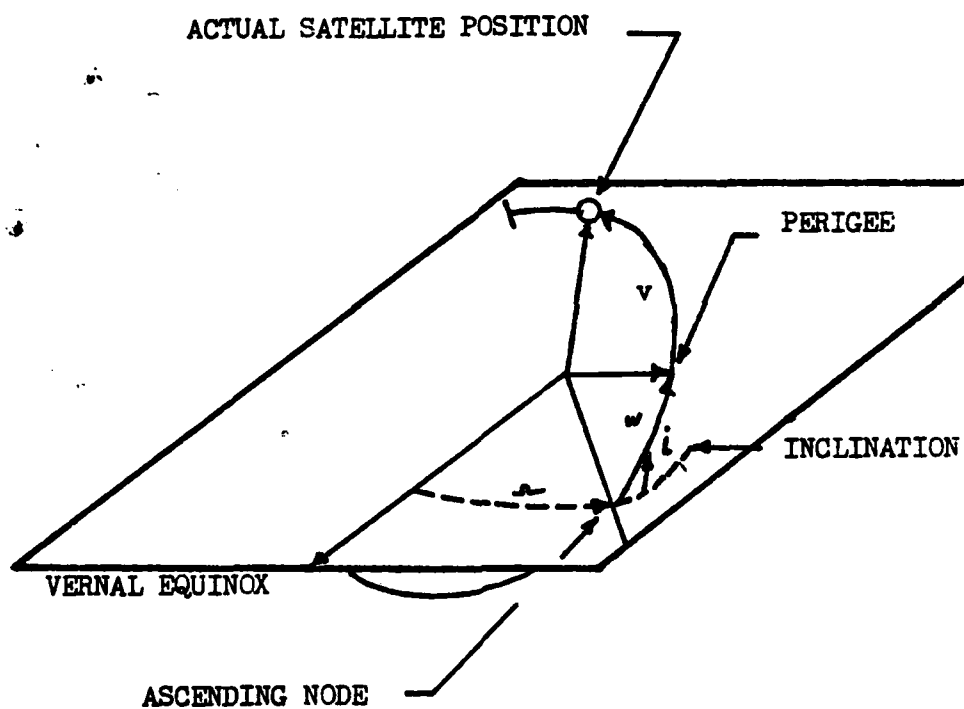


Figure 1. Geocentric equatorial reference.

clear line of sight to the target. Second, the sensor cannot operate in the presence of cloud cover or with the earth between it and its target.

Once these preconditions have been satisfied, the differences between the sensors become important. The sensor class of primary interest here (like the GEODSS system) uses the sunlight reflected by the target satellites to detect them. The amount of sunlight which the targets reflect is dependent upon the relative positions of the sun, the target, and the sensor. This relationship is illustrated in Figure 2. For the sake of simplicity, all of the targets in the EOBASE simulation are modeled as cylinders with an earth center orientation. In addition, the irradiance of the sun (H_0) is assumed to be constant throughout the orbits of the target satellites. In this case, the irradiance of the light reflected by the target at the sensor can be calculated if the following is known (Ref 19:12, 15, and 84-86): the distance between the target and the sensor (R), the sensor aspect angle (α), the solar aspect angle (β), the phase angle (ϕ), the reflectivity of the cylinder (ρ_c) and the endplate (ρ_p), and the projected area of the cylinder (A_c) and the endplate (A_p). The following formulas are employed.

$$H_p = \frac{H_0 \rho_p A_p \cos \alpha \cos \beta}{\pi R^2}$$

$$H_c = \frac{H_0 \rho_c A_c \sin \alpha \sin \beta (\sin \theta + [\pi - \theta] \cos \theta)}{4 \pi R^2}$$

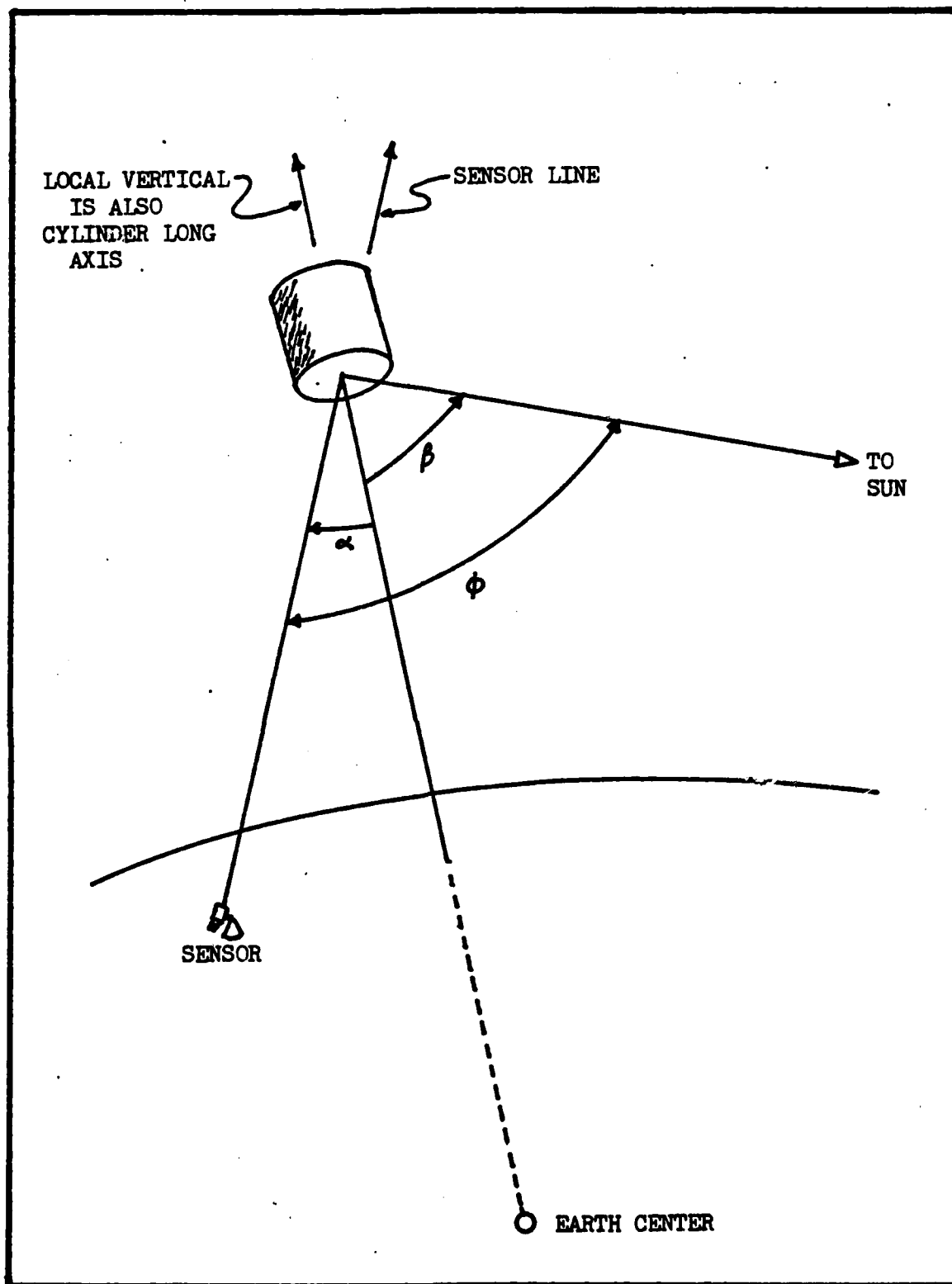


Figure 2. Sunlight reflection geometry.

where

H_p = the irradiance at the sensor due to the end plate

H_c = the irradiance at the sensor due to the cylinder

$$\theta = \cos^{-1} (\cos \phi - \cos \alpha \cos \beta \sin \alpha \sin \beta)$$

The final value is computed in units of visual magnitudes of light.

$$MAG = M_{v\odot} - 2.5 \log_{10} \left[\frac{H_p + H_c}{H_o} \right]$$

where

MAG = the visual magnitude of the target at the sensor
number

$M_{v\odot}$ = the visual magnitude of the sun at the target
= -26.78 M_v

The visual magnitude of light from the target can then be compared with the amount of light that the sensor needs to detect the target. If the number is low enough (the smaller the number the more light), then the sensor can detect the target.

The second sensor which can be considered using EOBASE detects satellites from their thermal emissions in the long wavelength infrared (LWIR) range of 8 to 14 micrometers. Unlike the reflected sunlight employed by the previous sensor, the emissions come directly from the satellite itself, and their intensity and wavelength are primarily

dependent upon the temperature of the satellite. The emissions can be modeled using Planck's Blackbody Radiation Law (Ref 20:Ch 1).

As indicated in Chapter I in the introduction, some experimental work has been done with this kind of sensor using a U-2 aircraft (Ref 3). However, the sensitivity of this system was not great enough to detect deep space satellites (Ref 3:Ch 3). The system ultimately was limited by background infrared emissions from the atmosphere and the telescope itself. Nonetheless, this type of sensor has been included as an EOBASE sensor option since it is conceivable that further improvements in detector technology could make it feasible to use it for deep space satellite tracking. Such a breakthrough, the development of the vidicon imaging tube, has been extremely important in the development of visible wavelength sensors for satellite tracking (Ref 21). The extremely small image cell diameters or detector spot sizes which can be achieved with these tubes are to a great extent responsible for the high sensitivity of the GEODSS system.

So, the long-wavelength infrared sensor is included in EOBASE with two assumptions. First, the sensor will be either in a space-based or air-based mode. The ground-based mode will be excluded because of the relatively much higher sky background at lower altitudes and because the presence of water vapor prohibits cooling the optics to liquid nitrogen temperatures. Second, it will be assumed that the sensor has sufficient sensitivity to track target satellites in geosynchronous orbits in a reasonable time frame.

Because of the effect that the earth's atmospheric radiance has upon the LWIR Air-Based Sensor, an effort has been made to have EOBASE account for the loss of sensitivity as the zenith angle increases with

respect to the sensor's line of sight to the target satellite. Therefore, EOBASE calculates the irradiance at the sensor due to both the target satellite and the atmosphere. The formula used to determine the irradiance at the sensor (ϵ_T) from the target is based upon the point source approximation (Ref 22:App 5)

$$\epsilon_T = \frac{L_{\lambda}(\bar{\lambda}) a^2 \tau_A \Delta\lambda}{r^2}$$

where

$L_{\lambda T}(\bar{\lambda})$ = the radiance of the target at the middle of the sensor's spectral band

a = the radius of the target

τ_A = the average atmospheric transmittance

$\Delta\lambda$ = the bandwidth of the sensor

r = slant range to the target

The irradiance at the sensor on a single detector field of view due to the atmosphere (ϵ_B) is calculated by (Ref 20):

$$\epsilon_B = \Omega_1 L_{\lambda A} \tau_A$$

where

Ω_1 = the field of view of a single detector

$L_{\lambda A}$ = the radiance of the atmosphere over the spectral band of the sensor

Once the irradiance at the sensor is known, the current response both due to the target irradiance and due to the atmosphere can be calculated (Ref 20). The current (i_T) produced by the target can be calculated by:

$$i_T = \frac{S_R \eta(\bar{\lambda}) \epsilon_T e}{hc/\bar{\lambda}}$$

where

S_R = the area of the receiving optics

$\eta(\bar{\lambda})$ = quantum efficiency of the detector at the mean wavelength of the sensor's spectral band

h = Planck's constant

= 6.63×10^{-34} Watts second⁺²

c = speed of light

= 3.00×10^8 meters second⁻¹

$\bar{\lambda}$ = the mean of the sensor's spectral band

e = the charge on an electron

= 1.6×10^{-19} Coulombs

The current response (i_B) due to the atmospheric irradiance is:

$$i_B = \frac{S_R \eta(\bar{\lambda}) \epsilon_B e}{hc/\bar{\lambda}}$$

Once the current response is known, the signal to noise ratio (S/N), assuming there is no source of noise other than atmospheric radiance, can be calculated by:

$$S/N = \frac{i_T/e \sqrt{\tau D}}{\sqrt{i_T/e + i_B/e}}$$

If the signal to noise ratio is sufficiently large, then the target can be tracked.

Submodel Descriptions

The ten major subroutines associated with the program EOBASE are SPHERE, CART, TARGET, SUNPOS, SIGHT, VISBLE, SLWIR, SIDEN, CLOUD, and TRACK. Each is briefly described in this section. Expanded descriptions of underlying models for these subroutines are found in the next chapter.

SPHERE and CART. When EOBASE is used to select the most efficient sensor system, SPHERE and CART are called to generate a sphere of operations for each sensor type. Together these subroutines calculate and store 410 points that are spread uniformly over this sphere of operations which is fixed in the geocentric equatorial coordinate system. Note that the radius of each sphere is defined by the altitude of the sensor for which it is calculated. See Figure 3 for a functional flow of SPHERE.

TARGET and SUNPOS. TARGET is used to randomly place all selected targets into their proper orbits and store the cartesian coordinates of their locations. The TARGET algorithm uses a random selection from a uniform (0,2 π) distribution for the mean anomaly, a root solution

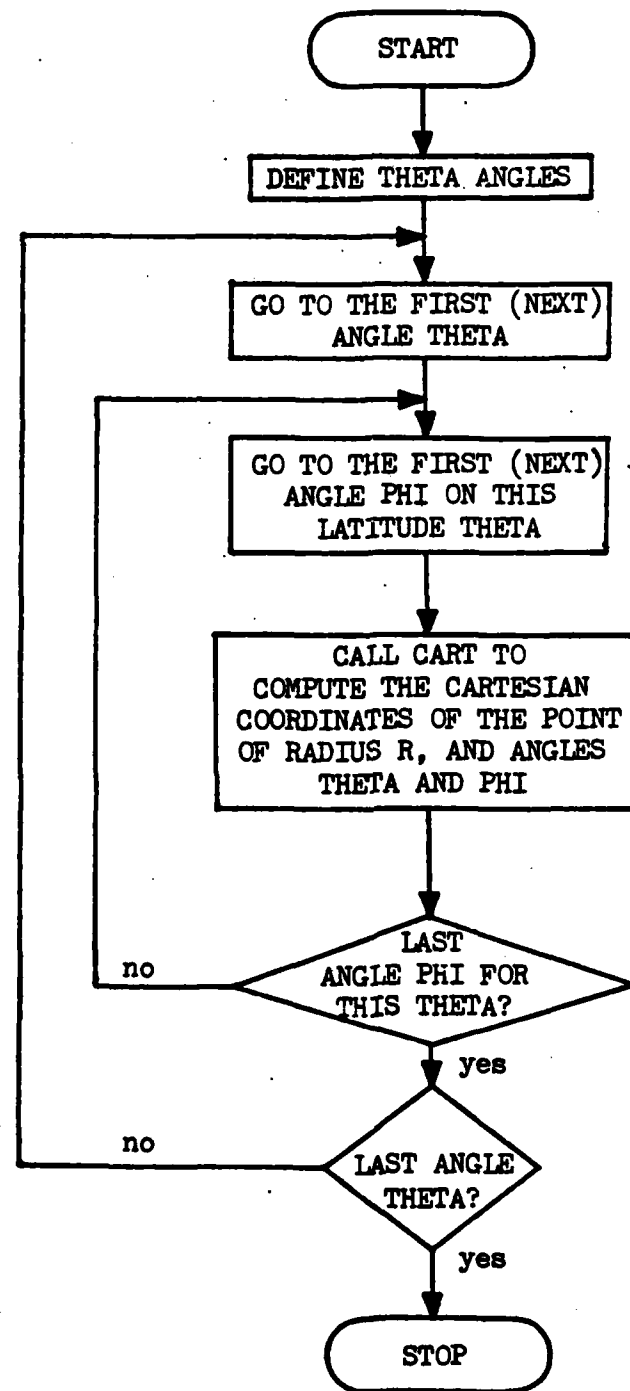


Figure 3. Submodel SPHERE logic diagram

to Kepler's equation for the eccentric anomaly, and a conversion to the true anomaly. In addition, TARGET calls subroutine SUNPOS to randomly place the position of the sun with respect to the latitude and longitude that is oriented over the earth. See Figure 4 for the functional flow of TARGET.

SIGHT. The purpose of SIGHT is to determine whether or not a target can be tracked by a particular sensor from a given location. SIGHT's answer is yes or no. If the target cannot be tracked, SIGHT returns the calling program a score of 0.0. Conversely, if the target can be tracked, SIGHT returns a value of 1.0. SIGHT uses the subroutine VISBLE or the subroutine LWIR. See Figure 5 for the functional flow of SIGHT.

VISBLE. Subroutine VISBLE is used to determine if the amount of visible radiation from the sun reflected to a particular sensor is sufficient for the target to be detected. For the sake of simplicity, the algorithm used in VISBLE assumes that the target is a simple earth center oriented cylinder. See Figure 6 for the functional flow of VISBLE.

SLWIR. The purpose of subroutine SLWIR is to determine if a LWIR sensor can track a target satellite. SLWIR assumes the target is a Lambertian surface at 300 degrees Kelvin with one square meter of surface area presented to the sensor. See Figure 7 for the functional flow of LWIR.

SIDEN. Subroutine SIDEN uses the subroutines TARGET and SIGHT to generate an "average target system sighting efficiency" value for each point on each sensor type's sphere of operations. Subroutine SIDEN

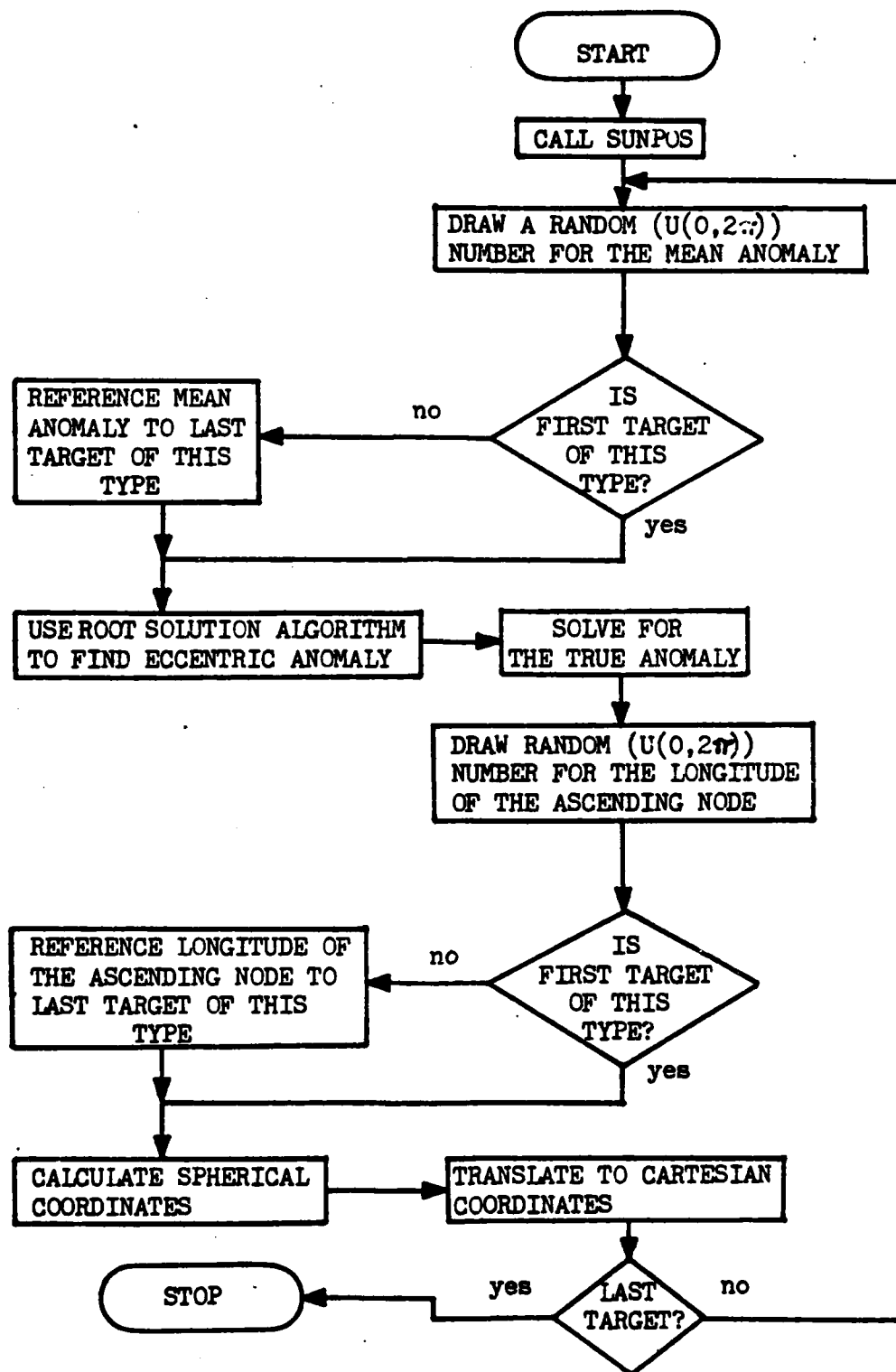


Figure 4. Submodel TARGET logic diagram.

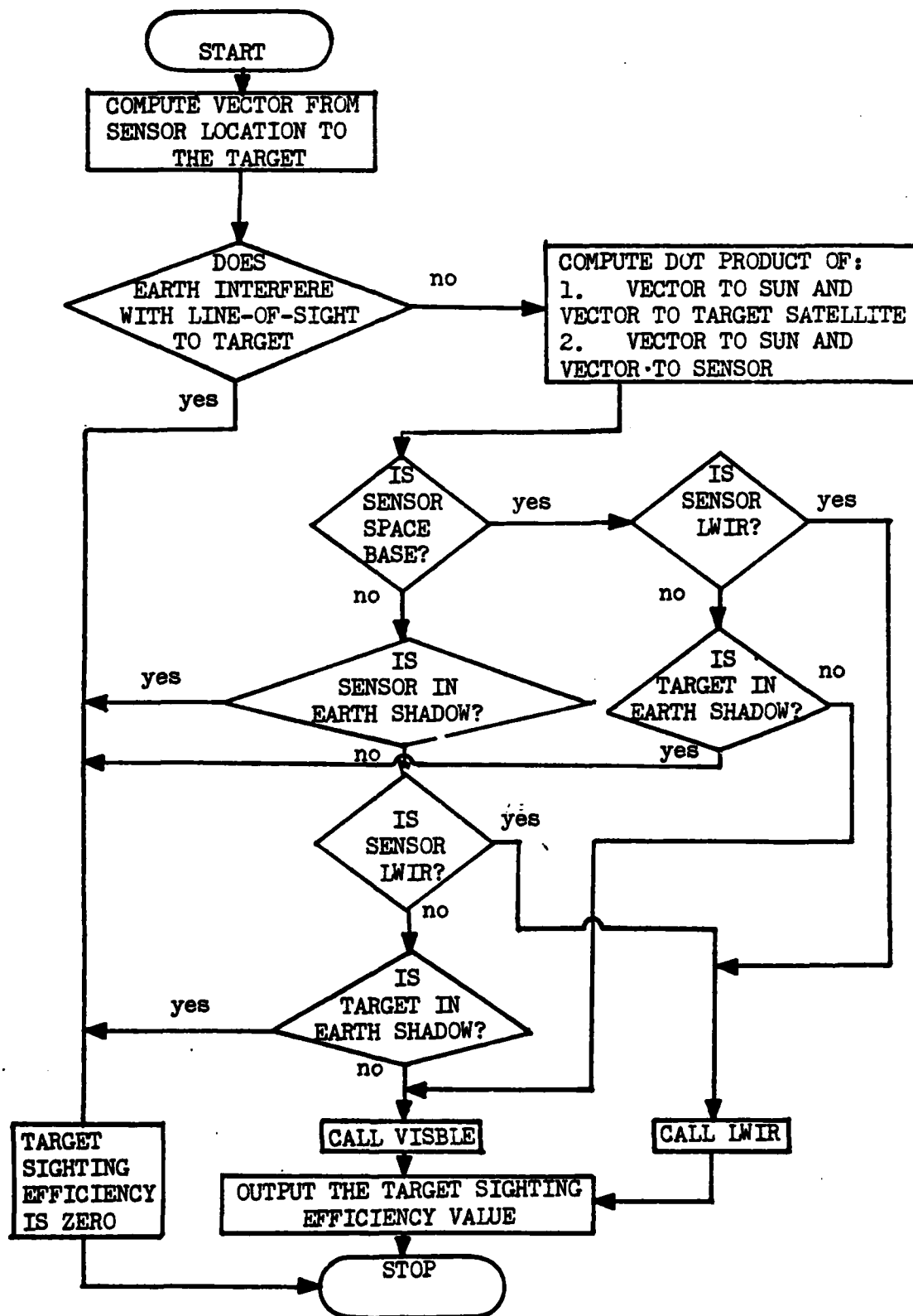


Figure 5. Submodel SIGHT logic diagram.

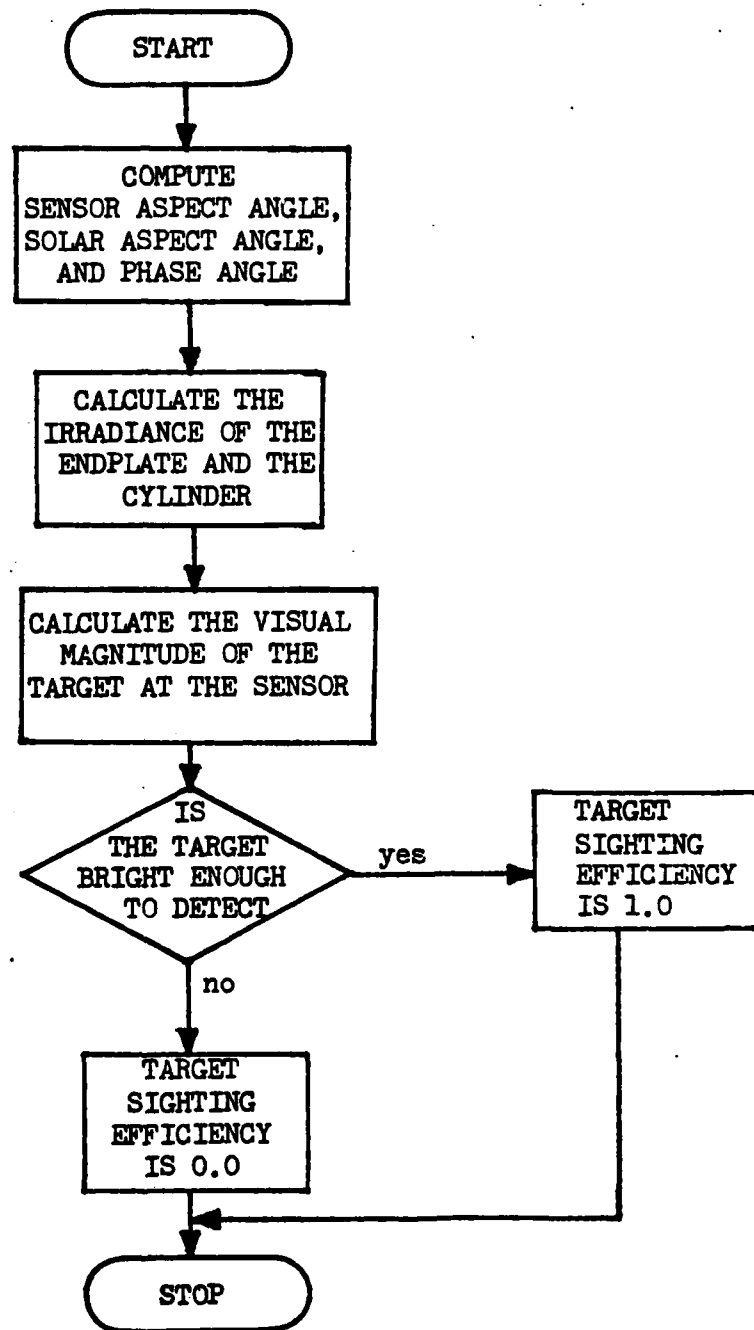


Figure 6. Submodel VISBLE logic diagram.

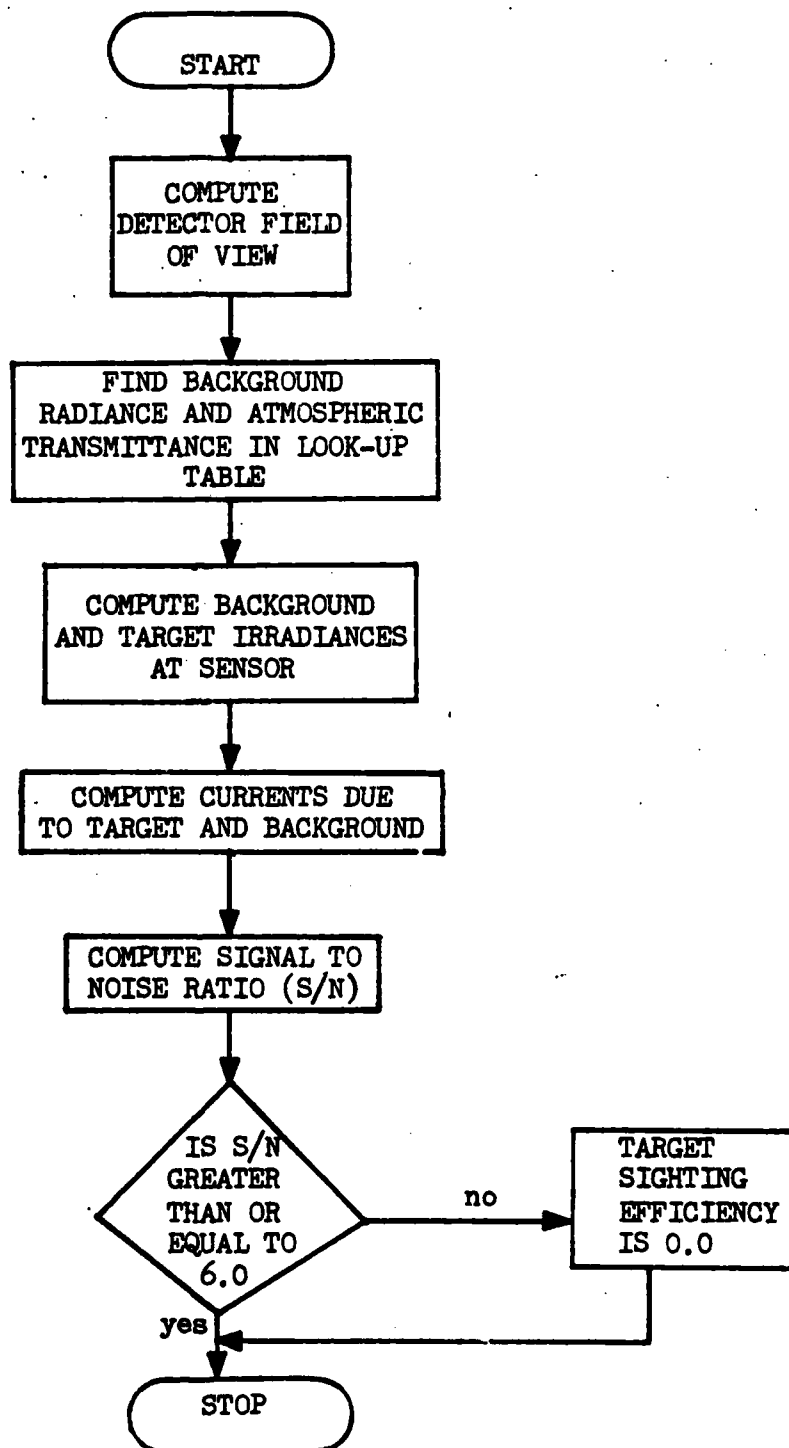


Figure 7. Submodel SLWIR logic diagram.

does this by having TARGET randomly place the targets into their orbits and then it uses SIGHT to score each point on each sphere of operations with respect to each target. See Figure 8 for the functional flow of SIDEN.

CLOUD. The purpose of subroutine CLOUD is to simulate the amount of cloud cover at ground-based sensor site locations and then determine if the sensor is still functional. CLOUD is called only when preselected ground-based sensor site locations have been entered into the program. See Figure 9 for the functional flow of CLOUD.

TRACK. Subroutine TRACK is the portion of the EOBASE model in which the simulation takes place. TRACK uses either the user supplied sensor system or the sensor system selected by EOBASE to attempt tracking the target system within the mission completion time. TRACK uses subroutines TARGET, SIGHT, and CLOUD. See Figure 10 for the functional flow of TRACK.

Main Program EOBASE

The main program, EOBASE, acts as a controlling program. EOBASE is divided into three sections, an input section, an optimization section, and a confidence section. The optimization and confidence sections of EOBASE, together with its various subroutines, provide the EOBASE with the capability to select the most efficient sensor system from the input sensor types to accomplish a given mission. In the event the user wishes to evaluate a preselected weapons system, the optimization section is bypassed and TRACK is called the number of times requested. See Figure 11 for a functional flow of EOBASE.

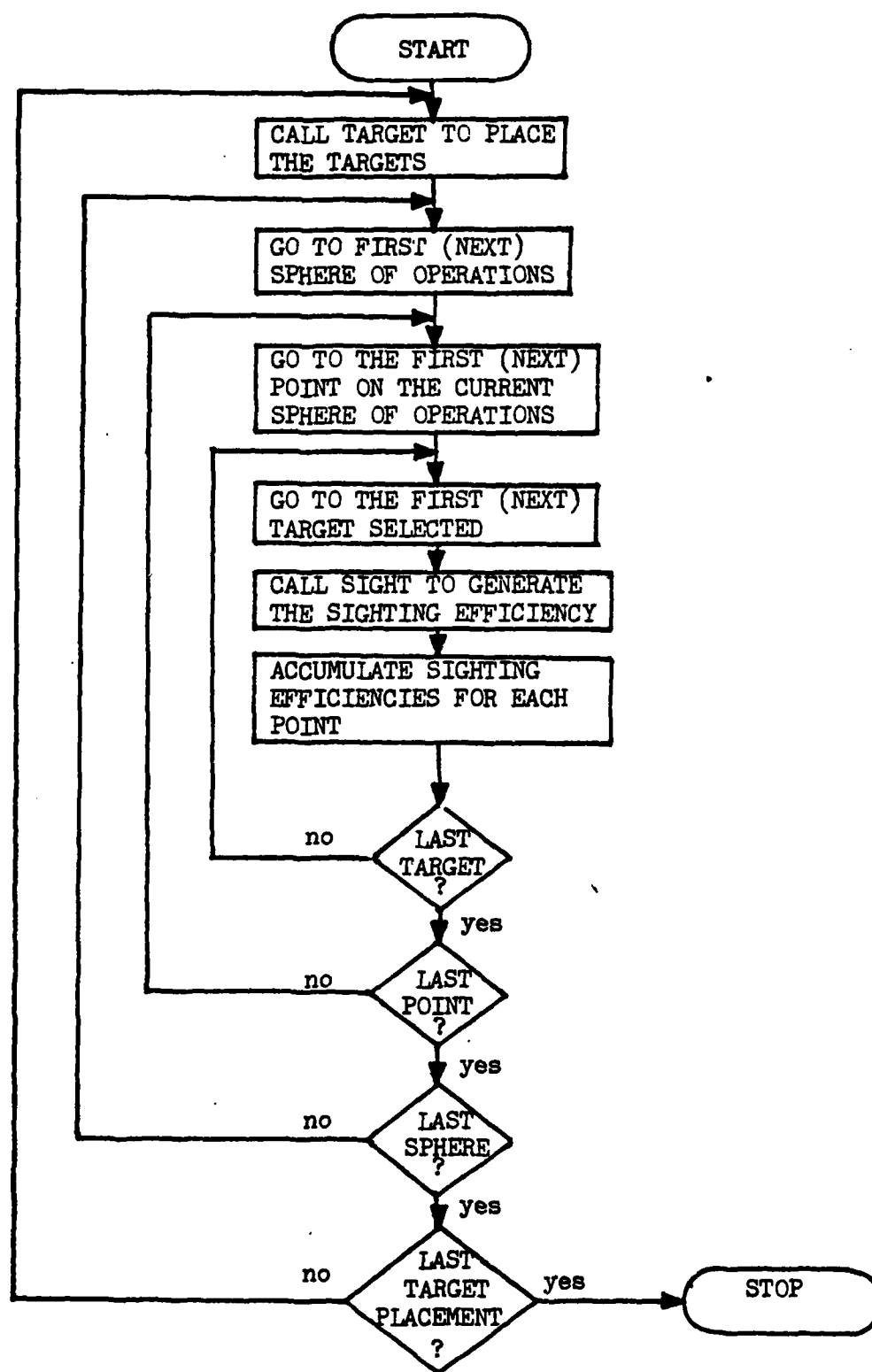


Figure 8. Submodel SIDEN logic diagram.

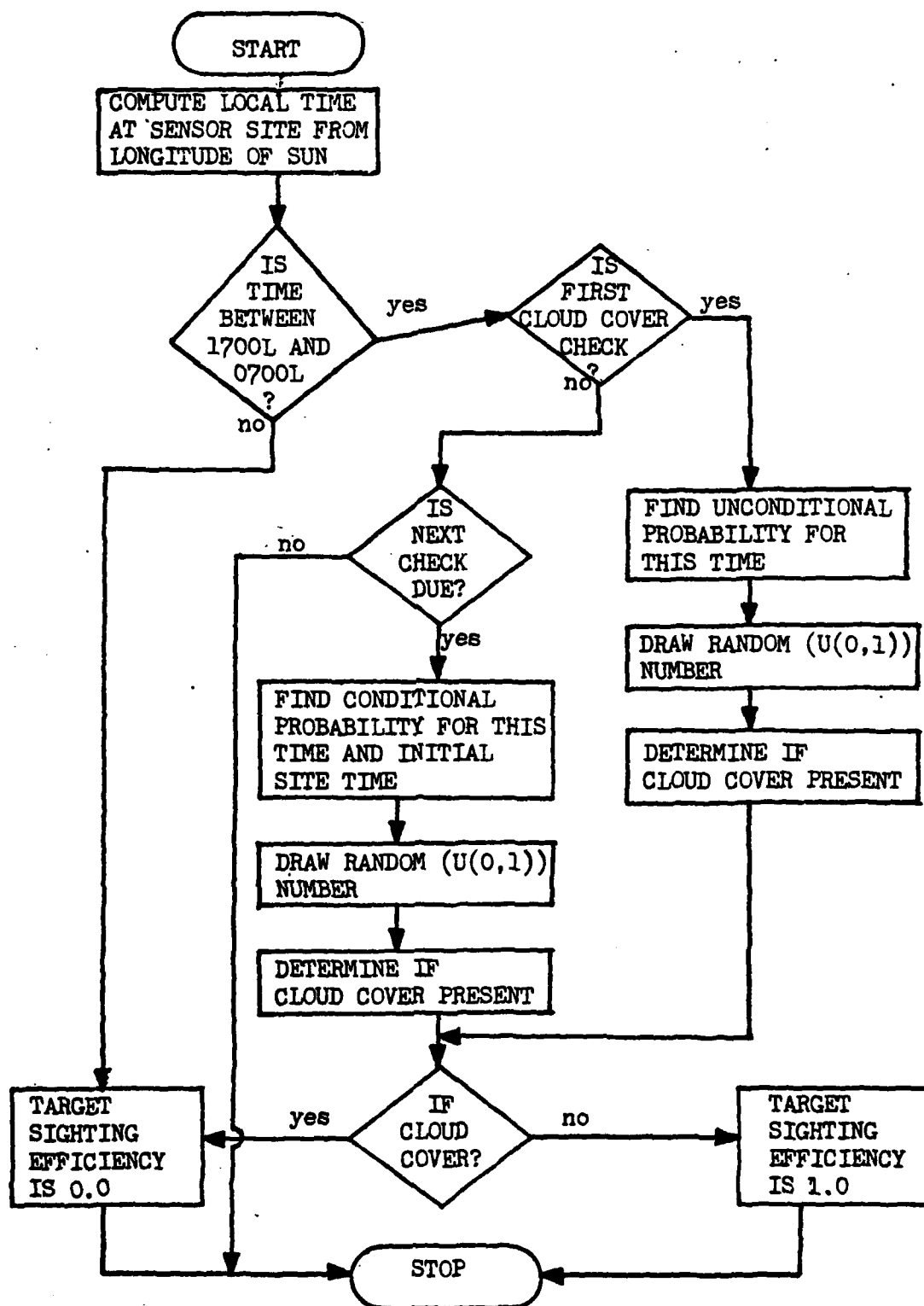


Figure 9. Submodel CLOUD logic diagram.

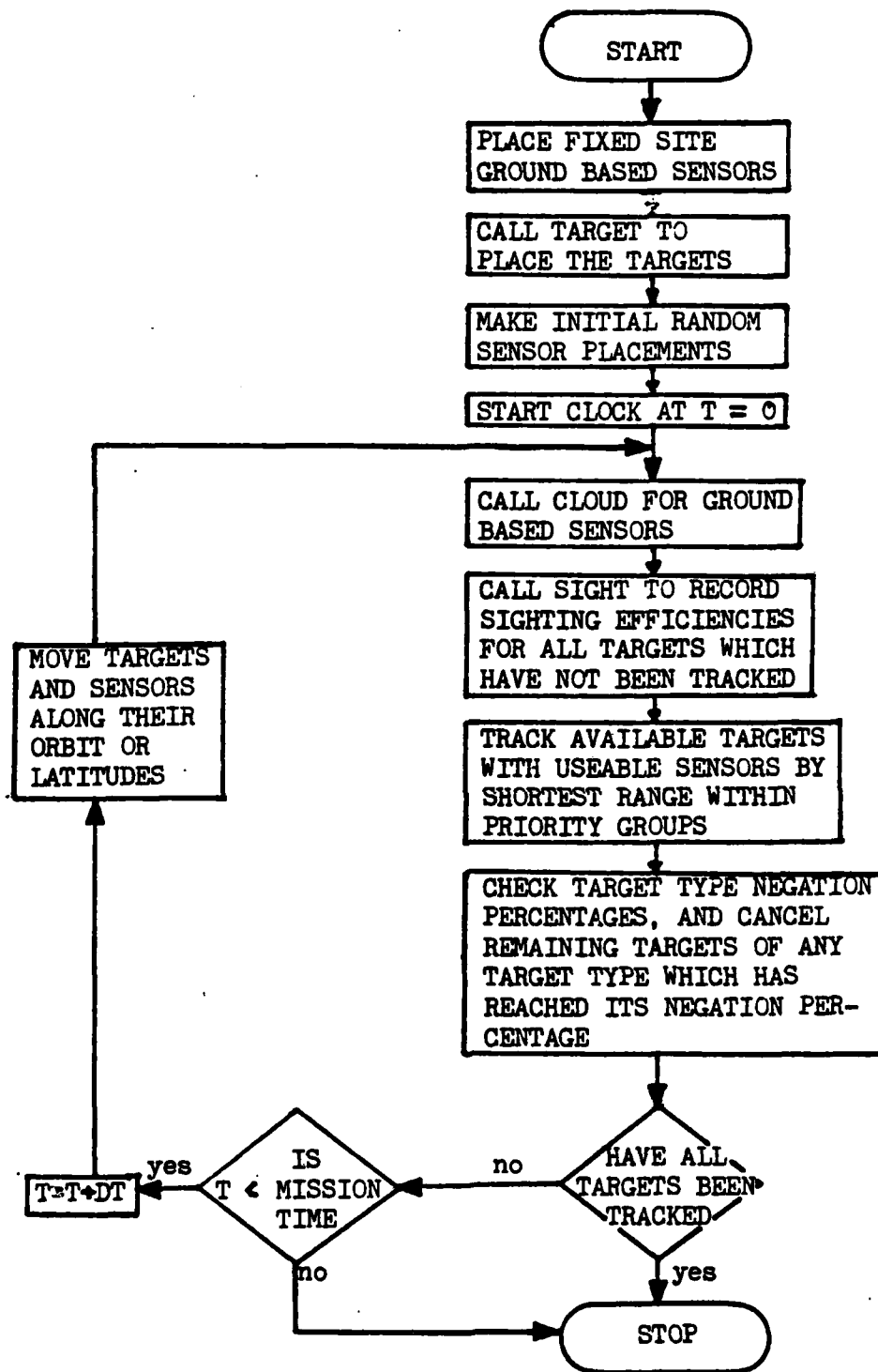


Figure 10. Submodel TRACK logic diagram.

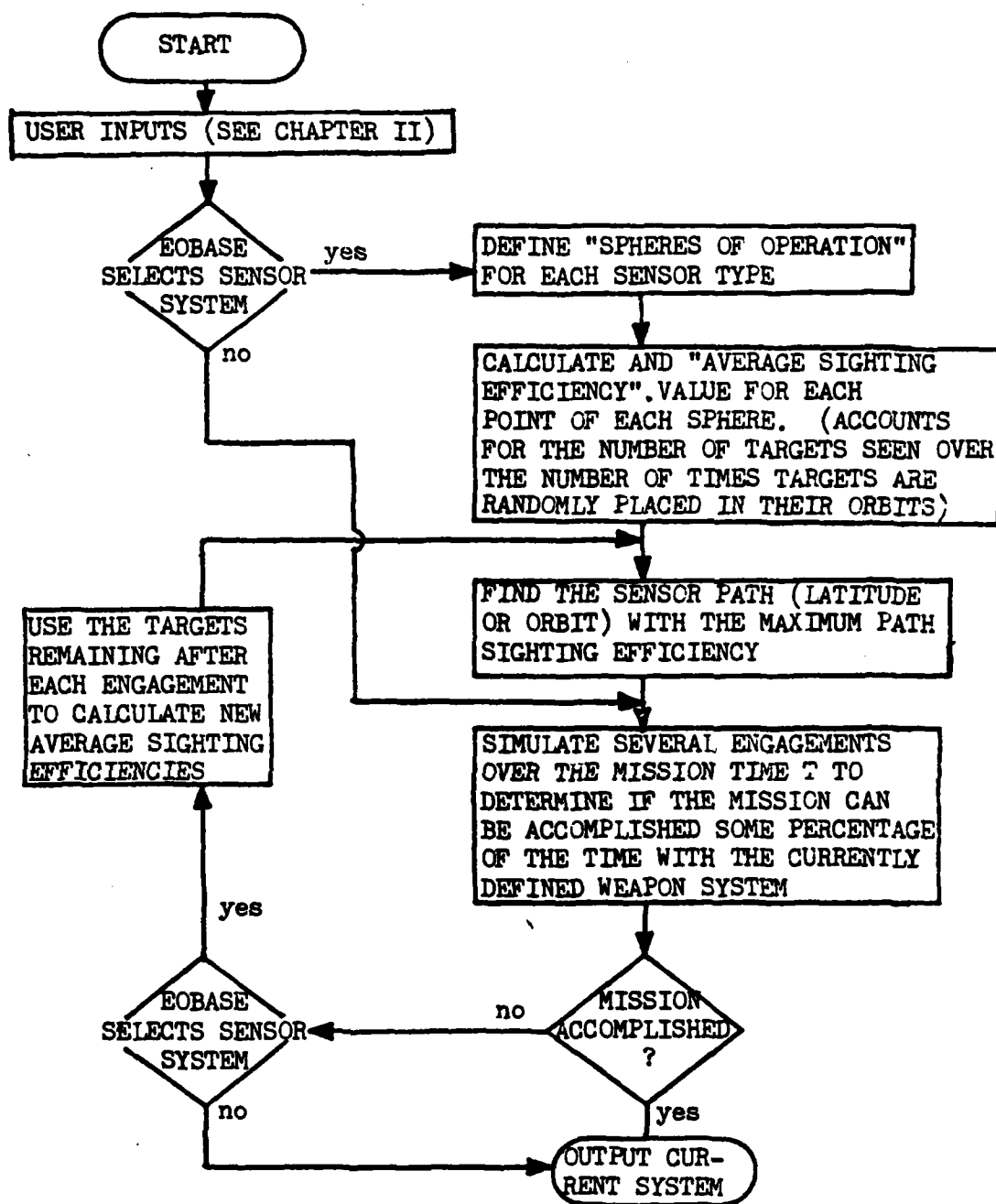


Figure 11. EOBASE function flow.

Input Section. This section of EOBASE reads in all user inputs and writes them back for verification. In addition, SPHERE is called to generate the sphere of operations for each sensor type when the user directs EOBASE to select the most weapons system.

Optimization Section. The purpose of this section of the program is to place the first (next) best sensor in the most efficient orbit or latitude. The average target system sighting efficiencies, generated by SIDEN, are used to decide the first (next) best sensor/path choice. SIDEN is called each time a sensor is placed.

Confidence Section. The confidence section of the program runs TRACK several times to determine if the selected sensor system can meet mission requirements. If EOBASE is being used to select the most efficient sensor system, the percentage of time the selected sensor meets mission requirements is compared with some user selected percentage. In the event that the user selected percentage is higher, SIDEN is called, and then control is passed to the optimization section and another sensor is added to the sensor system. Otherwise, EOBASE writes out the final selected sensor system. If the user wishes to use EOBASE to evaluate a preselected sensor system, the confidence section is used to run TRACK the requested number of times.

Summary. The purpose of the EOBASE simulation program is twofold; the program can be used to select the most efficient sensor system which will meet mission requirements given no knowledge of the time of the tracking sequence initiation, or the program can be used to evaluate a preselected system. This chapter has included a functional description of EOBASE and its submodels, and it is concluded with a

table summarizing these submodels, their functions, inputs, and outputs see Table V). Chapter III provides an explanation of the concepts employed by each of the EOBASE submodels, and it describes the efforts which were made to validate the EOBASE program.

TABLE V
Summary of Submodel Functions

<u>Submodel</u>	<u>Function</u>	<u>Inputs</u>	<u>Outputs</u>
SPHERE	Calculate and store cartesian coordinates of points on a sphere of operations	Radius	Cartesian coordinates of a sphere of operation
TARGET	Place targets randomly into orbits	Target type selections	Cartesian coordinates of all targets
SUNPOS	Place sun above earth	Sun type selection	Unit vector to and longitude of sun
SIGHT	Determines feasibility of sighting target	Target, sun, and sensor locations, sensor type, and target type	Target sighting efficiency
VISBLE	Calculates visual magnitude of target at sensor	Sensor type, vectors to target from origin and sensor, vector to sun, and range to target	Target sighting efficiency
SLWIR	Calculates signal to noise ratio for target irradiance versus background irradiance	Sensor type, zenith angle, range to target	Target sighting efficiency
SIDEN	Establishes the target system sighting efficiency for each point on each sphere of operations	Sensor type, target type, sun type, and spheres of operation	Values of target system sighting efficiency

(continued)

TABLE V (continued)

Summary of Submodel Functions

<u>Submodel</u>	<u>Function</u>	<u>Inputs</u>	<u>Outputs</u>
CLOUD	Simulates effect of cloud cover on ground based sensor	Longitude of sun, longitude of sensor, sky cover probabilities	Target sighting efficiency
OPTIMIZE	Select most efficient sensor orbit or latitude to place first (next) sensor	Average target system sighting efficiencies	Sensor system locational parameters
TRACK	Engage targets in accordance with mission data	Sensor system, target system, mission data	Number of targets tracked and target system tracking time

III Model Development

The previous chapter provided a functional description of EOBASE and its submodels. This chapter contains a description of the concepts employed by each of the various submodels described in Chapter II. In addition, the efforts made to validate EOBASE are presented.

Sphere of Operations (Subroutine SPHERE)

A "sphere of operations" is a stationary sphere in the celestial reference system, and it is used to represent all of the possible basing locations for a particular sensor type (see Refs 17 and 18 for a more complete explanation).

Placement of Points. EOBASE uses 410 points to define a sphere of operations. This number is the same as chosen for HELBASE (Ref 18:Ch 2, 29), and it was chosen as a tradeoff between accuracy run time and computer core memory requirements. The 410 points are distributed among 19 latitudes starting with the equator and heading north and south in 10 degree increments. The number of points on each latitude is the number of points required to achieve the closest approximation to a 10 degree arc spacing (see Table VI). Subroutine SPHERE calculates the cartesian coordinates for each of the 410 points for each sphere of operations.

Ground and Air Basing Modes. The sphere of operations for ground based sensors is the mean surface of the earth. For air-based sensors,

TABLE VI

Number of Points on Each 10 Degrees of Latitude

<u>True Latitude (degrees)</u>	<u>Number of Points</u>
0	36
10	35
20	34
30	31
40	27
50	23
60	18
70	12
80	6
90	1

Note: The southern hemisphere is a mirror image of the northern hemisphere.

the sphere of operations is 21 kilometers (70,000 feet) above the mean surface of the earth. The choice of this altitude is due to the existence of a minimum wind velocity at this altitude (Refs 11 and 23). A typical example of this minimum is shown in Figure 12. As noted by Petrone and Wessel (Ref 11), although a considerable penalty in weight and complexity is exacted at this altitude, the required power is much less (except of course at altitudes near sea level). As a first approximation, drag (power consumption) and lift (power available) are proportional to density while power consumption increases as the cube of the velocity; thus a minimum in the velocity altitude curve represents an optimal point for operations.

The possible alternatives for positioning a sensor in these modes are limited to the set of latitudes from 60 degrees north through 60 degrees south spaced in 10 degree intervals. The position of both ground-and air-based sensors is considered fixed with respect to the

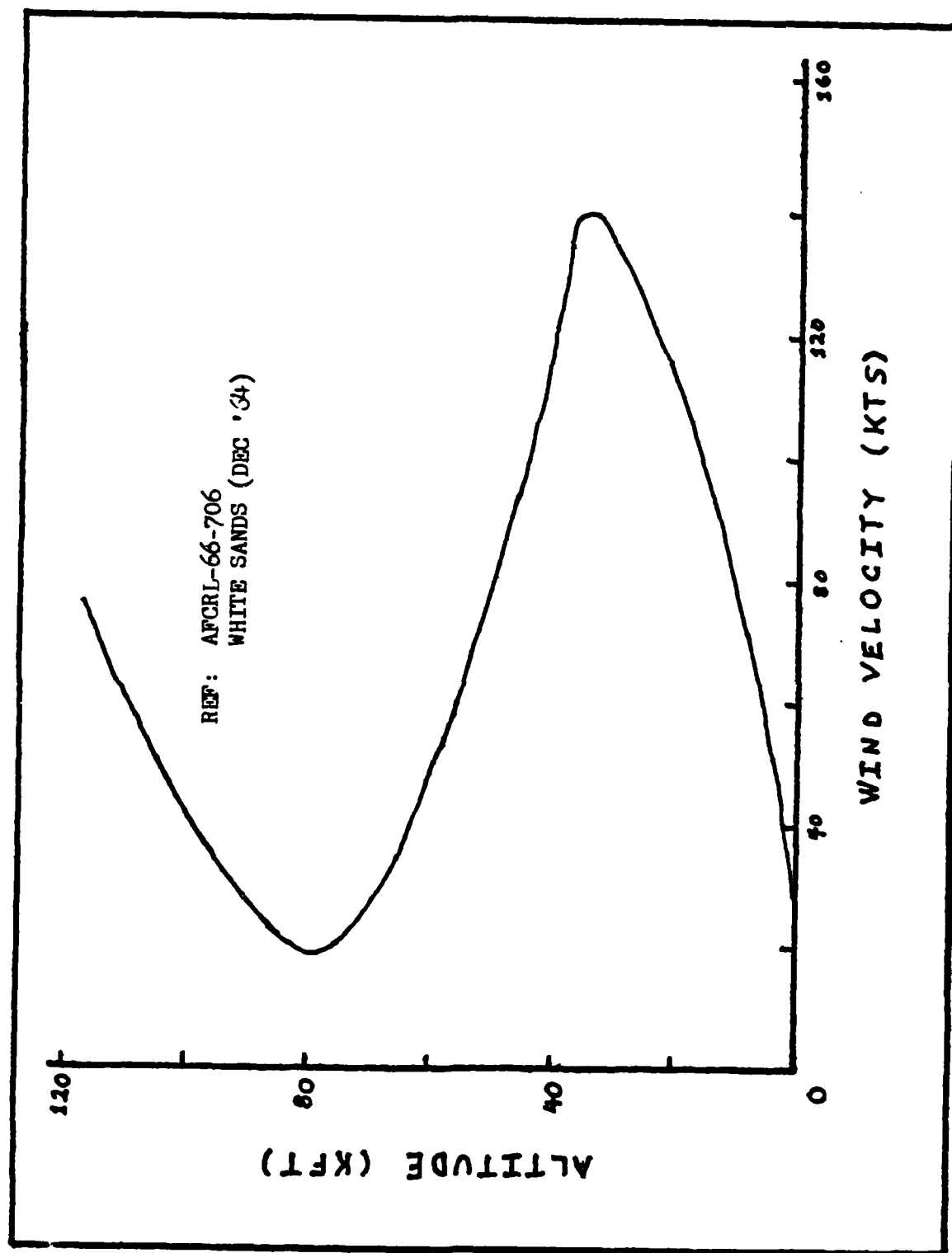


Figure 12. Typical wind velocity profile.

earth, however, since the earth rotates over time, selection of a particular longitude is not necessary. So, the sighting efficiency for a latitude is approximated using the average sighting efficiency of the set of evenly spaced points at that latitude.

Space-Basing Mode. The space-basing mode is also available in EOBASE. The sphere of operations for a sensor type in the space-based mode is defined by a sphere at some given radius from the earth's center. Since orbits precess at different rates based upon their altitude, inclination, and eccentricity, the longitude of the ascending node for a sensor is randomly chosen by EOBASE. The inclination of an orbit is the only parameter which must be selected. The inclinations considered are 0, 15, 25, ..., 85, and 90 degrees. Each inclination alternative is defined by the points which lie over a latitude which is less in degrees from the equator than the inclination of the orbit. These points are used to model the band swept out by an orbit as it precesses around the earth in time. The average of the sighting efficiencies for all the points which fall within the band is used to describe the sighting of the orbit.

TARGET and SUNPOS

Subroutine SUNPOS, when called by TARGET, uses the user input SUNTYP to determine how to place the sun over the earth. SUNTYP can have the values 1, 2, 3, or 4. With the values 1, 2, or 3, the latitude over which the sun is oriented is fixed. The value 1 causes the sun to be placed over the equator, 2 at 23 degrees north, and 3 at 23 degrees south. The value of 4 causes the sun to be randomly placed between 23 degrees north and 23 degrees south. The procedure for

randomly placing the sun assumes a circular orbit for the earth around the sun so that the number of days since the last vernal equinox can be randomly chosen from a uniform (0,365.25) distribution. Then the angle between the earth at its randomly chosen position and its position at the vernal equinox (relative to the sun) can be calculated by:

$$\theta = \frac{2\pi \text{ rad.}}{365 \text{ days/year}} \text{ number of days since last vernal equinox}$$

From θ the declination angle (δ) to the sun, that is the angle between the earth's equatorial plane and the vector to the sun, can be calculated as shown below (Ref 24).

$$\delta = \sin^{-1} (\sin \epsilon \sin \theta)$$

where

$$\begin{aligned} \epsilon &= \text{the angle between the earth's equatorial plane and the} \\ &\quad \text{ecliptic plane} \\ &= 23 \text{ degrees} \end{aligned}$$

If a spherical earth is assumed, this last calculation provides the latitude over which the sun resides since latitude and declination angle then become equivalent concepts. In all four cases or sun types, the longitude is randomly selected from a uniform (0,2 π)

distribution. Once the latitude and longitude are chosen, SUNPOS then calculates a unit vector to the sun.

Subroutine TARGET itself uses the orbital parameters of the selected target satellites to randomly place them into their orbits. Two orbital parameters are randomly selected, mean anomaly (M) and the longitude of the ascending node (Ω). Both are randomly drawn from a uniform $(0, 2\pi)$ distribution. In order to position the satellite, the mean anomaly is converted to the true anomaly using the "mean anomaly to true anomaly technique" (Ref 25:185). M is related to the eccentric anomaly by:

$$M = E - e \sin E$$

where

e = the orbital eccentricity

A numerical technique is used to find E . Then E is used to calculate the true anomaly, V , by:

$$V = \cos^{-1} \left[\frac{e - \cos E}{e \cos E - 1} \right]$$

Note that the numerical solution procedure is not necessary where $e = 0$, since in this case $M = E = V$.

SIGHT

Subroutine SIGHT is used to determine the feasibility of tracking a target at one point by a sensor at another given location. Several

checks are made by Subroutine SIGHT. The first check is for line-of-sight interference with the earth. Next, in the case of ground and air based sensors, a check is made to determine if the sensor is on the dark side of the earth. Then, in the case of sensors employing visible light, a check is made to determine if the target is in the earth's shadow. Finally, Subroutines VISBLE (for visible light detecting sensors) and SLWIR (for LWIR detecting sensors) are used to determine if the quantity of light from the target reaching the sensor is sufficient for detection of the target to occur. If any of these checks are violated, the subroutine returns a sighting efficiency value of 0.0 for negative acquisition. However, if all the checks are passed, a value of 1.0 is returned which indicates that tracking of the target is feasible.

All of these checks are made with vector algebra using the appropriate vectors. For example, whether or not ground and air-based sensors are on the earth's dark side is determined using the inner dot product of the vector to the sensor and the unit vector to the sun. A negative value indicates that the sensor is in the earth's shadow.

VISBLE and SLWIR

The basic principles employed in VISBLE and SLWIR have been previously explained as part of sensor operations in Chapter II.

In the case of the visible light detecting sensors, Subroutine VISBLE is used to calculate the required angles: α , β , and ϕ . These angles together with the target's range from the sensor, and the target's plate and cylinder areas (these areas are stored with the target's orbital parameters) are used by VISBLE to calculate the visual

magnitude of the target at the sensor. The value must be less than the maximum required by the sensor for detection to occur.

Subroutine SLWIR is used in the case of the air-based LWIR sensor. SLWIR is supplied with the angular resolution of the telescope, which it converts to the detector field of view, and the detector dwell time as user inputs under sensor type. Subroutine SIGHT provides the angle from the zenith and the range to the target. Also, SLWIR uses two permanently stored arrays which contain the values for the atmospheric radiance and transmittance for a standard U.S. atmosphere (Ref 26) looking into space from 21 kilometers at zenith angles from 0 to 80 degrees at intervals of 10 degrees. In addition, SLWIR contains the assumptions that the target is a Lambertian surface 1.0 meter in diameter, at 300 degrees Kelvin, with a radiance of $(44/\pi)$ Watts meter⁻² steradian⁻¹ (over the spectral range from 10.5 micrometers to 12 micrometers); that the receiving optics are 1.0 meter in diameter; that the detector efficiency is .25; and the sensor has a bandpass 10.5 micrometers to 12 micrometers. With these assumptions and inputs, SLWIR calculates a signal to noise ratio. If the ratio is greater than or equal to 6.0, the sensor is considered capable of detecting the target satellite.

SIDEN

Subroutine SIDEN is used to calculate an average sighting efficiency for each point on the sphere of operations for each sensor type. These sighting efficiencies are used by the OPTIMIZE to generate path sighting efficiencies for all possible paths for each sensor type.

For one point looking at a target, Subroutine SIGHT returns with S, the sighting efficiency, with a value of 0.0, target not sighted, or

1.0, target sighted. With n targets, the target system sighting efficiency is calculated by:

$$\bar{S} = \sum_{k=1}^n S_k$$

where

S_k = the sighting efficiency of the k_{th} target

Since the targets and the sun are randomly placed, the system sighting concept can be extended for m iterations to achieve greater accuracy by calculating an average target system sighting efficiency (EFF). EFF is calculated by:

$$EFF = \sum_{j=1}^m \sum_{k=1}^n S_{jk}$$

where

S_{jk} = the sighting efficiency of the k_{th} target at the j_{th} iteration

The input variable JCOUNT is equal to j and determines the number of iterations used to calculate EFF.

CLOUD

Subroutine CLOUD is called by Subroutine TRACK to simulate the interference of cloud cover with ground-based sensor operations. The

major assumptions demonstrated in this submodel are: (1) a ground based sensor is relatively ineffectual at greater than $3/8$ sky cover and effective at less than or equal to $3/8$ sky cover, (2) the percentage of total sky cover tends to be either extremely low or extremely high, and (3) the amount of total sky cover does not tend to change radically in less than 3 hour intervals. The basis for the first assumption is the Air Defense Command's (ADCOM) criteria for site selection for the GEODSS sites (Ref 27). ADCOM has used the decimal fraction of less than or equal to $3/10$ sky cover over the tracking period (1800 hours to 0600 hours) as one measure of effectiveness for the candidate GEODSS sites. Previous experience with the Baker-Nunn camera system has found that the average number of tracks submitted is approximately equal to the square of the probability of less than or equal to $3/10$ sky cover times the number of scheduled tracks. The $3/8$ sky cover figure was used in this study for two reasons: (1) sky cover is usually reported in eighths and (2) GEODSS is expected to do 30 to 40 percent better than the Baker-Nunn system (Ref 27). The second assumption is based upon existing data and observations. For example, Lund and Shanklin (Ref 28) report that, of over 12,000 observations, 57 percent were either $0/10$ sky cover or $10/10$ sky cover. The third assumption is also based upon observation. Lund and Shanklin (Ref 29) indicate that initial conditions for a line of sight will on the average persist, whether cloud free or cloudy, for a greater than 3 hour period more than 50 percent of the time

CLOUD operates in the following sequence. First, CLOUD determines the local site time relative to the longitude over which the sun

resides. Then, if the time falls between 1700 hours and 0700 hours local, CLOUD checks the appropriate (see Table IV in Chapter II) unconditional probability for that time relative to a random number selected from a uniform (0,1.0) distribution. Thereafter, based upon the results of the comparison, the initial sky cover condition is established and the appropriate conditional probability is checked at 3-hour intervals.

OPTIMIZE

OPTIMIZE, a section of the main program EOBASE, is used when the user wishes to have EOBASE identify the most efficient sensor system. OPTIMIZE uses the output from SIDEN to search all the allowable paths for the path with the highest "path sighting efficiency." For ground and air-based sensors, a "path sighting efficiency" at each latitude from 60 degrees north to 60 degrees south at 10 degree intervals is calculated. For space-based sensors, there are ten orbital "bands" which are defined by the inclinations of the orbits. As noted in the first section of this chapter, "Spheres of Operation," the coordinates supplied by Subroutine SPHERE are used to model these orbital and latitudinal paths (see Refs 17 and 18 for further details).

TRACK

Subroutine TRACK is used by the confidence section of EOBASE to simulate, at some random starting time, a tracking engagement between the selected sensor and target systems over the mission time. TRACK has dual purposes. If the sensor system is supplied by the user, TRACK merely simulates the number of tracking engagements indicated. If,

however, the sensor system is supplied by EOBASE, then the confidence section of EOBASE uses TRACK to check the adequacy of the sensor system in terms of meeting the mission requirements. If the sensor system is found to be inadequate, then OPTIMIZE is used to select another sensor for the sensor system.

Sensor Placement. Several methods are used to place sensors. These methods differ according to the basing mode of the sensors and according to whether or not the sensor system is user or EOBASE selected. In the case of user selected ground-based sensors, the sensor's coordinates are already specified, latitude, longitude, and altitude. So, TRACK merely converts these coordinates to cartesian coordinates. In the case of air- and space-based sensors, only the latitude or the inclination and the altitude respectively are supplied by the user. Therefore, TRACK must calculate the remaining positioning coordinates. Air-based sensors are placed so that the sensors occupy equally spaced longitudes around the globe. The basing longitude of the first sensor to be placed is randomly chosen, and all the other air-based sensors are located with respect to it. The sensors on the latitude on which the most sensors are located are placed first to prevent a large number of sensors from being clumped together on the same latitude on the same side of the globe. Then the latitude with the next largest number of sensors is considered, and so forth. Space-based sensors are arranged by giving sensors which share the same inclination equally spaced values for the mean anomaly and the same value for the longitude of the ascending node. EOBASE selected ground-based sensors are placed in the same way as air-based sensors.

It should be emphasized that TRACK does not consider geographical features as part of the sensor placement process. Sensors, therefore, may be placed at unrealistic locations such as broad ocean areas or even the Soviet land mass. Nonetheless, the system configuration selected by EOBASE is a good indication of what the relative positions of the sensors should be.

Target and Sensor Movement at Each Δt . All sensors and targets are assigned initial locations at the beginning of each tracking sequence. For targets and space sensors, the initial position in orbit is determined by a random selection of the mean anomaly and the longitude of the ascending node. At each time increment (Δt), the mean anomaly advances (ΔM). This effect is given by:

$$\Delta M = (\mu/a^3)^{1/2} (\Delta t)$$

where

$$\mu = 3.986 \times 10^5 \text{ km}^3/\text{sec}^2$$

a = semimajor axis of the orbit

The new mean anomaly is then calculated and converted to the true anomaly, and from this, the new position is found.

The movement of ground and air-based sensors is due to the rotation of the earth with respect to the fixed geocentric coordinate frame. The effect of the earth's rotation can be determined by adding the rotation of the earth to the previous location; thus moving the sensor to a new longitude L . The new L is calculated by:

$$L = L_o + 2\pi (\Delta t/1440)$$

where

L_o = the previous longitude

EOBASE Validation

The "Towards Validation" methodology proposed by Haley and Gnelber (Ref 30) was used as a guideline for the EOBASE validation process.

The process is divided into four parts: (1) conceptualization, (2) verification, (3) credibility, and (4) confidence.

Conceptualization. The purpose of this step is to determine if the early stages of model development are reasonable and valid. This includes a statement of the model's purpose, degree of accuracy, assumptions, limitations, and a structural framework. These items are contained in Chapters I and II and in this chapter and have been coordinated with experts in the areas of operations research, physics, and astrodynamics.

Verification. There are four parts to the verification process: (1) structural walk-through, (2) verification of technical processes, (3) simulation of predictable states, and (4) testing of stochastic events. The structured walk-through was accomplished for all subroutines as well as the overall EOBASE simulation. See Chapter II for descriptions of the event-path logic flow diagrams for all subroutines. The technical processes associated with EOBASE are discussed in detail in this chapter. Proper coding of these processes was checked by comparing subroutine outputs with hand calculations. In some cases the set of predictable states was chosen based upon extremes of what could occur in the real world. For all experiments, a basic scenario was chosen and the parameters were identical to those in Table VII unless otherwise specified. Table VIII provides the experiments (variations from Table VII) and Table IX provides a

TABLE VII
Basic Scenario

Initialization

SEED	421. --
JCOUNT	40 --
NOWT	1 --
ICOUNT	40 --
DT	5. minutes
P	.899
INPUT	3
INPUT2	0
SUNTYP	1

Sensor

Mode	1.
Type	1.
Cutoff/detector field of view	16. visual magnitudes
Altitude	0. kilometers
Cycle time	120 seconds
Dwell time	0. seconds

Target Selection and Mission Data

Target type	4
Negation percentage	100
Negation time	1440 minutes
Tracking priority	1

Ground Site Data*

Latitude	1.5708 radians
Longitude	0. radians
Altitude	0. kilometers
Sensor type	1.0 ---
Sky cover probabilities	.5#

* Three sites are entered separated by $(2\pi/3)$ radians of longitude.

All elements of the sky cover probabilities array are set equal to .5.

TABLE VIII

Experiment Descriptions

-
1. Three sensors: on the equator, 120 degrees apart
Four sensors: on the equator, 90 degrees apart
 2. Make one run with Target Type 4 only
Make one run with Target Types 3 and 4
 3. Three sensors: sensitivity cutoff equal to 13.5 visual magnitudes
Three sensors: sensitivity cutoff equal to 16 visual magnitudes
 4. Make one run with sky cover probabilities all equal to .5
Make one run with sky cover probabilities all equal to 1.0
 5. Three sensors: equally spaced around the globe at 30°N, 0°, and 30°S, SUNTYP = 2
Three sensors: equally spaced around the globe at 30°N, 0°, and 30°S, SUNTYP = 3
-

TABLE IX

Experiment Results

<u>Experiment</u>	<u>Predicted results</u>	<u>Actual results</u>
1	Target system negation times shorter with four sensors	*
2	Target system negation times longer with second target type	*
3	Sensor system with lower sensitivity cut-off has longer target system negation times	*
4	Run with sky cover probabilities equal to 1.0 has shorter target system negation times	*
5	Sensors in summer hemisphere track fewer targets than sensor in winter hemisphere	*

* Actual results matched predictions.

comparison of expected results to the actual results. Testing of stochastic events was unwarranted since all random numbers were selected from a uniform distribution using Fortran IV's random number generator.

Credibility. The third phase, credibility, deals with intuitive (face validation) and statistical (sensitivity analysis) appeal of EOBASE. Face validation of EOBASE was accomplished by consultation with experts in operations research and physics concerning the physical processes modeled and the structure of the model. Sensitivity analysis was performed on two variables to determine their effect on accuracy and processing time. JCOUNT was varied to determine how large it has to be to get consistent path selections from EOBASE for an air-based visible light detecting sensor. The same inputs described in Table VII were used except INPUT was set equal to zero, Target Types 2 and 3 were selected, and the sensor location and sky cover probability inputs were deleted. A STOP was inserted into the program so that only the first sensor path choice was output. Ten trials each of JCOUNT were made at values of 5, 10, 20, 40, and 80. The results indicate that JCOUNT must be at least 20 to obtain consistent path selections. Target Type 2 appears to have the most influence upon path selection in this case and causes the most northern latitudes to be favored. The simulation time step Δt was also subjected to sensitivity analysis. The same inputs as shown in Table VII were used except Target Types 2 and 3 were selected and ICOUNT was set equal to 10. As shown in TABLE X, Δt was varied from 5 through 80. The results confirmed that the number of successful missions increases as Δt decreases until Δt

equals 10 minutes. Then there is essentially no difference in the average target system tracking time using 5 minutes versus using 10 minutes for Δt .

Confidence. Further confidence in the ability of the EOBASE model was built by examining the cost/benefit of additional information and

TABLE X

Δt Experiment Results

Δt	Number of successful missions*
5	9
10	9
20	8
40	7
80	6

* Out of 10 trials.

by proper documentation of the model. Analysis of the sensitivity of EOBASE to JCOUNT and Δt indicated the cost of further information. Each iteration of JCOUNT with one sensor and six targets requires 0.3 seconds of execution time. Each time increment in TRACK with three sensors and six targets averages 0.03 seconds of execution time.

The documentation of EOBASE is fairly thorough. A "documentation list" described by Shannon (Ref 31, 262) requires the following:

Flow diagrams of each module and the overall model

--Chapter II

Description of inputs necessary for executing the program

--Chapter II, Appendix A, and Appendix B

Definitions of the program variables not used as inputs

--Appendix B

Verbal description of the purpose and function of all modules

--Chapter II and Chapter III

Input deck set up to run

--Provided separately

Listing of program

--Appendix B

The validation results indicate EOBASE is performing as described. The conceptual validity of the underlying physical processes and techniques described in this chapter and Chapter II has been coordinated with experts in physics, operations research, and astrodynamics. Chapter IV will present analysis results comparing the ability of ground- and air-based sensors.

IV Sensor System Basing Mode Analysis

The purpose of this analysis is to compare the Ground-based Electro-Optical Deep Space Surveillance (GEODSS) system with a hypothetical system of air-based sensors. The GEODSS system is a military project, built for the Air Force to replace the quartet of Baker-Nunn photographic telescopes (Refs 32 and 33). The first GEODSS station began operations in May of this year at White Sands Missile Range southeast of Socorro, New Mexico, and three other installations are expected to take shape during the next two years on Mount Haleakala, Hawaii; at Taeger, Korea; and at the naval base on Diego Garcia in the Indian Ocean. A fifth site is planned for either Ascension Island or the Iberian Peninsula.

Each of the GEODSS sites houses three tracking instruments. Two of the three have 1-meter apertures and a 2.1-degree field of view. Three telescopes can detect objects as faint as magnitude 18.5, however, in normal operation, the cutoff is 16.0. The third telescope has a 0.4-meter aperture, a 6.0-degree field of view, and its magnitude cutoff is 14.5. The wider field of view and faster slow rate of the small instrument make it better suited to the study of lower altitude, brighter satellites.

The principle advantage of the GEODSS system is that the data analysis is rapid. The time required per track is about one minute.

Unlike the Baker-Nunn cameras which use photographic film, a GEODSS sensor uses a SIT vidicon imaging tube, an advanced television camera, so that data processing can be computer assisted. Thus the time consuming process of photographic development required for the Baker-Nunn camera is avoided.

The characteristics of the hypothetical air-based sensor are less easily defined. But, it is obvious that it should be like a GEODSS sensor in that it would use a vidicon tube and computer assisted data processing. Unfortunately it is also apparent that the sensor will have to weigh much less and that both this lower weight and the sensor's mode of basing would contribute to less pointing stability in the telescope. The reduced pointing stability would reduce the image stability in the focal plane; hence, the sensitivity of the telescope could be reduced. Fortunately, high pointing accuracy is possible with an air-based telescope. The 36-inch aperture telescope which NASA has on board a C-141 can maintain a line of sight stability of 2 arc seconds root mean square while in flight for at least 30 minutes (Ref 34). So, it is possible that the pointing stability problem can be solved.

Also, the air-based telescope has several relevant advantages. The air-based telescope receives a satellite's image with much less loss in intensity due to atmospheric absorbency. This is critical at high line of sight angles to the zenith. The LOWTRAN program was used to estimate this loss using the program's model for a standard rural atmosphere (Ref 27). The transmittance to the air-based sensor at 23 kilometer above sea level was found to be virtually 100 percent at the zenith and 38.8 percent at 90 degrees to the zenith. However, the

transmittance to the ground-based sensor was much less, only 44.6 percent at the zenith, and the transmittance dropped off as the zenith angle increased. At 60 degrees to the zenith the transmittance begins to drop off rapidly, and at 80 degrees, a sensor with a magnitude 16.0 cutoff receives too little light from a target presenting 1.0 square meters of surface area to detect it even when haze conditions are favorable. The other advantage of the air-based sensor is that the image which it receives does not suffer significantly from the atmospheric effect "seeing," which is caused by small fluctuations in the index of refraction of the atmosphere (Ref 19:26). Seeing causes a blurring of the image and thus reduces the sensitivity of the telescope.

Since these advantages may just about make up for the pointing stability problem, the sensitivity of the hypothetical air-based telescope will be treated here as equal to that of the ground-based telescope.

Methodology

The analysis was conducted in two stages. First the ability of the GEODSS system to detect the target system was characterized using the EOBASE program and then EOBASE was used to choose an air-based sensor system and assess its ability to detect the target system relative to the GEODSS system.

The data required to characterize the GEODSS system came from several sources. The literature was consulted (Refs 32 and 33) to get estimates of the sensitivity of the sensor and the rate at which data from it could be processed. The coordinates of the GEODSS system used

in this study are from a list provided by DODR, NORAD Headquarters, Colorado Springs, Colorado. Table XI provides a list of the five sites selected for this study. While this list does not necessarily represent the final configuration of the GEODSS system, it is a viable one. The sky cover probabilities for each of these sites was provided by the USAF Environmental Technical Applications Center using data from their nearest reporting station (see Table XII). Unfortunately the proximity of the weather station and GEODSS site was not always as close as desired. Thus, the data for the GEODSS site at Mount Haleakala, Hawaii, is not as accurate as desired. This GEODSS site is 3000 meters above sea level whereas the weather station is near sea level. Nevertheless, the sky cover probabilities for this site still indicates predominately clear skies. Also, as indicated in the earlier part of this chapter, LOWTRAN (Ref 27) was used to assess the atmospheric transmittance at sea level and at 23 kilometers above sea level. As a result, the SIGHT subroutine was modified to score a line of sight with a zenith angle of greater than 70 degrees as 0.0 for ground-based sensors, and thus not a clear line of sight. As indicated in the first part of this chapter, the transmittance at zenith angles above 70 degrees tends to drop off rapidly.

The capabilities of the GEODSS system were characterized in the following way. First, the ability of the system to detect each target type in a 24 hour tracking period was determined. A separate program run was used to determine the capability of the GEODSS system to track each target type, and the results of these runs were used to set the mission inputs for each target type in all of the subsequent runs.

TABLE XI

Locations of GEODSS sites

<u>Site</u>	<u>Name</u>	<u>Latitude</u>	<u>Longitude</u>
1	Faro, Portugal	37.00N	7.92W
2	White Sands Missile Range, New Mexico	33.82N	106.66W
3	Mount Haleakala, Hawaii, AFB	20.71N	156.26W
4	Taegeer, Korea	35.74N	231.39W
5	Diego Garcia	7.20S	287.75W

TABLE XII

Locations of Weather Stations

<u>Site</u>	<u>Name</u>	<u>Latitude</u>	<u>Longitude</u>
1	not substituted		
2	Holloman AFB, New Mexico	32.87	106.10
3	Kahuli, Hawaii	20.78	15.47
4	Taegeer ARTCC, Korea	35.74	231.38
5	not substituted		

Next, the ability of the GEODSS system to track all four target types simultaneously was evaluated. The average annual ability of the GEODSS system to track the target system was estimated using the average annual sky cover probabilities with the position of the sun with respect to its latitudinal position over the earth randomly chosen. The impact of the seasonal variation of the sun's position and weather patterns was estimated in separate program runs using the sky cover probabilities at the winter solstice (month of December) and at the summer solstice (month of June) with the sun at its appropriate latitudinal position. In addition, the extent to which the cloud cover diminishes the effectiveness of the GEODSS system was estimated by setting the sky cover probabilities all to 1.0. the GEODSS system experiments required eight computer runs.

The capabilities of the air-based sensor were modeled around those of the GEODSS sensor. Like the GEODSS sensors, tracks for the air base sensors were limited to those with a line of sight less than or equal to 70 degrees to the zenith. This cutoff was again chosen since the intensity of the night sky background can be significantly larger beyond this point (Ref 19:19-23). For example, night airglow emission increases with increasing zenith angle because the telescope looks through a larger emitting air mass.

The first step in evaluating the air-based system was to use EOBASE to choose an air-based system sufficient to match or better the performance of the GEODSS system in tracking all four target types simultaneously. This system was chosen with the longitudinal position of the sun randomly chosen. Then this system was evaluated in

separate computer runs with the sun in its winter and summer solstice positions. Next EOBASE was used to choose a sensor system with five air-based sensors as opposed to five GEODSS sensors. Then the ability of this system to track the target system was evaluated to determine how well five air-based sensors could track the target system as opposed to five GEODSS sensors.

Results and Discussion

As indicated in the previous section, the first step in characterizing the ability of the GEODSS system to track the target system was to assess its ability to track each individual target type. The purpose of this step was to determine the maximum percentage of each target type that the GEODSS system could reasonably be expected to track in a 24-hour period. So, the GEODSS system was run against each target type with the tracking negation percentage set to 100 percent, the mission time to 1440 minutes, and the tracking priority to 1. The initialization and sensor type inputs used for these experiments and the remaining GEODSS characterizations are shown in Table XIII unless otherwise specified. Also, the average annual sky cover probabilities were used unless otherwise indicated.

The ability of the GEODSS system to track the first target type, a satellite in the highly eccentric Molynia orbit, was never 100 percent in a 24-hour period. Apparently, the apogee of at least one target satellite of this type is always oriented toward the sun where it could not be sighted by any earth based sensor. Note that if the angle between the sun and the sensor (with the target at the vertex) is greater than 90 degrees, very little sunlight, if any, is

TABLE XIII

Basic Initialization and Sensor Inputs
for GEODSS System Simulation

Initialization

SEED	151 - -
JCOUNT	0 - -
NOWT	1 - -
ICOUNT	40 - -
DT	10. minutes
P	.5 - -
INPUT	5 - -
INPUT 2	0 - -
SUNTYP	4 - -

Sensor

Mode	1.0 - -
Type	1.0 - -
Cutoff	16.0 visual magnitudes
Altitude	0.0 kilometers
Cycle time	120.0 seconds
Dwell time	0.0 seconds

reflected by the target to the sensor by an earth oriented cylinder. This problem is not remedied by placing a target (of type 1) with the apogee of its orbit oriented toward the sun in another part of its orbit because the very small portion of its orbit which is not oriented to the sun is mostly in the earth's shadow where there is no sunlight to reflect. The perigee of target type one is only 300 kilometers high. Nevertheless, since the longitude of the ascending mode of this target type is always 120 degrees apart, the GEODSS system can track at least two targets. In only three cases out of 40 trials was only one target tracked, and two targets were tracked in all other cases. As a result the GEODSS system could be expected to track two

targets of this type, and so a tracking percentage of 65 percent was used in all subsequent runs.

Target type 2 produced similar results, and it is also in a high eccentric orbit. However, the longitude of the ascending nodes for this target type are separated by only 90 degrees. So, in this case two targets could be oriented toward the sun. In 10 of 40 trials only two targets were tracked. In the remaining trials, three targets were tracked. So, the mission negation percentage was again set to 65 percent in all subsequent runs.

Target types 3 and 4 produced similar results because both use geosynchronous orbits. With target type 3, 28 out of 40 trials resulted in all targets tracked; and with target type 4, 27 out of 40 trials resulted in all targets tracked. Thus, in both cases, the mission negation percentage was set to 100 percent in all subsequent computer runs.

The next step in evaluating the GEODSS system was to test its ability to track all the target types simultaneously. The results of these runs are shown in Table XIV. These four experiments suggest that cloud cover has an important effect in reducing the effectiveness of the GEODSS system. The number of successful runs increases quite significantly when the sky cover probabilities are all set to 1.0. The latitudinal position of the sun is also important. All but one of the GEODSS sites is in the northern hemisphere, and Diego Garcia, the site in the southern hemisphere, is very close to the equator. Thus, the latitudinal position of the sun can significantly alter the number of hours the sites spend in daylight and are therefore not functional.

TABLE XIV

Results of GEODSS System Encounters with the
Four Target Type Target System

<u>Experiment</u>	<u>Number of Successful Trials</u>
1. Average Environment	15
- Annual sky cover probabilities	
- Random sun	
2. Winter Solstice Environment	26
- December sky cover probabilities	
- Sun at winter solstice	
3. Summer Solstice Environment	12
- June sky cover probabilities	
- Sun at summer solstice	
4. Cloudless environment	34
- Sky cover probabilities all set to 1.0	
- Random sun	

* Out of 40 trials.

This effect is important because the sun spends considerable time near its latitudinal extremes, hence the name solstice. The seasonal variation in cloud cover may also be important. Although the sites are widely dispersed, with one exception, they all experience the same seasons at the same time. Since the unconditional probability of less than or equal to $3/8$ sky cover varies with the time of year (see Table XV), the probability of good weather at the sites may vary as a whole

TABLE XV

Average Nighttime Probability of Less than
or Equal to $3/8$ Sky Cover

<u>Site</u>	<u>Annual</u>	<u>June</u>	<u>December</u>
1	.70	.75	.55
2	.70	.78	.73
3	.64	.65	.66
4	.52	.72	.35
5	.33	.38	.34

Note: These nighttime probabilities are defined by observations taken at the weather stations between 2,000 hours and 0400 hours local time.

so that the system performance may be dependent upon the time of year. Table XV indicates that better weather occurs in June at most of the GEODSS sites than in December.

The air-based system was chosen using the inputs shown in Table XVI. This resulted in the selection of three sensors. The sensors were located on lines of longitude separated by 120 degrees. Two sensors were located 10 degrees north, and one sensor was located 10 degrees south.

This system was able to track the target system (all 4 target types) 27 out of 40 times during a 24-hour period. In all cases the target satellites in geosynchronous orbits were target within 24 hours. The satellites in subsynchronous orbits limited the mission success rate. The system was also evaluated with the sun at the winter and summer solstices. With the sun in the winter position, 40 out of 40 trials were successful in meeting the mission requirements. Twenty-five trials were successes with sun in the summer position.

These runs strongly indicate that if all other aspects of the air- and ground-based modes are equal, that is sensor performance and reliability, three air-based sensors can match or exceed the performance of the GEODSS system which includes five sensors.

EOBASE was also used to choose an air-based system composed of five sensors. The same inputs shown in Table XVI were used except the sensor system was required to track the target system in 1200 minutes with a probability of .99. The program was allowed to run until it ran out of CPU time. At this point five sensors had been chosen.

TABLE XVI

Inputs Used To Choose The Air Based System

Initialization

SEED	151 - -
JCOUNT	40 - -
NOWT	1 - -
ICOUNT	40 - -
DT	10. minutes
P	.375 - -
INPUT	0 - -
INPUT 2	0 - -
SUNTYP	4 - -

Sensor

Mode	1.0 - -
Type	1.0 - -
Cutoff	10.0 visual magnitudes
Altitude	23.0 kilometers
Cycle time	120.0 seconds
Dwell time	0.0 seconds

Note: The same target selection and mission inputs used to characterize the GEODSS system were used to select the air-based system.

These five sensors were located as shown in Table XVII. This system was able to track the target system 37 out of 40 times in 24 hours. The target satellite located in geosynchronous orbit were always tracked within 24 hours. The performance of this system was about as good as the GEODSS system in the absence of cloud cover.

The experiments with the air-based sensors indicate air basing could significantly increase the frequency deep space satellites are tracked. Three air-based sensors could conceivably match or surpass the performance of the GEODSS system. In addition, a reliable air-based system could assure that all geosynchronous satellites would be tracked within any 24-hour period. This comparative analysis of the GEODSS system with a system of hypothetical air-based sensors was conducted in two phases. First, the capabilities of the GEODSS system to track all four target types was determined, and the position of the sun and cloud cover conditions were varied so that their effect upon the capabilities of the GEODSS system could be estimated. The results of these experiments showed that it was possible for an earth based sensor to consistently track only two of the three type 1 targets and three of the four type 4 targets in a 24-hour period. All of the type 1 and type 4 targets could be track in a 24-hour period. These experiments also showed that cloud cover significantly reduces the effectiveness of the GEODSS system and that the latitudinal position of the sun causes the effectiveness of the GEODSS system to vary considerably. Next, a system of air-based sensors was chosen which could match the GEODSS system's capability to track the target system.

TABLE XVII

Five Sensor Air-Based System

<u>Sensor</u>	<u>Latitude</u>	<u>Relative Longitude*</u> <u>(degrees)</u>
1	1.4039	0
2	1.4039	144
3	2.1041	216
4	0.6930	288
5	1.5708	72

Note: The longitude of the first sensor is randomly chosen and the remaining sensors are placed relative to it

Only three air-based sensors were needed. When a system of five air-based sensors were chosen, it was found that this system could be tracked within 24 hours nearly 100 percent of the time.

Unfortunately it cannot be stated without reservation that these air-based systems would perform as well as indicated. As noted in Chapter III under "Sensor Placement," submodel TRACK does not consider geographic features as part of the sensor placement process. Since it is possible that the desired system configuration might not be achievable in the real world, in practice these air-based systems might not perform as well as indicated by the model.

In the next chapter, the information contained in this study will be summarized. Then some conclusions will be presented. Finally, this work will close with some recommendations for further study.

V Conclusion

The primary purpose of this thesis has been to evaluate the possible benefits of an air-based system of electro-optical telescopes. As a prerequisite, some effort has been made to show the need for and the plausibility of such a system.

Summary

The presence of the atmosphere is a serious hindrance to a ground-based astronomical telescope. Because of this, the satellite tracking telescopes of the Air Force's SPADATS network tend to be located at remote sites at high elevation. The use of air-based sensors has been suggested as a possible solution for this problem. This approach has already been adopted by astronomers who use balloons and airplanes to carry their infrared telescopes into the stratosphere.

Several efforts are currently under way to develop a high altitude airship which can remain on station for extended periods of time. The Air Force's program has already demonstrated the feasibility of this kind of vehicle with the launch of High Platform II in May of 1970, and the Navy, as demonstrated by its Hi Spot, is seriously considering the high altitude airship for operational use. On the other hand, NASA is studying the value of this kind of airship for commercial use. NASA has purposed the HAPP concept which utilizes a microwave transmitter to power a high

concept which utilizes a microwave transmitter to power a high altitude airship or perhaps a high altitude airplane.

The program EOBASE has been developed to estimate the value of a high altitude platform for satellite tracking. The program can be used to assess the gain in performance conferred by the airship's high operating altitude and flexibility in site selection. The program simulates getting the first track on each satellite of a system of deep space satellites using either a system of user input sensors or a system of sensors selected by EOBASE.

The EOBASE program has been used here in a comparative analysis of the GEODSS system with a hypothetical system of air-based sensors. This analysis was conducted in two phases. First, the EOBASE program was used to assess the capability of the GEODSS system to track four target types, both individually and collectively. This analysis showed that the affect of weather is quite detrimental to the GEODSS system, and that the changing position of the sun can cause its performance to vary considerably. Second, EOBASE was used to choose an air-based sensor system based upon its ability to track all four target types simultaneously at least as well or better than the GEODSS system. Only three air-based sensors were needed to match the performance of the GEODSS system. The performance of this system was also found to be dependent upon the position of the sun. EOBASE was also used to select an air-based system of five air sensors. This system was able to track the target system within 24 hours nearly 100 percent of the time.

Conclusions

While the results of this study with EOBASE are not sufficient grounds for launching a program to develop a system of air-based satellite tracking telescopes, they do demonstrate that such a system may have value. The possibility that three air-based sensors could match the performance of the GEODSS system means that there could be possible cost savings promising air-based sensors instead of ground-based sensors. Also, the air-based sensor could have greater value in the early warning role than the GEODSS system. The air-based system is consistently able to track all the satellites in geosynchronous orbit in less than 24 hours because unlike a ground-based system, it is unaffected by weather. However, it should be emphasized that because of the dearth of basing restrictions in the sensor placement process in practice, the air-based system may not perform quite as well as indicated.

Based upon the results of their study, the concept of using air-based satellite surveillance telescopes warrants an engineering feasibility study. This study is needed to determine if the required sensitivity can be obtained with a sensor light enough to be carried by a high altitude airship or perhaps a high altitude airplane. Also, this study is needed to establish a basis for a cost analysis.

Recommendations

Further refinements of the results obtained with EOBASE could be useful. Following is a list of recommendations which should lead to an improved understanding of the problems involved in choosing the proper basing mode.

1. Allow the user to input the target satellite orbital and shape parameters of his choice.
2. Allow different negation times for each target type.
3. Revise subroutine VISIBLE to include the effect of atmospheric transmittance.
4. Include basing restrictions in the sensor placement algorithm.

Bibliography

1. E40BF2031-001/E4AOF27650-007. Space Systems Operations. Study Guide. Keesler AFB, Mississippi: Keesler Technical Training Center, July 1, 1981.
2. Luke, Charles A. Design Study for Airborne Electro-optical Surveillance Experimentation. Final Technical Report. Wright-Patterson AFB, Ohio: Air Force Avionics Laboratory, October 1967. (AD 386 262)
3. Carlson, Donald J., Shanley, Thomas J. B., and McClarty, John R. High-Altitude Infrared Detection Techniques. Final Technical Report. Wright-Patterson AFB, Ohio: Air Force Avionics Laboratory, April 1972. (AD 520 093)
4. "Telescope in C-141 to Gather IR Data," Aviation Week & Space Technology, 97(21): 71-72 (November 20, 1972).
5. Hudson, Richard D. Infrared System Engineering. New York: John Wiley & Sons, 1969.
6. Fazio, G. G. "A 102-cm Balloon Borne Telescope for Far-Infrared Astronomy," Optical Engineering, 16(6): 551-557 (December 1977).
7. Boggess, N. W. "Infrared Instrumentation on NASA Airborne Observatories," Optical Engineering, 16(6): 528-532 (December 1977).
8. Office of the Assistance for Study Support. Spacetrack Augmentation Tradeoff Study, Annex B- Augmentation Options. Final Report. Kirtland AFB, New Mexico: DCS/Development Plans, Air Force Systems Command, November 1973. (AD 528 642)
9. Beemer, Jack D., Parsons, Roger R., Rueter, Loren L., Seufferer, Paul A., and Swiden, LaDell R. POBAL-S, The Analysis and Design of a High Altitude Airship. Final Technical Report. Sioux Falls, South Dakota: Raven Industries Inc., February 1975. (AD A012 292)
10. Scales, Stewart H. and McComas, C. B. High Altitude Superpressured Powered Aerostat (HASPA) Demonstration Program. Final Technical Report. Denver, Colorado: Denver Division, Martin Marietta Aerospace, October 1977. (AD B021 939L)
11. Wessel, P. R. and Petrone, F. J. "Special Problems and Capabilities of High Altitude Lighter Than Air Vehicles," Proceedings of the Interagency Workshop on Lighter Than Air Vehicles. 595-603. Cambridge, Massachusetts: Flight Transportation Laboratory, Massachusetts Institute of Technology,, 1975.

12. Greenstone, Reynold. Environmental and Technological Uncertainties Related to the High Altitude Powered Platform (HAPP) Concept. Technical report proposed under Contract No. NASW-2961 for NASA. Silver Spring, Maryland: ORI, Silver Spring, Maryland.
13. Marcy, William L. and Hookway, Ralph O. Propulsion Options for the HI Spot Long Endurance Drone Airships. Final Technical Report. Denver, Colorado: Denver Division, Martin Marietta Aerospace, September 1979. (AD A074 595)
14. Elson, Benjamin M. "Cost Factor Key to Unmanned Vehicles," Aviation Week and Space Technology, 117(8): 65-73 (August 9, 1982).
15. Sinko, James W. "High-Altitude Powered Platform: A Microwave Powered Airship," A Collection of Technical Papers. 212-218. Palo Alto, California: AIAA Lighter-than-Air Conference, New York, New York, July 1979.
16. Kuhner, Mark B. "Application of the High-Altitude Powered Platform (HAPP)," A Collection of Technical Papers. 146-154. Palo Alto, California: AIAA Lighter-than-Air Conference, New York, New York, July 1979.
17. Dutton, Jeffrey L. HELBASE: A Tool for the Analysis of High Energy Laser Development, Deployment, and Operation. Unpublished M.S. Thesis. Wright-Patterson, AFB, Ohio: Air Force Institute of Technology, 1980. (AD A094854)
18. Copeland, William R. A Validation Study of HELBASE: A Tool for the Analysis of Strategic High Energy Laser Weapon System Development and Operation. Unpublished M.S. Thesis. Wright-Patterson AFB, Ohio: Air Force Institute of Technology, December 1981. (AD B067181)
19. AVCO Systems Division. Satellite Photometry. Study Guide. Wilmington, Massachusetts: AVCO Systems Division, January 31, 1977.
20. Wolfe, William L. And Zissis, George J., ed. The Infrared Handbook. Technical Handbook. Arlington, Virginia: Office of Naval Research, Department of the Navy, 1978.
21. Weber, Robert. "The Ground-Based Electro-Optical Detection of Deep-Space Satellites." Applications of Electronic Imaging Systems. SPIE Vol. 143 (1978).
22. Slater, Phillip N. Remote Sensing. Reading, Massachusetts: Addison-Wesley Publishing Company 1980.

23. Strganac, Thomas W. "Wind Study for High Altitude Platform Design," A Collection of Technical Papers. 155-161. Palo Alto, California: AIAA Lighter-than-Air Conference, New York, New York, July 1979.
24. Richardson, M. Plane and Spherical Trigonometry. New York: The MacMillan Company, 1950.
25. Bate, Roger R., et al. Fundamentals of Astrodynamics. New York: Dover Publications Inc., 1971.
26. Kneizys, F. X., et al. Atmospheric Transmittance/Radiance Computer Code LOWTRAN 5. Scientific report. Defense Hanscom AFB, Massachusetts: Optical Physics Division, Air Force Geophysics Laboratory, February 21, 1980. (AFGL-TR-80-0067)
27. ADCOM/J3Z. Alternatives for GEODSS Sites Four and Five.
28. Lund, Iver A. and Shanklin, Milton D. "Photogrammetrically Determined Cloud-Free Lines-of-Sight Through the Atmosphere," Journal of Applied Meteorology. 11: 773-782 (August 1972).
29. ——— "Universal Methods for Estimating Probabilities of Cloud-Free Lines-of-Sight Through the Atmosphere," Journal of Applied Meteorology. 12: 1040-1043 (September 1973).
30. Haley, Charles and Ghelber, Craig. A Methodology for Validation of Complex Multivariable Military Simulation Models. Unpublished M.S. Thesis. Wright-Patterson AFB, Ohio: Air Force Institute of Technology, 1980.
31. Shannon, Robert E. System Simulation—The Art and Science. Englewood Cliffs, New Jersey: Prentice Hall, Inc. 1975.
32. Otten, David G., et al. "GEODSS Heavenly Chronicles," Quest. 3-23 (Autumn 1980).
33. Beatty, J. Kelly. "The GEODSS Difference," Sky and Telescope. 469-473 (May 1982).
34. Mobley, R. E. and Cameron, R. M. "NASA-ARC 36-Inch Airborne Infrared Telescope." Technical report. Moffet Field, California: Ames Research Center, National Aeronautics and Space Administration, June 1972.

APPENDICES

A Use of the Model

The purpose of this section is to acquaint the EOBASE user with the various input possibilities, how to interpret the data, and how to interpret the output. As an aid to explanation, specific examples will be used.

Inputs

All input is free formatted with both integer and real variables. The first input card contains nine inputs. (1) SEED - the random number generator argument (real), (2) JCOUNT - the number of times the targets are placed to calculate sighting efficiencies (integer), (3) NOWT - the number of sensor types choices to be input (integer), (4) ICOUNT - the number of times TRACK is called to build confidence in the selected sensor system (integer), (5) DT - the time increment in TRACK in minutes (real), (6) P - the probability of success required for a given mission (real), (7) INPUT - the number of preselected ground based sensors to be entered (integer), (8) INPUT2 - the number of preselected air and/or space sensors to be entered (integer), and (9) SUNPOS - this number, 1-4, indicates the way the latitudinal position is to be chosen (integer). See Table XVIII.

The next set of data cards contains sensor type information. A separate card is input for each sensor type, and contains all the information given in Table XVIII. All inputs are real.

Table XVIII

Example Scenario

Initialization

SEED	4239.- -
JCOUNT	50 - -
NOWT	1 - -
ICOUNT	10 - -
DT	10. minutes
P	.8 - -
INPUT	0 - -
INPUT 2	0 - -
SUNTYP	4 - -

Sensor

Basing Mode	1.0 - -
Sensor	1.0 - -
Cutoff	16.0 visual magnitudes
Altitude	0. kilometers
Minimum tracking time per cycle	120.0 seconds
Dwell time	0.0 seconds

Mission Data

Target type	4 - -
Target type tracking percentage	100 - -
Mission time	1440 minutes
Target type tracking priority	1 - -

The third set of data cards contain the target types selected and their associated mission data. For each target type selected, a single card with that target type number is included (real), followed by a card containing the mission data for that target type (integer). This is repeated for all target types selected, followed by a "termination" card with a 99. on it (not needed if all target types are selected). Again see Table XVIII.

If both INPUT and INPUT2 equal zero, then the above mentioned inputs and the data are entered as shown in Table XIX, otherwise sensor location data is needed.

TABLE XIX

Input Data Format for Preselected Ground Base Sensors

Card #	Contents								
1	4239.	50	1	10	10.	.8	0	0	4
2	.1	1.	.16	0.	120.	0.			
3	4.								
4	4	.93	100	1440	1				
5	99.								

The location of ground-based sensors are entered first in the next set of cards. For each site entered, a single card containing the sensor type, the latitude, longitude, and the altitude (all real) is included in the order just given. The following cards provide the sky cover probabilities (see Table IV in Chapter II for the format). Table XX provides an example input.

Air- and space-based sensors are input next. A card is entered for each sensor and includes the sensor type, the orbital radius or coordinate theta for air-based sensors, the eccentricity, the inclination or coordinate theta, longitude of the ascending node, and the argument of perigee in the order just given. See Table XXI.

TABLE XX

Input Data Format for Preselected Ground Base Sensors

Card #	Contents								
1	1.	.925		6.145	0.				
2	.54	.93	.32	.93	.48	.91	.50	.83	.45
3	.65	.94	.31	.92	.37	.83	.36		
4	.72	.93	.21	.82	.28				
5	.72	.85	.18						
6	.66								

Note: This card represents the GEODSS site at Faro, Portugal located at 37.0 degrees north and 7.917 degrees west. In Card 1, degrees have been converted to radians in the geocentric coordinate referenced system. Cards 2-6 contain the annual sky cover probabilities.

TABLE XXI

Input Data Format for Preselected Air and Space Based Sensor

Card #	Contents				
1	1.	1.5708	0.	1.5708	0.0
2	1.	1000.	0.	1.5708	0.0

Note: Card 1 represents an air-based sensor located on the equator. Card 2 represents a space-based sensor in a 90-degree, 1000-kilometer circular orbit. Angular measurements are input in radians.

Output

All sensor types, target types, sensor location, and sky cover probabilities are printed out in an easy to read well documented format. At the start of each TRACK run, the track run is printed, followed by all the sensors selected. When a target satellite is tracked, the target number and sensor number are printed. At the completion of each successful tracking sequence, the total time and the number of targets tracked is printed. If tracking sequence is unsuccessful, only the number of targets tracked is printed. After all the tracking sequences have been completed, the number of successful sequences and the total number of sequences are printed. If the sensor system meets mission requirements, the sensor types and location parameters for all sensors in the sensor system are printed. All output is well documented.

B EOBASE Listing

```

130- CAPT RICHARD T. SALMON
140- PROGRAM ECBASE(INPUT,OUTPUT)
150- DIMENSION SENSOR(6,5),T(14,11),MISSION(4,4),TAROPR(14),
160- C SUMEFF(5,410),X(5,410),VIS(410),Z(5,410),XT(14),YT(14),
170- C ZT(14),EOSEL(50,6),PATH(5,19),TH(19),SITE(50,4),NU(50),
180- C SKVC(50,25)
190- INTEGER SUNTYP
200- COMMON/DIR/TRANSNT(9),BKGD(19)
210- DATA (BKGD(1),1-1,9)/.00236,.0024,.00251,.00272,.00306,.00362,
220- C .00467,.00671,.0129/
230- DATA (TRANSNT(1),1-1,9)/.9992,.9992,.9992,.9992,.9991,.9990,.9988,.9985,
240- C .9978,.9958/
250- C *****
260- C SEED IS THE RANDOM NUMBER GENERATOR SEED (REAL).
270- C JCOUNT IS THE NUMBER OF TIMES THE TARGETS ARE RANDOMLY PLACED TO
280- C CALCULATE THE AVERAGE SIGHTING EFFICIENCY FOR EACH POINT ON A
290- C SPHERE OF OPERATIONS (INTEGER).
300- C NOUT IS THE NUMBER OF SENSOR TYPES (INTEGER).
310- C ICOUNT IS THE NUMBER OF TIMES TRACK IS CALLED TO BUILD CONFIDENCE
320- C IN THE SELECTED SENSOR SYSTEM (INTEGER).
330- C DT IS THE TIME INCREMENT IN TRACK (REAL).
340- C P IS THE PROBABILITY OF SUCCESS REQUIRED FOR THE SELECTED SENSOR SYST
350- C INPUT IS THE NUMBER OF GROUND-BASED SENSORS WHOSE COORDINATES ARE TO
360- C ENTERED (INTEGER).
370- C INPUT2 IS THE NUMBER OF AIR AND SPACE BASED SENSORS (INTEGER).
380- C SUNTYP IS USED TO SELECT TH THETA VALUE OF THE SUM (INTEGER).
390- C READX,SEED,JCOUNT,NOUT,ICOUNT,DT,P,INPUT,INPUT2,SUNTYP
400- C P-P-.001
410- C
420- C THE FOLLOWING IS USED TO CONTROL THE NUMBER OF TIMES SIDEN IS
430- C IS RUN BY TRACK TO PROVIDE SIGHTING EFFICIENCIES TO CHOOSE THE
440- C THE NEXT BEST SENSOR PATH COMBINATION.
450- C
460- C COUNT=ICOUNT
470- C KCOUNT=JCOUNT/ICOUNT
480- C IF(KCOUNT.LE.0)KCOUNT=1
490- C CALL RANSET(SEED)
500- C *****
510- C THE FIRST SECTION IS DESIGNED TO ACCEPT USER INPUTS
520- C INPUTS ARE READ IN THE FOLLOWING ORDER...
530- C SENSOR TYPES
540- C TARGET TYPES
550- C MISSION DATA
560- C SITE LOCATIONS
570- C SKYCOVER PROBABILITIES
580- C AIR AND SPACE BASED SENSOR PARAMETERS
590- C *****
600- C SENSOR INPUTS ARE STORED IN MATRIX SENSOR (6,5)
610- C
620- C UP TO FIVE DIFFERENT SENSOR TYPES MAY BE INPUT, 1 CARD PER SENSOR TY
630- C EACH CARD IS FREE FORMATTED, WITH ENTRIES BEING SEPARATED BY COMMAS
640- C SPACES.
650- C
660- C
670- C
680- C

```

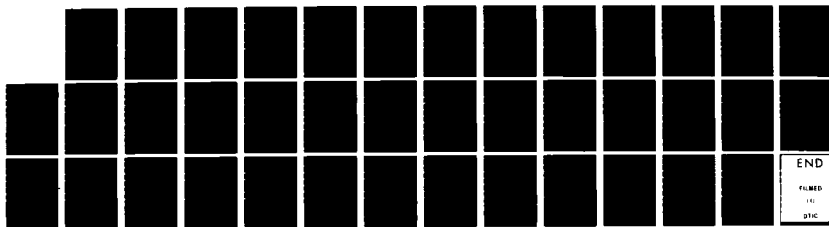
AD-A124 734

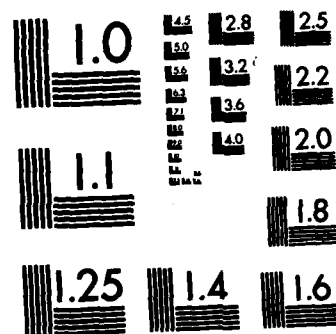
AN EVALUATION OF THE EFFECTIVENESS OF DEPLOYING
ELECTRO-OPTICAL TELESCOPE. (U) AIR FORCE INST OF TECH
WRIGHT-PATTERSON AFB OH SCHOOL OF ENGI... R T SALMON
DEC 82 AFIT/GSO/OS/82D-4 F/G 17/8

2/2

UNCLASSIFIED

NL





MICROCOPY RESOLUTION TEST CHART
NATIONAL BUREAU OF STANDARDS-1963-A

```

710-
720-
730-
740-
750-
760-
770-
780-
790-
800-
810-
820-
830-
840-
850-
860-
870-
880-
890-
900-
910-
920-
930-
940-
950-
960-
970-
980-
990-
1000-
1010-
1020-
1030-
1040-
1050-
1060-
1070-
1080-
1090-
1100-
1110-
1120-
1130-
1140-
1150-
1160-
1170-
1180-
1190-
1200-
1210-
1220-
1230-
1240-
1250-
1260-
1270-
..

60
65
70
75
80
85
90
95
100
105
110

A "0" MAY BE INPUT WHERE ALLOWED TO ACCEPT THE DEFAULT VALUE.
THE VARIABLE ORDER ON EACH CARD IS AS FOLLOWS
NODENO.....MODE NUMBER(REAL)..(1-GROUND, 2-AIR, 3-SPACE)(MANDAT
TYPE.....SENSOR TYPE(REAL)..(1-VISIBLE, 2-LIIR)
CUTOFF.....MINIMUM SIGNAL STRENGTH (VISUAL MAGNITUDES)
OR LIIR SENSOR ANGULAR RESOLUTION(RADIANS)
ALT.....SENSOR ALTITUDE (KILOMETERS)
MODE 1: 0
MODE 2: 21.3 KM
MODE 3: (MANDATORY)
DELTRN.....MINIMUM CYCLE TIME (SEC)
DULTRN.....LIIR DETECTOR DWELL TIME(SEC)

#####
TARGET TYPE INPUTS ARE STORED IN MATRIX T(14,7)
4 TARGET TYPES, 14 TOTAL TARGETS
T(1,1) IS TARGET TYPE NUMBER.
T(1,2) IS SEMI-MAJOR AXIS OF ORBIT.
T(1,3) IS ORBITAL ECCENTRICITY.
T(1,4) IS ORBITAL INCLINATION.
T(1,5) IS LONGITUDE OF THE ASCENDING NODE.
T(1,6) IS ARGUMENT OF PERIGEE.
T(1,7) IS MEAN ANOMALY.
T(1,8) IS THE PROJECTED AREA OF THE CYLINDER WRT TO THE SENSOR.
T(1,9) IS THE REFLECTIVITY OF THE CYLINDER.
T(1,10) IS THE PROJECTED AREA OF THE PLATE.
T(1,11) IS THE REFLECTIVITY OF THE PLATE.

#####
MISSION DATA INPUTS ARE STORED IN MATRIX MISSION(4,4) (INTEGER)

THREE VARIABLES FOR EACH TARGET TYPE ARE ALLOWED
A CARD MUST BE INPUT FOR EACH TARGET TYPE SELECTED.
AS BEFORE, INPUT 1 CARD FOR EACH TARGET TYPE.
CARD FORMAT IS AGAIN FREE FIELD

TYPE.....TARGET TYPE (1,2,3, OR 4.) (MANDATORY)
TYPNEG.....TARGET TYPE NEGATION PERCENTAGE (MANDATORY)
TNEG.....TARGET SYSTEM NEGATION TIME (MINUTES) (MANDATORY).
NOTE... TNEG MUST BE THE SAME FOR ALL TARGET TYPES SELECTED.
PRIPRI... TRACK PRIORITIES (1,2,3,4) (4 THE LOWEST) (MANDATORY)

#####
SITE LOCATIONS ARE STORED IN SITE(50,4)
SITE(1,1).....LATITUDE
SITE(1,2).....LONGITUDE
SITE(1,3).....ALTITUDE
SITE(1,4).....SENSOR TYPE

#####
SKYCOVER PROBABILITIES ARE STORED IN SKYC(50,25)
ARRAY ELEMENTS ARE STORED AS SHOWN BELOW:
INITIAL STATE INITIAL +3HR +6HR +9HR +12HR
TIME

```



```

3660- PRINT*, 'LATITUDE.....', SITE(I,1), 'RADIANS'
3670- PRINT*, 'LONGITUDE.....', SITE(I,2), 'RADIANS'
3680- PRINT*, 'ALTITUDE.....', SITE(I,3), 'KILOMETERS'
3690- PRINT*, 'SKY COVER PROBABILITIES:'
3700- PRINT 111, (SKYC(I,IU), IU=1,9)
3710- PRINT 111, (SKYC(I,IU), IU=10,16)
3720- PRINT 111, (SKYC(I,IU), IU=17,21)
3730- PRINT 111, (SKYC(I,IU), IU=22,24)
3740- PRINT 111, SKYC(I,25)
3750- FORMAT(F9.2,F8.2,F8.2,F8.2,F8.2,F8.2,F8.2,F8.2)
3760- CONTINUE
3770- IF (INPUT2.EQ.0) GO TO 785
3780- CONTINUE
3790- PRINT*, '***** AIR AND SPACE BASED SENSOR LOCATION PARAMETERS *****'
3800- C
3810- PRINT*, ' '
3820- I=INPUT2+INPUT
3830- J=INPUT +1
3840- DO 786 IOUT=J,1
3850- PRINT*, 'SENSOR TYPE.....', EOSEL(IOUT,1)
3860- PRINT*, 'ORBITAL RADIUS.....', EOSEL(IOUT,2), 'KILOMETER'
3870- PRINT*, 'ECCENTRICITY.....', EOSEL(IOUT,3)
3880- PRINT*, 'INCLINATION.....', EOSEL(IOUT,4), 'RADIANS'
3890- PRINT*, 'ASCENDING NODE.....', EOSEL(IOUT,5), 'RADIANS'
3900- PRINT*, 'ARGUMENT OF PERIGEE.....', EOSEL(IOUT,6), 'RADIANS'
3910- PRINT*, ' '
3920- C
3930- CONTINUE
3940- CONTINUE
3950- PRINT*, '*****'
3960- PRINT*, '*****'
3970- C
3980- ZERO THE SUNEFF MATRIX.
3990- C
4000- DO 337 I=1,NOUT
4010- DO 339 J=1,410
4020- SUNEFF(I,J)=0.
4030- CONTINUE
4040- C
4050- 339 CONTINUE
4060- C
4070- IC=1
4080- IF ((INPUT.GT.0).OR.(INPUT2.GT.0)) IC=0
4090- IF ((INPUT.GT.0).OR.(INPUT2.GT.0)) GO TO 922
4100- CALL SPHERE FOR EACH SENSOR TYPE.
4110- C
4120- DO 340 I=1,NOUT
4130- R=SENSOR(4,I) +6378.145
4140- CALL SPHERE(R,I,X,Y,Z,TH)
4150- CONTINUE
4160- C
4170- *****
4180- *****
4190- *****
4200- *****
4210- *****
4220- *****
4230- C
4240- THIS SECTION IS SUB-MODEL 'OPTIMIZE'
4250- C
4260- THE PURPOSES OF 'OPTIMIZE' ARE TO PLACE THE FIRST (OR NEXT) SENSOR I
4270- THE 'MOST EFFICIENT' ORBIT OR LATITUDE, AND TO DETERMINE WHEN THE
4280- DEPLOYED SENSOR SYSTEM BECOMES ENOUGH TO SATISFY THE MISSION

```



```

4840-
4850-
4860-
4870-
4880-
4890-
4900-
4910-
4920-
4930-
4940-
4950-
4960-
4970-
4980-
4990-
5000-
5010-
5020-
5030-
5040-
5050-
5060-
5070-
5080-
5090-
5100-
5110-
5120-
5130-
5140-
5150-
5160-
5170-
5180-
5190-
5200-
5210-
5220-
5230-
5240-
5250-
5260-
5270-
5280-
5290-
5300-
5310-
5320-
5330-
5340-
5350-
5360-
5370-
5380-
5390-
5400-

425 CONTINUE
    PATH(1,5)=PTHEFF/23.
    C
    PTHEFF=0.
    DO 427 J=187,204
    PTHEFF=PTHEFF+SUNEFF(1,J)
    CONTINUE
    PATH(1,7)=PTHEFF/18.
    427 C
    PTHEFF=0.
    DO 429 J=205,216
    PTHEFF=PTHEFF+SUNEFF(1,J)
    CONTINUE
    PATH(1,8)=PTHEFF/12.
    429 C
    PTHEFF=0.
    DO 431 J=217,222
    PTHEFF=PTHEFF+SUNEFF(1,J)
    CONTINUE
    PATH(1,9)=PTHEFF/6.
    431 C
    PATH(1,10)=SUNEFF(1,223)
    C
    PTHEFF=0.
    DO 434 J=224,258
    PTHEFF=PTHEFF+SUNEFF(1,J)
    CONTINUE
    PATH(1,11)=PTHEFF/35.
    434 C
    PTHEFF=0.
    DO 436 J=259,292
    PTHEFF=PTHEFF+SUNEFF(1,J)
    CONTINUE
    PATH(1,12)=PTHEFF/34.
    436 C
    PTHEFF=0.
    DO 438 J=293,323
    PTHEFF=PTHEFF+SUNEFF(1,J)
    CONTINUE
    PATH(1,13)=PTHEFF/31.
    438 C
    PTHEFF=0.
    DO 440 J=324,350
    PTHEFF=PTHEFF+SUNEFF(1,J)
    CONTINUE
    PATH(1,14)=PTHEFF/27.
    440 C
    PTHEFF=0.
    DO 442 J=351,373
    PTHEFF=PTHEFF+SUNEFF(1,J)
    CONTINUE
    PATH(1,15)=PTHEFF/23.
    442 C
    PTHEFF=0.
    DO 444 J=374,391
    PTHEFF=PTHEFF+SUNEFF(1,J)
    CONTINUE
    444

```

```

5430-
5440-
5450-
5460-
5470-
5480-
5490-
5500-
5510-
5520-
5530-
5540-
5550-
5560-
5570-
5580-
5590-
5600-
5610-
5620-
5630-
5640-
5650-
5660-
5670-
5680-
5690-
5700-
5710-
5720-
5730-
5740-
5750-
5760-
5770-
5780-
5790-
5800-
5810-
5820-
5830-
5840-
5850-
5860-
5870-
5880-
5890-
5900-
5910-
5920-
5930-
5940-
5950-
5960-
5970-
5980-
5990-

515 C      PATH(I,16)=PTHEFF/18.
      PTHEFF=0.
      DO 446 J=392,403
      PTHEFF=PTHEFF+SUMEFF(I,J)
      CONTINUE
      PATH(I,17)=PTHEFF/12.
520 C      PTHEFF=0.
      DO 448 J=404,409
      PTHEFF=PTHEFF+SUMEFF(I,J)
      CONTINUE
      PATH(I,18)=PTHEFF/6.
525 C      PATH(I,19)=SUMEFF(I,410)
      DO 2 J=1,19
      PRINT2,I,PATH(I,J)
      PRINT2,1.
530 C      THIS COMPLETES THE FINDING OF THE 'PATH EFFICIENCIES' FOR EACH
      C      SENSOR TYPE OF NODES 1. AND 2.
      C      IF(SENSE(I,1).LT.2.5)GO TO 500
535 C
      C      CALCULATE 'PATH AVERAGE TARGET SYSTEM SIGHTING EFFICIENCY' FOR THE
      C      VARIOUS ORBITAL INCLINATIONS
540 C      DO 491 N=2,10
      C      EFF=0.
      C      DO 490 J=2,N
      C      EFF=EFF+PATH(I,J)
      C      N=J+9
      C      EFF=EFF+PATH(I,N)
      C      CONTINUE
      C      PATH(I,N)=(EFF+PATH(I,1))/((N-1)*2+1)
      C      PRINT2,I,PATH(I,N)
      C      CONTINUE
      C      CONTINUE
545 C      THE PATH MATRIX NOW CONTAINS 'PATH SIGHTING EFFICIENCY' VALUES
      C      FOR ALL POSSIBLE PATHS OF ALL SENSOR TYPES.
550 C
      C      NODES 1 AND 2 SENSOR TYPES WILL HAVE 19 VALUES IN A ROW.
      C      HOWEVER, LATITUDES MORE THAN 60 DEGREES FROM THE EQUATOR
      C      WILL NOT BE CONSIDERED AS POSSIBLE BASING LOCATIONS.
      C      NODE 3 SENSOR TYPES WILL HAVE 10 VALUES IN A ROW.
555 C      CHOOSE THE PATH WITH THE MAXIMUM EFFICIENCY.
560 C      LET IMAX BE THE SENSOR TYPE (INTEGER), AND JMAX THE LATITUDE OR ORDI
      C      NATE.
      C      XMAX=0.
      C      DO 540 I=1,NOUT
      C      L=10
      C      IF(SENSE(I,1).LT.3)L=12
      C      DO 550 J=1,1
      C      IF(SENSE(I,1).LT.2.5).AND.(J.GT.7).AND.(J.LT.11))
570 C

```

```

6020- C PATH(I,J)=0.
6030- IF((SENSOR(I,1).LT.2.5).AND.(J.GT.16))PATH(I,J)=0.
6040- IF(PATH(I,J).GT.XMAX)IMAX=J
6050- IF(PATH(I,J).GT.XMAX)JMAX=J
6060- IF(PATH(I,J).GT.XMAX)XMAX=PATH(I,J)
6070- CONTINUE
6080- PRINT2, .
6090- PRINT2, I,J,XMAX,IMAX
6100-
6110- C SO THE SENSOR SELECTED BY OPTIMIZE TO BE ADDED TO THE SENSOR SYSTEM
6120- C SENSOR IMAX IN LATITUDE OR ORBIT JMAX.
6130-
6140- C *****
6150- C THE MATRIX SUMEFF HAS NOW SERVED ITS PURPOSE, AND IS ZEROED.
6160-
6170- DO 650 I=1,NOUT
6180- DO 640 J=1,410
6190- SUMEFF(I,J)=0.
6200- CONTINUE
6210-
6220- C *****
6230- C THE PARAMETERS OF THE SELECTED SENSOR ARE STORED IN EOSL(50 BY 6)
6240- C USE BY TRACK AND FOR OUTPUT AS THE FINAL SENSOR SYSTEM.
6250- C EOSL(IC,1) IS THE SENSOR TYPE (REAL).
6260-
6270- EOSL(IC,1)=IMAX
6280-
6290- EOSL(IC,2) IS THE ORBITAL RADIUS (NOSE 3), OR THE SPHERICAL COORDI
6300- C THETA (NODES 1 OR 2).
6310-
6320- IF(SENSOR(1,IMAX).EQ.3.) EOSL(IC,2)=SENSOR( 4,IMAX)*6378.145
6330- IF(SENSOR(1,IMAX).LT.3.) EOSL(IC,2)=TH(JMAX)
6340-
6350- EOSL(IC,3) IS THE ORBITAL ECCENTRICITY, AND IS ZERO.
6360-
6370- EOSL(IC,4) IS THE ORBITAL INCLINATION
6380- C OR THE SPHERICAL THETA (NODES 1 AND 2)
6390-
6400- RINC=(JMAX-1)*218+5
6410- EOSL(IC,4)=(RINC/180.)23.14159
6420- IF(JMAX.EQ.1) EOSL(IC,4)=0.
6430- IF(JMAX.EQ.10) EOSL(IC,4)=1.570796
6440-
6450- EOSL(IC,5) IS THE LONGITUDE OF THE ASCENDING NODE (RANDOM).
6460-
6470- EOSL(IC,6) IS THE ARGUMENT OF PERIGEE, AND IS ZERO.
6480-
6490- DO 20 J=1,1C
6500- NU(J)=0
6510- DO 30 I=1,1C
6520- IF(( EOSL(I,1).EQ. EOSL(J,1)).AND.( EOSL(I,4).EQ. EOSL(J,4)))
6530- C NU(J)=NU(J)+1
6540- CONTINUE
6550-
6560- C *****
6570- C *****
6580-

```

```

6610-
6620-
6630-
6640-
6650-
6660-
6670-
6680-
6690-
6700-
6710-
6720-
6730-
6740-
6750-
6760-
6770-
6780-
6790-
6800-
6810-
6820-
6830-
6840-
6850-
6860-
6870-
6880-
6890-
6900-
6910-
6920-
6930-
6940-
6950-
6960-
6970-
6980-
6990-
7000-
7010-
7020-
7030-
7040-
7050-
7060-
7070-
7080-
7090-
7100-
7110-
7120-
7130-
7140-
7150-
7160-
7170-

C THIS COMPLETES THE STORAGE OF THE SELECTED SENSOR PARAMETERS IN EOS
C *****
C THIS SECTION OF SUBMODEL OPTIMIZE RUNS TRACK ENOUGH TIMES
C TO DEVELOP A CONFIDENCE OF .9 THAT THE CURRENT SENSOR SYSTEM (SENSOR
C SELECTED BY OPTIMIZE AND STORED IN EOSEL) EITHER CAN OR CANNOT
C MEET THE MISSION REQUIREMENTS SPECIFIED BY THE USER.
C
C SUCESA=0.
C DO 700 I1=1,ICOUNT
C PRINT2, I1, ICOUNT
C PRINT2, I1, TRACK RUN NUMBER ',I1
C PRINT2, I1, I1
C CALL TRACK( MISSION,EOSEL, I,SENSOR,TAROPP,XT,YT,ZT,J9,IC,NU,NOUT,
C DT,YB,INPUT,INPUTB,SUNTP,SITE,SKVC)
C J9=J9-(14-J999)
C IF((INPUT.GT.0).OR.(INPUT2.GT.0))GO TO 888
C IF(J9.LT.J999)CALL SIDENT(I,XT,YT,ZT,SENSOR,X,Y,Z,SUPEFF,EOSEL,
C TAROPP,KCOUNT,NOUT,SUNTP)
C
C J9 IS THE NUMBER OF TARGETS NEGATED DURING THIS RUN OF TRACK.
C
C PRINT2, I1, I1
C PRINT2, J9, ' TARGETS TRACKED FOR TRACK RUN NUMBER',I1
C PRINT2, I1, I1
C PRINT2, '*****'
C SUCESS=0.
C IF(J9.EQ.J999)SUCESS=1.
C SUCESA=SUCESA+SUCESS
C CONTINUE
C PRINT2, I1, I1
C PRINT2, SUCESA, ' OUT OF ',ICOUNT, ' TRACK RUNS WERE SUCCESSFUL'
C PRINT2, I1, I1
C PRINT2, '*****'
C SUCESA=SUCESA/COUNT
C
C IF THIS IS ONLY A SIMULATION RUN, THEN DO NOT GET ANOTHER SENSOR.
C
C IF((INPUT.GT.0).OR.(INPUT2.GT.0))GO TO 1000
C
C IF THE AVERAGE OF SUCESS IS .GE. TO P, THE CURRENT SENSOR SYSTEM
C MEETS THE MISSION REQUIREMENTS, AND THE SENSOR SYSTEM MAY BE OUTPUT
C
C IF(SUCESA.GE.P)GO TO 1000
C
C IF THE AVERAGE OF SUCESS IS .LT. P, ANOTHER SENSOR IS NEEDED.
C
C IC=IC+1
C GO TO 343
C CONTINUE
C
C 1000
C OUTPUT THE FINAL SENSOR SYSTEM WHICH MEETS MISSION REQUIREMENTS.
C 1015 CONTINUE

```

```

7200- PRINTZ, ' '
7210- PRINTZ, ' '
7220- PRINTZ, ' '
7230-
7240-
7250-
7260-
7270-
7280-
7290-
7300-
7310-
7320-
7330-
7340-
7350-
7360-
7370-
7380-
7390-
7400-
7410-
..

685 PRINTZ, ' '
686 PRINTZ, ' '
687 PRINTZ, ' '
688
689
690
691
692
693
694
695
696
697
698
699
700
701
702
703
704
705
706
707
708
709
710
711
712
713
714
715
716
717
718
719
720
721
722
723
724
725
726
727
728
729
730
731
732
733
734
735
736
737
738
739
740
741
742
743
744
745
746
747
748
749
750
751
752
753
754
755
756
757
758
759
760
761
762
763
764
765
766
767
768
769
770
771
772
773
774
775
776
777
778
779
780
781
782
783
784
785
786
787
788
789
790
791
792
793
794
795
796
797
798
799
800
801
802
803
804
805
806
807
808
809
810
811
812
813
814
815
816
817
818
819
820
821
822
823
824
825
826
827
828
829
830
831
832
833
834
835
836
837
838
839
840
841
842
843
844
845
846
847
848
849
850
851
852
853
854
855
856
857
858
859
860
861
862
863
864
865
866
867
868
869
870
871
872
873
874
875
876
877
878
879
880
881
882
883
884
885
886
887
888
889
890
891
892
893
894
895
896
897
898
899
900
901
902
903
904
905
906
907
908
909
910
911
912
913
914
915
916
917
918
919
920
921
922
923
924
925
926
927
928
929
930
931
932
933
934
935
936
937
938
939
940
941
942
943
944
945
946
947
948
949
950
951
952
953
954
955
956
957
958
959
960
961
962
963
964
965
966
967
968
969
970
971
972
973
974
975
976
977
978
979
980
981
982
983
984
985
986
987
988
989
990
991
992
993
994
995
996
997
998
999

```



```

9000-
9000-
9010-
9020-
9030-
9040-
9050-
9060-
9070-
9080-
9090-
9100-
9110-
9120-
9130-
9140-
9150-
9160-
9170-
9180-
9190-
9200-
9210-
9220-
9230-
9240-
9250-
9260-
9270-
9280-
9290-
9300-
9310-
9320-
9330-
9340-
9350-
9360-
9370-
9380-
9390-
9400-
9410-
9420-
9430-
9440-
9450-
9460-
9470-
9480-
9490-
9500-
9510-
9520-
9530-
9540-
9550-
..

1      SUBROUTINE SPHERE(R,RC,X,Y,Z,TH)
        DIMENSION X(5,410),Y(5,410),Z(5,410),TH(19)
        INTEGER RC
C
C PROVIDES 3-D CARTESIAN COORDINATES OF ALL 410 POINTS ON THE
C SPHERE OF OPERATIONS FOR A SINGLE RADIUS
C CALL STATEMENT MUST SPECIFY WHICH RADIUS AND ENUMERATOR IS TO BE USE
C
        TH(1)=1.5708
        TH(2)=1.4039
        TH(3)=1.2359
        TH(4)=1.0374
        TH(5)=.8693
        TH(6)=.6930
        TH(7)=.5236
        TH(8)=.3546
        TH(9)=.1875
        TH(10)=.0
        TH(11)=1.7376
        TH(12)=1.9057
        TH(13)=2.1041
        TH(14)=2.2723
        TH(15)=2.4485
        TH(16)=2.6180
        TH(17)=2.7870
        TH(18)=2.9741
        TH(19)=3.1416
C
C POINTS 1 THRU 36
C
C
C
        XC=0.
        DO 1 I=1,36
          PHI=XC*6.28318/36.
          CALL CART(R,RC,TH,PHI,I,1,X,Y,Z)
          XC=XC+1.
          CONTINUE
C
C POINTS ON LAT. 2 AND 11
C
C
        XC=0.
        DO 3 I=37,71
          PHI=XC*6.28318/35.
          CALL CART(R,RC,TH,PHI,I,2,X,Y,Z)
          CALL CART(R,RC,TH,PHI,I+187,11,X,Y,Z)
          XC=XC+1.
          CONTINUE
C
C POINTS FOR LAT. 3 AND 12
C
C
        XC=0.
        DO 5 I=72,105
          PHI=XC*6.28318/34.
          CALL CART(R,RC,TH,PHI,I,3,X,Y,Z)
          CALL CART(R,RC,TH,PHI,I+187,12,X,Y,Z)
          XC=XC+1.
          CONTINUE
C
C
55      B C

```


10170-	115	CALL CART(R,RC,TH,PHI,1+187.18,X,Y,Z)
10180-		XC-XC+1.
10190-	17	CONTINUE
10200-	C	
10210-	C	POINT FOR LAT. 10
10220-	C	
10230-		PHI=0.
10240-		CALL CART(R,RC,TH,PHI,223.10,X,Y,Z)
10250-		
10260-	C	POINT FOR LAT. 19
10270-		PHI=6.28318
10280-		CALL CART(R,RC,TH,PHI, 410.19,X,Y,Z)
10290-		RETURN
10300-		END

10590-
10700-
10710-
10720-
10730-
10740-
10750-
10760-
..

1
5
SUBROUTINE CART(R,RC,TH,PHI,IX,JX,X,Y,Z)
DIMENSION TH(19),X(5,410),Y(5,410),Z(5,410)
INTEGER RC
X(RC,IX)=R*SIN(TH(JX))*COS(PHI)
Y(RC,IX)=R*SIN(TH(JX))*SIN(PHI)
Z(RC,IX)=R*COS(TH(JX))
RETURN
END

```

10990-
11000-
11010-
11020-
11030-
11040-
11050-
11060-
11070-
11080-
11090-
11100-
11110-
11120-
11130-
11140-
11150-
11160-
11170-
11180-
11190-
11200-
11210-
11220-
11230-
11240-
11250-
11260-
11270-
11280-
11290-
11300-
11310-
11320-
11330-
11340-
11350-
11360-
11370-
11380-
11390-
11400-
..

SUBROUTINE SIDE(T,X,T,VT,ZT,SENSOR,X,Y,Z,SUMEFF,EOSEL,TAROPP,
CJCOUNT,MOJ,T,SUNTYP)
INTEGER SENSNO,PTNO,TGTNO,SUNTYP
DIMENSION X(5,410),Y(5,410),Z(5,410),T(14,11),XT(14),
CVT(14),ZT(14),SENSOR(5,5),SUMEFF(5,410),EOSEL(50,6),TAROPP(14)
C
C THE PURPOSE OF THIS SUB-MODEL IS TO GENERATE THE "TARGET SYSTEM
C SIGHTING EFFICIENCY" VALUES FOR EACH POINT ON EACH SPHERE OF OPERATI
C (STORED IN MATRIX SUMEFF)
C
C DO 10 I=1,JCOUNT
C
C CALL TARGET TO INITIALLY PLACE THE TARGETS
C
C CALL TARGET(T,X,T,VT,ZT,TAROPP,SUNTYP,SNXCOS,SNYCOS,SNZCOS,SUNPHI)
C
C SENSNO= SENSOR TYPE NUMBER
C
C DO 20 SENSNO=1,NOUT
C
C PTNO=POINT ON SPHERE OF OPERATIONS
C
C DO 30 PTNO=1,410
C
C TGTNO = TARGET NUMBER BEING LOOKED AT
C
C DO 40 TGTNO=1,14
C
C IF THE TARGET WAS NOT SELECTED BY THE USER OR WAS SEEN
C DON'T CALL SIGHT
C
C IF(TAROPP(TGTNO).EQ.0.100 TO 40
C CALL SIGHT(SENSNO,TGTNO,SENSOR,T,X(SENSNO,PTNO),
C Y(SENSNO,PTNO),Z(SENSNO,PTNO),XT(TGTNO),YT(TGTNO),ZT(TGTNO),S,
C SNXCOS,SNYCOS,SNZCOS,RANGE)
C SUMEFF(SENSNO,PTNO)=SUMEFF(SENSNO,PTNO)+S
C CONTINUE
C CONTINUE
C CONTINUE
C CONTINUE
C RETURN
C END

```



```

12410-
12420-
12430-
12440-
12450-
12460-
12470-
12480-
12490-
12500-
12510-
12520-
12530-
12540-
12550-
12560-
12570-
12580-
12590-
12600-
12610-
12620-
12630-
12640-
12650-
12660-
12670-
12680-
12690-
12700-
12710-
12720-
12730-
12740-
12750-
12760-
12770-
12780-
12790-
12800-
12810-
12820-
12830-
12840-
12850-
12860-

```

IF THE TARGET HAS ECCENTRICITY OF 0, THE MEAN ANOMALY, ECCENTRIC AND
 AND TRUE ANOMALY ARE THE SAME.
 IF(T(1,3).EQ.0.)ETA=XN
 IF(T(1,3).EQ.0.)GO TO 50
 E=T(1,3)
 A=XN-E
 B=XN+E
 CALL ROOT(E,XN,A,B,EAN)
 STEP 3- THE TRUE ANOMALY ETA IS THEN CALCULATED USING THE ECCENTR
 ANOMALY EAN
 ETA=ACOS((E-COS(EAN))/(E+COS(EAN))-1.)
 CONTINUE
 SELECT LONGITUDE OF THE ASCENDING NODE RANDOMLY FOR EACH TARGET TYPE
 RINC=1-1.
 RN=RN*(DUM)
 T(1,5)=RN*STUOP1
 IF(1.E-2).AND.(1.E-3))T(1,5)=T(1,5)+2.0948RINC
 IF(1.E-5).AND.(1.E-7))T(1,5)=T(1,5)+1.57078(RINC-3)
 IF(1.E-9).AND.(1.E-10))T(1,5)=T(1,5)+2.0948(RINC-7)
 IF(1.E-11))T(1,5)=0.
 CALCULATE R, THETA, AND PHI FROM ORBITAL PARAMETERS
 R=T(1,2)*(1.-T(1,3)*E2)/(1.+T(1,3)*COS(ETA))
 THETA=ASIN(SIN(T(1,4))*SIN(ETA)+T(1,6)))
 THETA=(PI/2.0)-THETA
 IF(T(1,4).LT..0001)PHIS=ETA+T(1,8)+T(1,5)
 IF(T(1,4).LT..0001)GO TO 70
 ASP=TAN(THETA)/TAN(T(1,4))
 ACP=COS(ETA+T(1,8))/COS(THETA)
 PHIS=ATAN2(ASP,ACP)+T(1,5)
 CALCULATE CARTESIAN COORDINATES
 XT(1)=R*SIN(THETA)*COS(PHIS)
 YT(1)=R*SIN(THETA)*SIN(PHIS)
 ZT(1)=R*COS(THETA)
 CONTINUE
 RETURN
 END

```

13300-
13310-
13320-
13330-
13340-
13350-
13360-
13370-
13380-
13390-
13400-
13410-
13420-
13430-
13440-
13450-
13460-
13470-
13480-
13490-
13500-
..
1
SUBROUTINE ROOTLE,X,A,B,EAN)
F(E,XM,EAN)=EAN-ESIN(EAN)-XM
F1=F(E,XM,A)
IF(F1.GT.-.001)EAN=A
IF(F1.GT.-.001)GO TO 100
F2=F(E,XM,B)
IF(F2.LT..001)EAN=B
IF(F2.LT..001)GO TO 100
IF((F1.GE.-.01).AND.(F2.LE..01))EAN=(A+B)/2.0
IF((F1.GE.-.01).AND.(F2.LE..01))GO TO 100
C=(A+B)/2.0
F3=F(E,XM,C)
IF(F3.GT.0.001)F2=F3
IF(F3.GT.0.001)B=C
IF(F3.GT.0.001)GO TO 50
IF(F3.LT.-.001)F1=F3
IF(F3.LT.-.001)A=C
IF(F3.LT.-.001)GO TO 50
EAN=C
RETURN
END
50
100
20

```



```

13750-
13800-
13810-
13820-
13830-
13840-
13850-
13860-
13870-
13880-
13890-
13900-
13910-
13920-
13930-
13940-
13950-
13960-
13970-
13980-
13990-
14000-
14010-
14020-
14030-
14040-
14050-
14060-
14070-
14080-
14090-
14100-
14110-
14120-
14130-
14140-
14150-
14160-
14170-
14180-
14190-
14200-
14210-
14220-
14230-
14240-
14250-
14260-
14270-
14280-
14290-
14300-
14310-
14320-
14330-
14340-
14350-
..

SUBROUTINE SIGHT(N,TGTNO,SENSOR,T,XS,YS,ZS,XTS,YTS,ZTS,S,SNKCOS,
C SNKCOS,SNKZCOS,RANGE)
DIMENSION T(14,11),SENSOR(6,5)
REAL MCNDENO
REAL KX,KY,KZ ,KTGT,LXTS,LVTS,LZTS,LDOTTS,LDOTS
INTEGER TGTNO

222 THE FOLLOWING ARE INPUT VARIABLES TO SIGHT222
N= CURRENT LEAPON NUMBER (INTEGER)
T= TARGET CHARACTERISTICS MATRIX
TGTNO= CURRENT TARGET NUMBER (INTEGER)
XS,YS, AND ZS ARE COORDINATES OF SENSOR POINT
XTS,YTS, AND ZTS ARE COORDINATES OF TARGET
SNKCOS,SNKZCOS, AND SNKZCOS ARE THE DIRECTION COSINES TO THE SUN

2222 THE OUTPUT IS S THE TARGET SIGHTING EFFICIENCY FOR THIS ONE
ON ONE; ONE-TIME SIGHTING ATTEMPT 22222
S IS EITHER 0 OR 1.
SUBROUTINE 'SIGHT' IS USED BY BOTH 'SIDEN' AND 'TRACK'
'SIGHT' IS PROVIDED A SENSOR AND ITS INSTANTANEOUS POSITION, AND
THE POSITION OF A SPECIFIC TARGET
THE PURPOSE OF 'SIGHT' IS TO DETERMINE WHETHER THAT TARGET COULD
BE TRACKED BY THAT SENSOR WITH THE GEOMETRY IMPLIED
COMPUTE VECTORXL, YL, ZL FROM THE SENSOR (OR POINT) TO THE TARGET.

XL=XTS-XS
YL=YTS-YS
ZL=ZTS-ZS

COMPUTE RANGE FROM SENSOR OR POINT TO TARGET

RANGE=SQRT(XL**2+YL**2+ZL**2)

COMPUTE DIRECTION COSINES OF VECTOR FROM SENSOR OR POINT
TO TARGET

XLCOS=XL/RANGE
YLCOS=YL/RANGE
ZLCOS=ZL/RANGE

COMPUTE DIRECTION COSINES OF VECTOR TO SENSOR OR POINT

R=SQRT(XS**2+YS**2+ZS**2)
XSCOS=XS/R
YSCOS=YS/R
ZSCOS=ZS/R

COMPUTE ANGLES COM AND PSI.

COSCOM=XLCOS*SNKCOS+YLCOS*YSCOS+ZLCOS*ZSCOS
COM=ABS(ACOS(COSCOM))
COSCON=ABS(COSCON)
MODENO=SENSOR(1,N)

```

14970-			
14980-			
14990-			
15000-			
15010-			
15020-			
15030-			
15040-			
15050-			
15060-			
..			

115		C	TO TRACK IT.
		C	CALL VISIBLE(SENSEOR N, TGTNO, T, MTS, YTS, ZTS, S, SNXCOS,
			C SNXCOS, SNXCOS, RANGE, XL, YL, ZL)
			RETURN
	799		S=1.
120			RETURN
	300		S=0.0
	100		RETURN
			END

```

15550- SUBROUTINE VISBLE(SENSE,N,TGNO,XTS,VTS,ZTS,S,SNXCOS,
15560- C,SNXCOS,SNXCOS,RANGE,XL,YL,ZL)
15570- DIMENSION SENSE(6,5),T(14,11)
15580- REAL IRCVL,IRPLT,MAG
15590- INTEGER TGNO
15600-
5      THIS SUBROUTINE CALCULATES THE VISUAL MAGNITUDE OF AN EARTH-CENTER
15610- STABLE CYLINDER WITH ENDPLATES AND DETERMINES IF THE SENSOR CAN
15620- SEE THE SATELLITE.
15630- AREAC=T(TGNO,8)
15640- REFC=T(TGNO,9)
15650- AREAP=T(TGNO,10)
15660- REFP=T(TGNO,11)
15670- AS SHOWN LATER IN THE OPTIMIZE SECTION.
15680- CUTOFF=SENSE(3,N)
15690-
15700- COMPUTE BETA
15710-
15720- RTGT=ABS(SORT(XTS*Z2+YTS*Z2+ZTS*Z2))
15730- TGTSLN=SNXCOS(-XTS)+SNXCOS(-VTS)+SNXCOS(-ZTS)
15740- BETA=ACOS(TGTSLN/RTGT)
15750-
15760- COMPUTE ALPHA
15770-
15780- RANGE=ABS(RANGE)
15790- TGTSEN=(-XL)*(-XTS)+(-YL)*(-VTS)+(-ZL)*(-ZTS)
15800- ALPHA=ACOS(TGTSEN/RANGE*RTGT)
15810-
15820- COMPUTE PHIO
15830-
15840- SENSUN=SNXCOS(-XL)+SNXCOS(-YL)+SNXCOS(-ZL)
15850- PHIO=ACOS(SENSEN/RANGE)
15860-
15870- COMPUTE THTA
15880- THTA=((COS(PHIO)-(COS(ALPHA)*COS(BETA)))/(SIN(ALPHA)*
15890- C SIN(BETA)))
15900- IF(ABS(THTA)-GT.1.0)GO TO 901
15910- THTA=ACOS(THTA)
15920- GO TO 902
15930- CONTINUE
15940- THTA=0.
15950- CONTINUE
15960-
15970- CALCULATE IRRADIANCE OF CYLINDER AND ENDPLATES, IRCVL AND IRPLT.
15980-
15990- IRCVL=REFC*AREAC*SIN(ALPHA)*SIN(BETA)*SIN(THTA)/(ACOS(-1.0)
16000- C -THTA)*COS(THTA)/(4.0*(ACOS(-1.0))*RANGE*Z2)
16010-
16020- IRPLT=REFP*AREAP*COS(ALPHA)*COS(BETA)/(ACOS(-1.0)*RANGE*Z2)
16030-
16040- CALCULATE VISUAL MAGNITUDE OF TARGET AT SENSOR.
16050-
16060- IF(COS(BETA).LE.0.)IRPLT=0.
16070- IF((IRPLT,GT.0.).OR.(IRCVL,GT.0.))GO TO 866
16080- S=0.
16090- RETURN
16100- MAG=-25.78-2.58*LOG10(IRCVL+IRPLT)
16110-
866

```

16140-
16150-
16160-
16170-
16180-
16190-
16200-
..

60

C C

CHECK IF TARGET IS SEEN
IF(MAG.LE.CUTOFF)S=1.0
IF(MAG.GT.CUTOFF)S=0.0
RETURN
END

```

16640- SUBROUTINE SLUIR(N,COM,RANGE,SENSOR,S)
16650- THIS SUBROUTINE COMPUTES THE SIGNAL TO NOISE RATIO OF A
16660- LUIR SENSOR'S TARGET CURRENT(IT) TO ITS BACKGROUND CURRENT(IB) TO
16670- DETERMINE IF THE TARGET CAN BE TRACKED.
16680- INPUTS TO THE PROGRAM ARE THE ZENITH ANGLE(COM), THE RANGE
16690- (RANGE), THE SENSOR TYPE(N), AND THE SENSOR ARRAY.
16700- THE ANGULAR RESOLUTION AND THE DETECTOR DUELL TIME
16710- ARE EXTRACTED FROM THE SENSOR ARRAY.
16720-
16730- REAL IT,IB,IRADB,IRADT,LB
16740- DIMENSION SENSOR(6,5)
16750- COMMON/AIR/TRANSMT(S),BKGD(9)
16760- PI=ACOS(-1.)
16770-
16780- COMPUTE DETECTOR FIELD OF VIEW (SOLID) FROM ANGULAR RESOLU-
16790- TION.
16800- SOLID=((SENSOR(3,N)*PI/180.)*PI/4
16810-
16820- FIND THE APPROPRIATE VALUES FOR THE ATMOSPHERIC RADIANCE(LB)
16830- AND THE ATMOSPHERIC TRANSMITTANCE(TAO) BASED ON THE ZENITH
16840- ANGLE.
16850- DO 10 I=1,9
16860-   ANG=(10.*FLOAT(I)-5)*PI/180.
16870-   IF(ANG.GE.COM)GO TO 10
16880-   LB=BKGD(I)
16890-   TAO=TRANSMT(I)
16900-   CONTINUE
16910-
16920- COMPUTE TARGET AND BACKGROUND IRRADIANCES.
16930-
16940- IRADB=SOLID*LB*TAO
16950- IRADT=(PI*46.58*(1/PI**2)/RANGE**2)*TAO
16960-
16970- COMPUTE TARGET AND BACKGROUND CURRENTS
16980-
16990- IT=.81.25*IRADT/2.2E-20
17000- IB=.81.25*IRADB/2.2E-20
17010-
17020- COMPUTE SIGNAL TO NOISE RATIO(STON).
17030-
17040- STON=ITSORT(SENSOR(6,N))/SORT(IT+IB)
17050-
17060- IF STON GT 6. THEN S = 1.
17070- IF(STON.LT.6.)S=0.
17080- RETURN
17090- END
17100-
17110-

```

```

17530-
17540-
17550-
17560-
17570-
17580-
17590-
17600-
17610-
17620-
17630-
17640-
17650-
17660-
17670-
17680-
17690-
17700-
17710-
17720-
17730-
17740-
17750-
17760-
17770-
17780-
17790-
17800-
17810-
17820-
17830-
17840-
17850-
17860-
17870-
17880-
17890-
17900-
17910-
17920-
17930-
17940-
17950-
..

5
10
15
20
25
30
35
40
45

SUBROUTINE SUNPOS(SUNTYP,SNXCOS,SNYCOS,SNZCOS,SUNPHI)
THIS SUBROUTINE LOCATES THE SUN ON A RANDOM LONGITUDE AND AT A
LATITUDE CHOSEN ACCORDING TO SUNTYP.
INTEGER SUNTYP
SUNTYP IS USE TO LOCATE THE SUN IN ONE OF THREE POSITIONS
1.....ON THE EQUATOR
2.....MOST EXTREME NORTHERN LATITUDE
3.....MOST EXTREME SOUTHERN LATITUDE
4.....RANDOM POSITION
IF(SUNTYP.EQ.1)THETA=1.5708
IF(SUNTYP.EQ.2)THETA=1.1694
IF(SUNTYP.EQ.3)THETA=1.972
IF(SUNTYP.NE.4)GO TO 747
RN=RNMF(DUM)
CHOOSE RANDOM DAY AND FIND ANGLE FROM VERNAL EQUINOX(ANGLE).
DAY =RN*365.25
ANGLE=2.8ACOS(-1.)*DAY/365.25
DETERMINE LATITUDE OF SUN BASED ON TIME OF YEAR
THETA=ASIN(SIN(.40)*SIN(ANGLE))
IF(THETA.GT.0.)THETA=1.5708-THETA
IF(THETA.LE.0.)THETA=1.5708+THETA
CONTINUE
CHOOSE RANDOM LONGITUDE
RN=RNMF(DUM)
PHI=2.0*RN*ACOS(-1.0)
SUNPHI=PHI
CALCULATE DIRECTION COSINES
SNXCOS=SIN(THETA)*COS(PHI)
SNYCOS=SIN(THETA)*SIN(PHI)
SNZCOS=COS(THETA)
RETURN
END

```

```

18280- SUBROUTINE CLOUD(SKYC,I,TIME,S,ICFLAG,SUNPHI)
18290-
18300- SUBROUTINE CLOUD MODELS THE WEATHER OF THE NIGHT SKY.
18310- CLOUD IS MODELED AS HAVING A PROBABILITY OF CHANGING
18320- EVERY THREE HOURS.
18330-
18340- DIMENSION SKYC(50,25),ICFLAG(50),TIME(50,5),BFLAG(50)
18350-
18360- FIND THE POSITIVE ANGULAR DIFF BETWEEN THE LONGITUDINAL POSIT-
18370- OF THE SUN AND THE POSITION OF THE SENSOR TO DETERMINE THE
18380- TIME OF DAY AT THE SENSOR
18390-
18400- ADD=0.
18410- SUNLIN=SUNPHI
18420- IF(SUNPHI.LE.TIME(I,4))GO TO 949
18430- ADD=2.XACOS(-1.)-SUNPHI
18440- SUNLIN=0
18450- SENPHI=TIME(I,4)+ADD
18460- DIFF=SENPHI-SUNLIN
18470-
18480- DETERMINE IF THE SITE MUST BE IN DAYLIGHT. THEN TARGET NOT
18490- SEEN.
18500-
18510- IF((DIFF.LT.1.3089969).OR.(DIFF.GT.4.9741884))GO TO 948
18520-
18530- IF FIRST TIME CLOUD COVER HAS BEEN DETERMINED, USE INITIAL
18540- SKY COVER PROBABILITIES.
18550-
18560- IF(ICFLAG(I).GT.0)GO TO 947
18570-
18580- SET FLAG(ICFLAG) FOR INITIAL TIME CLOUD COVER DETERMINED.
18590-
18600- IF(DIFF.GT.1.3089969)ICFLAG(I)=1
18610- IF(DIFF.GT.2.0943951)ICFLAG(I)=2
18620- IF(DIFF.GT.3.8797933)ICFLAG(I)=3
18630- IF(DIFF.GT.3.6651914)ICFLAG(I)=4
18640- IF(DIFF.GT.4.4505896)ICFLAG(I)=5
18650-
18660- SET TIME TO NEXT WEATHER CHECK (TIME ARRAY ELEMENT FIVE).
18670-
18680- TIME(I,5)=.7853982
18690-
18700- FIND INITIAL CLOUD COVER PROBABILITY BASED ON INITIAL TIME.
18710-
18720- IF(ICFLAG(I).EQ.1)PROB=SKYC(I,1)
18730- IF(ICFLAG(I).EQ.2)PROB=SKYC(I,10)
18740- IF(ICFLAG(I).EQ.3)PROB=SKYC(I,17)
18750- IF(ICFLAG(I).EQ.4)PROB=SKYC(I,22)
18760- IF(ICFLAG(I).EQ.5)PROB=SKYC(I,25)
18770- RN=RN*(DUM)
18780- IF(RN.GE.PROB)S=0.
18790-
18800- BFLAG CONTAINS FLAG INDICATING CLOUD COVER STATE AT INITIAL
18810- TIME.
18820-

```

```

18350-
18360-
18370-
18380-
18390-
18400-
18410-
18420-
18430-
18440-
18450-
18460-
18470-
18480-
18490-
18500-
18510-
18520-
18530-
18540-
18550-
18560-
18570-
18580-
18590-
18600-
18610-
18620-
18630-
18640-
18650-
18660-
18670-
18680-
18690-
18700-
18710-
18720-
18730-
18740-
18750-
18760-
18770-
18780-
18790-
18800-
18810-
18820-
18830-
18840-
18850-
18860-
18870-
18880-
18890-
18900-
18910-
18920-
18930-
18940-
18950-
18960-
18970-
18980-
18990-
19000-
19010-
19020-
19030-
19040-
19050-
19060-
19070-
19080-
19090-
19100-
19110-
19120-
19130-
19140-
19150-
19160-
19170-
19180-
19190-
19200-
19210-
19220-
19230-
19240-
19250-
19260-
19270-
19280-
19290-
19300-
19310-
19320-
19330-
19340-
..

60      C      BFLAG(1)=S
        C      GO TO 946
        C      FIND IF TIME FOR NEXT CLOUD COVER CHECK.
        C
        C      947      IF(ICFLAG(1).EQ.1)FLAG2-DIFF-1.3089969
        C      IF(ICFLAG(1).EQ.2)FLAG2-DIFF-2.0943951
        C      IF(ICFLAG(1).EQ.3)FLAG2-DIFF-2.8797933
        C      IF(ICFLAG(1).EQ.4)FLAG2-DIFF-3.6651914
        C      IF(ICFLAG(1).EQ.5)FLAG2-DIFF-4.4505896
        C      IF(FLAG2.LT.TIME(1,5))GO TO 926
        C
        C      FIND APPROPRIATE UNCONDITIONAL CLOUD COVER PROBABILITY.
        C
        C      IF(IND-INT(TIME(1,5)/.7853982)
        C      IF(ICFLAG(1).NE.1)GO TO 945
        C      IF(IFIND.EQ.1)K=2
        C      IF(IFIND.EQ.2)K=4
        C      IF(IFIND.EQ.3)K=6
        C      IF(IFIND.EQ.4)K=8
        C      GO TO 928
        C      945      IF(ICFLAG(1).NE.2)GO TO 929
        C      IF(IFIND.EQ.1)K=11
        C      IF(IFIND.EQ.2)K=13
        C      IF(IFIND.EQ.3)K=15
        C      929      IF(ICFLAG(1).NE.3)GO TO 927
        C      IF(IFIND.EQ.1)K=18
        C      IF(IFIND.EQ.2)K=20
        C      GO TO 928
        C      927      K=23
        C
        C      CHECK IF THERE IS CLOUD COVER AND ADVANCE WEATHER CHECK TIME
        C      BY THREE HOURS.
        C
        C      928      IF(BFLAG(1).EQ.0.K=K+1
        C      RM-RANF(DUR)
        C      TIME(1,5)=TIME(1,5)+.7853982
        C      IF(RN.GT.SKYC(1,K))S=0.
        C
        C      STORE PRESENT SKY COVER STATUS IN TIME ARRAY 2.
        C
        C      946      TIME(1,2)=S
        C      GO TO 925
        C      948      ICFLAG(1)=0
        C      S=0.
        C      TIME(1,2)=S
        C      GO TO 925
        C      925      S=TIME(1,2)
        C      RETURN
        C      END

```



```

19720- SUBROUTINE TRACK(MISSION, EOSEL, T, SENSOR, TAROPP, XT, YT, ZT, J9, JU,
19730- C MI, ^CUT, IT, TB, INPUT, INPUT2, SUNTYP, SITE, SKVC,
19740- DIMENSION EOSEL(50,6), T(14,1), TAROPP(14), TRCTEF(50,4), NU(50),
19750- C SENSOR(6,5), XU(50), YU(50), ZU(50), TIME(50,5), XT(14), MISSION(4,4),
19760- C VT(14), ZT(14), N(50), SITE(50,4), SKVC(50,25), PUT(50), ICFLAG(50)
19770- INTEGER SUNTYP
19780- DO 15 I=1,50
19790- ICFLAG(I)=0
19800- N(I)=0
19810-
19820- BY OPTIMIZE CAN MEET THE MISSION REQUIREMENTS.
19830- THE PURPOSE OF TRACK IS TO DETERMINE IF THE SENSOR SYSTEM SELECTED
19840- C
19850- IN ADDITION, TRACK CAN BE USED TO TEST THE EFFECTIVENESS OF A
19860- C
19870- SYSTEM OF PRESELECTED SITES AND SENSORS.
19880-
19890- A 50 BY 5 MATRIX (TIME) IS USED TO STORE THE FOLLOWING VARIABLES...
19900-
19910- SENSOR SELECTION NUMBER.
19920- PRESENT SITE, SKY COVER STATUS.
19930- TAIL (TIME UNTIL SENSOR WILL BE AVAILABLE AGAIN).
19940- XT (MEAN ANOMALY OR PHI ANGLE).
19950- TIME FOR NEXT CLOUD COVER CHECK AT FIXED GROUND SITES.
19960-
19970- THE SENSOR SELECTIONS ARE TAKEN FROM THE EOSEL MATRIX GENERATED BY
19980- OPTIMIZE.
19990-
20000- ZERO THE TIME MATRIX.
20010-
20020- PI=ACOS(-1.)
20030- DO 10 I=1,50
20040- DO 5 J=1,5
20050- TIME(I,J)=0.
20060- CONTINUE
20070- CONTINUE
20080-
20090- ENTER SITE DATA INTO TIME AND EOSEL ARRAYS IF INPUT .GT. ZERO
20100- ALSO COMPUTE XU, YU, AND ZU SENSOR COORDINATES.
20110-
20120- IF (INPUT.LE.0) GO TO 944
20130- DO 943 I=1, INPUT
20140- TIME(I,4)=SITE(I,2)
20150- EOSEL(I,1)=SITE(I,4)
20160- EOSEL(I,2)=SITE(I,1)
20170- R=REARTH-6378.145
20180- THETA=EOSEL(I,3)
20190- PHIS=TIME(I,4)
20200- XU(I)=R*SIN(THETA)*COS(PHIS)
20210- YU(I)=R*SIN(THETA)*SIN(PHIS)
20220- ZU(I)=R*COS(THETA)
20230- CONTINUE
20240- 943 CONTINUE
20250- 944 CONTINUE
20260-
20270- C THE TARGETS AVAILABLE ARE REGISTERED IN MATRIX TAROPP (TARGET OFFSET

```

```

20290-
20300-
20310-
20320-
20330-
20340-
20350-
20360-
20370-
20380-
20390-
20400-
20410-
20420-
20430-
20440-
20450-
20460-
20470-
20480-
20490-
20500-
20510-
20520-
20530-
20540-
20550-
20560-
20570-
20580-
20590-
20600-
20610-
20620-
20630-
20640-
20650-
20660-
20670-
20680-
20690-
20700-
20710-
20720-
20730-
20740-
20750-
20760-
20770-
20780-
20790-
20800-
20810-
20820-
20830-
20840-
20850-

```

C TAROPP MATRIX IS THE FIRST COLUMN OF THE T MATRIX.
 C GENERATE THE TAROPP MATRIX.
 C DO 30 I=1,14
 C TAROPP(I)=T(I,1)
 C CONTINUE
 30
 C CALL SUBROUTINE TARGET TO INITIALLY PLACE THE SUM AND THE
 C AND THE TARGETS.
 C CALL TARGET(I,XT,YT,ZT,TAROPP,SUNTYP,SNXCOS,SNYCOS,SNZCOS,SUNPHI)
 C BEGIN PROCESS TO MAKE REMAINING SENSOR PLACEMENTS
 C I=INPUT+1
 C J=INPUT2+JU
 C CALCULATE NU MATRIX FOR PRESELECTED SPACE AND AIR BASED SENSORS.
 C IF(INPUT2.LE.0)GO TO 940
 C DO 942 K=I,J
 C NU(K)=0
 C DO 941 L=1,J
 C IF((EOSEL(K,1).EQ.EOSEL(L,1)).AND.(EOSEL(K,4).EQ.EOSEL(L,4)))NU(K)
 C C=NU(K)+1
 C 941 CONTINUE
 C 942 CONTINUE
 C 940 CONTINUE
 C PLACE AIR-BASED SENSORS AND GROUND-BASED SENSORS WHICH ARE
 C NOT FIXED-POSITIONED.
 C IF((INPUT.GT.0).AND.(INPUT2.EQ.0))GO TO 891
 C FIND THE NUMBER OF SENSORS INVOLVED(IONGRD) SO THE
 C SPACING(APART) CAN BE DETERMINED, AND A LONGITUDE(PUT ARRAY)
 C CAN BE DESIGNATED FOR EACH OF THESE SENSORS.
 C IONGRD=0
 C DO 891 K=1,J
 C NSEN=EOSEL(K,1)
 C IF(SENOR(1,NSEN).LT.2.5)IONGRD=IONGRD+1
 C CONTINUE
 C N=IONGRD
 C APART=2.84COS(-1.)/IONGRD
 C PUT(1)=2.84COS(-1.)*N
 C DO 892 K=2,IONGRD
 C K2=K-1
 C PUT(K)=PUT(K2)+APART
 C CONTINUE
 C 891
 C 892
 C ARRANGE THE SENSORS STORED IN THE EOSEL ARRAY IN TERMS OF THE
 C GREATEST NUMBER ON SAME LATITUDE.
 C DO 911 K=1,J
 C DO 912 L=K,J

```

20880- 115 IF(NU(K).GE.NU(L1))GO TO 913
20890- DO 929 L2=1,6
20900- HOLD-ESEL(K,L2)
20910- ESEL(K,L2)=ESEL(L1,L2)
20920- ESEL(L1,L2)=HOLD
20930- CONTINUE
20940- 909 HOLD=NU(K)
20950- NU(K)=NU(L1)
20960- NU(L1)=HOLD
20970- CONTINUE
20980- 913 CONTINUE
20990- 912 CONTINUE
21000- L3=0
21010- DO 904 L1=K,J
21020- IF((ESEL(K,1).EQ.ESEL(L1,1)).AND.(ESEL(K,4).EQ.ESEL(L1,4)))
21030- C.AND.(K.NE.L1))GO TO 908
21040- GO TO 907
21050- 908 L3=K+1
21060- DO 905 L2=1,6
21070- HOLD-ESEL(L3,L2)
21080- ESEL(L3,L2)=ESEL(L1,L2)
21090- ESEL(L1,L2)=HOLD
21100- CONTINUE
21110- 905 HOLD=NU(L3)
21120- NU(L3)=NU(L1)
21130- NU(L1)=HOLD
21140- CONTINUE
21150- 907 CONTINUE
21160- 904 CONTINUE
21170- 911 CONTINUE
21180- C
21190- C PLACE SPACE-, AIR-, AND REMAINING GROUND-BASED SENSORS
21200- C
21210- K=1
21220- IPLACE=1
21230- DO 53 I=K,J
21240- C
21250- C MSEN IS THE INTEGER SENSOR TYPE.
21260- C
21270- MSEN= ESEL(I,1)
21280- RN=RNPF(DUM)
21290- TIME(I,4)=RN*PI22.
21300- IF(M(MSEN).EQ.0)GO TO 56
21310- M=I-1
21320- NN= ESEL(M,1)
21330- IF(MN.EQ.MSEN).AND.( ESEL(I,4).EQ. ESEL(M,4)))GO TO 57
21340- M=M-1
21350- IF(M.EQ.0)GO TO 56
21360- GO TO 56
21370- C
21380- C SPACE BASED SENSORS WITH THE SAME INCLINATION ARE EQUALLY
21390- C AROUND THE SAME ORBIT USING THE NU ARRAY WHICH HOLDS THE NUM-
21400- C NUMBER OF SENSORS OF THE SAME TYPE WHICH ARE IN THE SAME
21410- C
21420- 57 RNJ=NU(I)
21430- TIME(I,4)=TIME(M,4)+(2.*PI/RNJ)
21440- ESEL(I,5)= ESEL(M,5)
21450- R=SENSOR(4,MSEN)+6378.145
21460- IF(SENSOR(1,MSEN).LT.R)GO TO 56

```

```

21470- ECSEL(1,5)=RAMP(DUM)P.22
21480- THETA=ASIN(SIN( ECSEL(1,4)*SIN(TIME(1,4)+ ECSEL(1,6)))
21490- THETA*PI/2.-THETA)
21500- IF( ECSEL(1,4).LT..0001)PHIS=TIME(1,4)+ ECSEL(1,6)+ ECSEL(1,5)
21510- IF( ECSEL(1,4).LT..0001)GO TO 51
21520- ASP=TAN(THETA)/TAN( ECSEL(1,4))
21530- PCP=COS(TIME(1,4)+ ECSEL(1,6))/COS(THETA)
21540- PHIS=ATAN(ASP,ACP)+ ECSEL(1,5)
21550- GO TO 51
21560- THETA= ECSEL(1,2)
21570- IF(1.EQ.1)GO TO 914
21580- ISKIP=IONGRD/NU(1)
21590- HOP=FLOAT(IONGRD)/FLOAT(NU(1))
21600- HOP=INT(HOP)
21610- HOP=HOP-FLOAT(HOP)
21620- IF(HOP.GT..5)ISKIP=ISKIP-1
21630- IF(PLACE=IPLACE)ISKIP
21640- IF(PLACE=GT.IONGRD)IPLACE=IPLACE-IONGRD
21650- IF(PLACE=GT.IONGRD)IPLACE=IPLACE-IONGRD
21660- IPLACE=IPLACE+1
21670- GO TO 914
21680- PHIS=PUT(IPLACE)
21690- IF(PHIS.GT.2.SACOS(-1.))PHIS=PHIS-2.SACOS(-1.)
21700- TIME(1,4)=PHIS
21710- PUT(IPLACE)=0.
21720- XU(1)=RHSIN(THETA)SACOS(PHIS)
21730- YU(1)=RHSIN(THETA)SIN(PHIS)
21740- ZU(1)=RHSIN(THETA)
21750- PRINT2, 'SENSOR SELECTED', I, 'TYPE', 'MSEN
21760- PRINT2, 'THETA', THETA, 'PHIS', PHIS
21770- N(MSEN)=1
21780- CONTINUE
21790- CONTINUE
21800- PRINT2, ' '
21810- C
21820- C
21830- C
21840- C
21850- C
21860- C
21870- C
21880- C
21890- C
21900- C
21910- C
21920- C
21930- C
21940- C
21950- C
21960- C
21970- C
21980- C
21990- C
22000- C
22010- C
22020- C
22030- C

```

```

22050-
22070-
22090-
22110-
22130-
22150-
22170-
22190-
22210-
22230-
22250-
22270-
22290-
22310-
22330-
22350-
22370-
22390-
22410-
22430-
22450-
22470-
22490-
22510-
22530-
22550-
22570-
22590-
22610-
22630-
22650-

C DELTA IS THE MEAN ANOMALY INCREMENT.
C
C DELTA=SQRT(XMU/CUBE(A))*DT*60.
C
C UPDATE THE MEAN ANOMALY IN MATRIX T.
C
T(I,7)=T(I,7)+DELTA
E=T(I,3)
IF(E.EQ.0.)ETA=T(I,7)
IF(E.EQ.0.)GO TO 46
XM=T(I,7)
A=XM*.5E
B=XM*.2E
CALL ROOT(E,XM,A,B,EAN)
ETA=ACOS((E-COS(EAN))/(E+COS(EAN))-1.)
CONTINUE
R=T(I,2)*(1.-T(I,3)*E2.)/(1.-T(I,3)*COS(ETA))
THETA1=ASIN(SIN(T(I,4)*XIN(ETA+T(I,6)))
THETA=(PI/2.0)-THETA1
IF(T(I,4).LT..0001)PHIS=ETA+T(I,6)+T(I,5)
IF(T(I,4).LT..0001)GO TO 47
ASP=TAN(THETA1)/TAN(T(I,4))
ACP=COS(ETA+T(I,6))/COS(THETA1)
PHIS=ATN2(ASP,ACP)+T(I,5)
XT(I)=RSSIN(THETA)*COS(PHIS)
YT(I)=RSSIN(THETA)*SIN(PHIS)
ZT(I)=RCOS(THETA)
CONTINUE
46
47
48
C
C TARGET COORDINATE MATRICES XT, YT, AND ZT ARE NOW UPDATED WITH CURRE
C TARGET POSITIONS.
C
C*****
C NOW MOVE THE SENSORS ALONG THEIR ORBITS OR LATITUDES.
C
J=INPUT+INPUT2+JU
DO 55 I=1,J
C
C DO GROUND- AND AIR-BASED SENSORS FIRST.
C
IF(SENSOR(I,MSEN).EQ.3.)GO TO 68
TIME(I,4)=TIME(I,4)+DT*.00436332
IF(TIME(I,4).GT.(2.*ACOS(-1.)))*TIME(I,4)-2.*ACOS(-1.)
IF((INPUT.GT.0.0).AND.(SENSOR(I,MSEN).LT.2.5))GO TO 939
R=SENSOR(I,MSEN)*6378.145
GO TO 938
938 CONTINUE
R=REARTH+SITE(I,3)
938 CONTINUE
THETA=EOSEL(I,2)
PHIS=TIME(I,4)
C
C CALCULATE CARTESIAN COORDINATES FOR THE SENSOR LOCATION AT THE CURRE
C TIME.
C
GO TO 64
22670-
22690-
22710-
22730-
22750-
22770-
22790-
22810-
22830-
22850-
22870-
22890-
22910-
22930-
22950-
22970-
22990-
23010-
23030-
23050-
23070-
23090-
23110-
23130-
23150-
23170-
23190-
23210-
23230-
23250-
23270-
23290-
23310-
23330-
23350-
23370-
23390-
23410-
23430-
23450-
23470-
23490-
23510-
23530-
23550-
23570-
23590-
23610-
23630-
23650-

```

```

22650- 52      CONTINUE
22660- C *****
22670- C FOLLOWING SECTION MOVES THE SPACE-BASED SENSORS ALONG THEIR ORBITS.
22680- C
22690- C ADVANCE THE MEAN ANOMALY.
22700- C
22710- C      CUBEA=( EOSEL(I,2))**3.
22720- C      DELXM=SQRT(XMU/CUBEA)*EDT360.
22730- C
22740- C UPDATE THE MEAN ANOMALY.
22750- C
22760- C      TIME(I,4)=TIME(I,4)+DELXM
22770- C
22780- C CALCULATE THE SPHERICAL COORDINATES.
22790- C
22800- C      ETA=TIME(I,4)
22810- C      R= EOSEL(I,2)
22820- C      THETA1=ASIN(SIN( EOSEL(I,4))*SIN(TIME(I,4)+ EOSEL(I,6)))
22830- C      THETA=PI/2.-THETA1
22840- C      IF( EOSEL(I,4).LT..0001)PHIS=TIME(I,4)+ EOSEL(I,6)+ EOSEL(I,5)
22850- C      IF( EOSEL(I,4).LT..0001)GO TO 54
22860- C      ASP=TAN(THETA1)/TAN(EOSEL(I,4))
22870- C      ACP=COS(TIME(I,4)+ EOSEL(I,6))/COS(THETA1)
22880- C      PHIS=ATAN2(ASP,ACP)+ EOSEL(I,5)
22890- C
22900- C CALCULATE THE CARTESIAN COORDINATES.
22910- C
22920- C      XU(I)=R*SIN(THETA)*COS(PHIS)
22930- C      YU(I)=R*SIN(THETA)*SIN(PHIS)
22940- C      ZU(I)=R*COS(THETA)
22950- C      CONTINUE
22960- C
22970- C 55
22980- C
22990- C 50 ALL THE USEABLE SENSORS ARE MOVED ALONG THEIR RESPECTIVE PATHS.
23000- C *****
23010- C
23020- C ADJUST THE TIME MATRIX ELEMENT YAVAIL.
23030- C
23040- C      K=INPUT+INPUT2+JU
23050- C      DO 70 I=1,K
23060- C      TIME(I,3)=TIME(I,3)-DT
23070- C      IF(TIME(I,3).LT.0.)TIME(I,3)=0.
23080- C      CONTINUE
23090- C
23100- C 70
23110- C
23120- C 11
23130- C
23140- C CONTINUE
23150- C
23160- C ZERO THE TRCTEF MATRIX.
23170- C
23180- C      DO 60 I=1,50
23190- C      DO 60 J=1,14
23200- C      TRCTEF(I,J)=0.
23210- C      CONTINUE
23220- C      CONTINUE
23230- C
23240- C 65
23250- C
23260- C *****
23270- C

```

```

C C CALL SIGHT TO BUILD TRCTEF FOR ALL SURVIVING TARGETS OVER ALL
C C CURRENTLY USEABLE SENSORS.
      M=0
      K=INPUT+INPUT2-JU
      DO 100 I=1,K
        C C MSEN IS THE INTEGER SENSOR TYPE.
        C C MSEN = EOSEL(I,1)
        C IF THE ITH SENSOR IS NOT CURRENTLY USEABLE, GO TO THE NEXT SENSOR,
        C IF(TIME(I,3).GT.DT)GO TO 100
        C DO 90 J=1,14
        C IF THE JTH TARGET HAS BEEN TRACKED, GO TO THE NEXT TARGET.
        C IF(TAROPPI(J).EQ.0.)GO TO 90
        C M=R+1
        C CALL CLOUD FOR GROUND-BASED SENSORS.
        C S=1.0
        C IF(SENSOR(1,MSEN).EQ.1.)CALL CLOUD(SKYC,I,TIME,S,ICFLAG,SUMPHI)
        C IF(S.EQ.0.)GO TO 90
        C CALL SIGHT FOR THE JTH TARGET AND THE ITH SENSOR.
        C CALL SIGHT(MSEN,J,SENSOR,T,XU(I),YU(I),ZU(I),XT(J),YT(J),ZT(J),S,
        C SMCOS,SNYCOS,SMZCOS,RANGE)
        C RECORD THE INVERSE OF THE RANGE TO THE TARGET IN TRCTEF OR A ZERO
        C IF THE TARGET IS NOT VISIBLE.
        C TRCTEF(I,J)=S
        C IF(S.GT.0.)TRCTEF(I,J)=1./RANGE
        C CONTINUE
        C CONTINUE
        C TRCTEF NOW CONTAINS ZEROS WHERE A SENSOR CANNOT SEE A TARGET DUE
        C TO ANY OF THE FOLLOWING REASONS.....
        C SENSOR IS CURRENTLY TRACKING A SATELLITE.
        C TARGET HAS ALREADY BEEN TRACKED.
        C TARGET IS NOT IN LINE-OF-SIGHT OF AN AVAILABLE SENSOR.
        C TRCTEF ALSO CONTAINS INVERSE OF THE RANGE TO THE TARGET IN ALL
        C OTHER LOCATIONS.
        C *****
        C TRACK THE TARGETS WITH THE SENSORS
        C DO 300 IPRIOR=1,4
        C *****

```

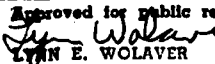

VITA

Richard T. Salmon was born at Scott Air Force Base, January 30, 1952. He graduated from Ocean Springs High School, Ocean Springs, Mississippi, in 1970. In 1974 he received a commission in the United States Air Force and a B.S. in Environmental Science from the University of Southern Mississippi, Hattiesburg, Mississippi. In 1979 he received a M.S. in Chemistry from Virginia Commonwealth University, Richmond, Virginia.

After graduation, he worked as an instructor of chemistry at John Tyler Community College, Chester, Virginia. He reentered the Air Force in 1980 and worked as an Orbital Analysis at NORAD's Cheyenne Mountain Complex City, Colorado Springs, Colorado, until he entered the Air Force Institute of Technology in June 1981.

He is married to the former Jo Sylvia Smith of Richmond, Virginia. They have one daughter, JoAnna.

Permanent address: 302 Teringo-Circle
Ocean Springs, MS 39564

REPORT DOCUMENTATION PAGE		READ INSTRUCTIONS BEFORE COMPLETING FORM
1. REPORT NUMBER AFIT/GSO/82D-4	2. GOVT ACCESSION NO.	3. RECIPIENT'S CATALOG NUMBER
4. TITLE (and Subtitle) AN EVALUATION OF THE EFFECTIVENESS OF DEPLOYING ELECTRO-OPTICAL TELESCOPES FOR SATELLITE TRACKING ON HIGH ALTITUDE POWERED PLATFORMS		5. TYPE OF REPORT & PERIOD COVERED Master's Thesis
		6. PERFORMING ORG. REPORT NUMBER
7. AUTHOR(s) Richard T. Salmon Capt		8. CONTRACT OR GRANT NUMBER(s)
9. PERFORMING ORGANIZATION NAME AND ADDRESS Air Force Institute of Technology (AFIT-EN) Wright-Patterson AFB, Ohio 45433		10. PROGRAM ELEMENT, PROJECT, TASK AREA & WORK UNIT NUMBERS
11. CONTROLLING OFFICE NAME AND ADDRESS		12. REPORT DATE December 1982
		13. NUMBER OF PAGES
14. MONITORING AGENCY NAME & ADDRESS (if different from Controlling Office)		15. SECURITY CLASS. (of this report) Unclassified
		15a. DECLASSIFICATION/DOWNGRADING SCHEDULE
16. DISTRIBUTION STATEMENT (of this Report)		
17. DISTRIBUTION STATEMENT (of the abstract entered in Block 20, if different from Report)		
18. SUPPLEMENTARY NOTES <div style="text-align: right;"> <p>Approved for public release: IAW AFR 190-17.  LYNN E. WOLAYER Dean for Research and Professional Development Air Force Institute of Technology (AIC) Wright-Patterson AFB OH 45433</p> </div>		
19. KEY WORDS (Continue on reverse side if necessary and identify by block number) Satellite tracking, powered balloons, airships, electro-optical telescope, astronomical telescope, remotely piloted vehicles		
20. ABSTRACT (Continue on reverse side if necessary and identify by block number) <p>The purpose of this research was to evaluate the possible benefits of an air based system of electro-optical satellite tracking telescopes. A computerized simulation model was developed to conduct a comparative analysis of a hypothetical system of air based telescopes with the Ground-Based Electro-Optical Deep Space Surveillance (GEODSS) System. The simulation includes a first order optimization process for selecting a satellite surveillance system and a many-on-many engagement model to test the</p>		

20. effectiveness of the surveillance system selected. In addition, the user can input a preselected surveillance system and test its effectiveness.

The user specifies the characteristics of the surveillance system and the basing locations, if they are preselected. Cloud cover data can be entered with preselected ground sites. Target satellites included four sets of representative satellite systems. The user selects the targets, defines the mission time, and determines the percentage of each target system which must be tracked.

Preliminary results indicate that an air based surveillance system with three dispersed telescope platforms could outperform a system of five candidate GEODSS sites.

END

FILMED

3-83

DTIC